FINAL TECHNICAL REPORT

Paleoseismology on the Owens Valley Fault and Latest Quaternary Stratigraphy in Owens Valley near Lone Pine, eastern California

Steven N. Bacon, Silvio K. Pezzopane, and R.M. Bud Burke (PI)

Humboldt State University, Department of Geology
Arcata, California 95521
(tel.) 707-826-4292
(e-mail) rmb2@humboldt.edu

U.S. Geological Survey
National Earthquake Hazard Reduction Program
Award Numbers 01-HQ-GR-0013 and 02-HQ-GR-0003

Program Element: NI

June, 2003

This research was supported by the U.S. Geological Survey (USGS), Department of the Interior, under USGS Awards 01-HQ-GR-0013 and 02-HQ-GR-0003. The views and conclusions contained in this document are those of the authors and should not be interpreted as necessarily representing the official policies, either expressed or implied, of the U.S. Government.

Paleoseismology on the Owens Valley Fault and Latest Quaternary Stratigraphy in Owens Valley near Lone Pine, eastern California

Award Numbers 01-HQ-GR-0013 and 02-HQ-GR-0003

Steven N. Bacon, Silvio K. Pezzopane, and R.M. Bud Burke (PI)

Humboldt State University, Department of Geology
Arcata, California 95521
(tel.) 707-826-4292
(e-mail) rmb2@humboldt.edu

Program Element: NI

Key words: Trench Investigation, Quaternary Fault Behavior, Recurrence Intervals, and Age Dating

Non-technical Summary

The Owens Valley fault is a normal oblique right-lateral fault that is bounded to the west by the Sierra Nevada frontal fault system and to the east by the White-Inyo fault zones. Understanding the seismogenic history on the Owens Valley fault is critical for evaluating strain partitioning within Owens Valley and the southern Walker Lane and northern Eastern California shear zone. Our research utilized detailed trench studies at three paleoseismic sites to improve our understanding of the timing of paleoearthquakes and displacement of the historic 1872 and penultimate events. Our principal results rely on the structural and geochronologic relations of latest Pleistocene to early Holocene fluvio-deltaic and lacustrine stratigraphy associated with oscillating pluvial water-levels in the lower Owens Lake basin near Lone Pine. Based on our paleoseismic and stratigraphic investigation, we present a latest Quaternary pluvial Owens Lake level curve that is a compilation of our data with that of other stratigraphic, geomorphic, and sediment core data from prior investigations.

Paleoseismology on the Owens Valley Fault and Latest Quaternary Stratigraphy in Owens Valley near Lone Pine, eastern California

Steven N. Bacon, Silvio K. Pezzopane, and R.M. Bud Burke (PI)

ABSTRACT

Two different paleoseismic sites (elev. 1115-1128 m) on the Owens Valley fault (OVF), located 4 and 7 km north of Lone Pine, eastern California, having a total of 7 trenches and 4 exploration pits, expose direct stratigraphic evidence for two earthquakes since ~15 cal. ka; the historic 1872 earthquake, the most recent event (MRE) and the penultimate event (PE). In addition to the paleoseismic sites, we investigated a graben that is located ~10 km north of Lone Pine at an elevation of 1160-1175 m. We used exploratory trenches across the graben and soil pits on different surfaces that bound the graben to provide information on the long-term paleoearthquake history on the OVF. The results indicate that the graben is associated with a lateral spread that occurred ~20 to ≥140 ka.

Our principal results rely on the structural and geochronologic relations of fluvio-deltaic and lacustrine stratigraphy associated with oscillating pluvial lake-levels in the lower Owens Lake basin near Lone Pine. Stratigraphic analyses of these sediments exposed in trenches, pits, and along 1.5 km of Owens River bluffs reveal a relatively complete record of ~15-7 cal. ka sequence stratigraphy. This study has documented an early Holocene transgression of pluvial Owens Lake between ~11-8 cal. ka. This early Holocene transgression postdates the lake's initial latest Pleistocene recession that occurred between ~15.5-11 cal. ka after it last overflowed. On the basis of tephra chronology, the early Holocene highstand occurred after ~8 cal. ka and reached an elevation of ~1135 m, ~10 m below the latest overflow sill of Owens Lake basin. This lake-level was short lived prior to lowering ~15 m to an elevation of ~1120 m where the lake eroded into older sediments and constructed a beach berm. The most recent fluctuating lake-levels and associated fluvio-deltaic systems modified and reset the landscape and evidence of pre-1872 fault scarps near and below the elevation of 1135 m between ~15.5-8 cal. ka.

The paleoseismic results provide average vertical offsets for the PE and MRE and a confident estimate of the age of the PE. Measured in 3 trenches from two sites, the cumulative vertical offset from the last two earthquakes (the PE and MRE) is 2.3 ± 0.3 m (2σ). In 5 trenches, the average vertical offset for the MRE is 0.9 ± 0.3 m (2σ). In each trench, the vertical offset of the MRE is subtracted from the cumulative vertical offset to derive an average vertical offset for the PE of 1.4 +0.3/-0.4 m (2σ). Analyses of ^{14}C in charcoal and tufa materials that bound the PE event horizon indicate the PE occurred between 10,210 ± 60 cal. yr B.P. and 8,790 ± 210 cal. yr B.P. The age of the PE is estimated at 9,300 ± 300 cal. yr B.P. on the basis of the PE horizon position with respect to the location of the ^{14}C ages and sedimentation rates. Accounting for the elapsed time between 1872 and 1950, the interseismic interval between the two earthquakes is ca. 9,500 to 8,900 yrs. The oldest sediment in the trench exposures that is not deformed by the antepenultimate event (APE) is ~15,000 ± 600 cal. ^{14}C yr B.P. This ca. 15 cal. ka age provides a minimum constraint for the APE. The maximum age of sediment deformed by the APE is 21,000 ± 1,300 ^{14}C yr B.P. (Lubetkin and Clark, 1988). Using the range of constraining ages of sediment that bound the APE, the event occurred 18,400 ± 4,000 cal. yr B.P. Given the poor age constraint of the APE, the interseismic interval estimate between the PE and APE is 12,800 to 5,400 yrs.

The average scaling ratio of 6:1 (horiz:vert; Beanland and Clark, 1994) is used with the average individual vertical and total vertical cumulative offsets of the PE and MRE to estimate the average horizontal displacements. The average horizontal displacements divided by their corresponding single interseismic intervals and age estimate of the APE, result in an average oblique slip rate estimate of 0.4-1.3 m/k.y. (2σ). Using the maximum scaling ratio of 10:1 with the average total vertical cumulative offset and the age estimate for the APE, result in a three event oblique slip rate estimate of 1.0-1.6 m/k.y.

TABLE OF CONTENTS

LIST OF TABLES

LIST OF FIGURES

INTRODUCTION

The Owens Valley fault (OVF) is located within the southern half of Owens Valley in east-central California. The fault zone is located in the central axis of Owens Valley, bounded to the west by Sierra Nevada Frontal-faults, to the east by the White-Inyo Mountain fault zones, and to the south by the Coso Range (Fig. 1). The Owens Valley is a graben that forms the western margin of the Eastern California shear zone (ECSZ) north of the Garlock fault (Fig. 1). The ECSZ is an active transtentional seismic belt that collectively accommodates 12 ± 2 mm/yr (25%) of contemporary relative dextral motion between the Pacific and North American plates inboard of the San Andreas plate boundary (Sauber et al., 1994).

The most recent event (MRE) on the OVF occurred on March 26, 1872 at 2:30 a.m., with a magnitude of M_w 7.5-7.7 (Beanland and Clark, 1994), which is the third largest magnitude historical earthquake in the western United States. An after shock of M_I 6.5 occurred 3.5 hours after the main event. Two additional M_I 6.1 and M_I 6.6 after shocks occurred 8 and 16 days after the main trembler, respectively (Ellsworth, 1990). Displacement was oblique, having 6.0 ± 2.0 m of right-lateral displacement with 1.0 ± 0.5 m of normal slip (Beanland and Clark, 1994). The surface rupture extended 100 ± 10 km from the southern shores of Owens Lake to just north of Big Pine, with ground-shaking effects documented as far north as Bishop (Oakeshott et al., 1972; dePolo et al., 1991; Vittori et al., 1993; Beanland and Clark, 1994; Fig. 2).

The paleoearthquake history and a long-term (mid to late Quaternary) slip rate are poorly known for the OVF near Lone Pine. The OVF seismic history and slip rate have important implications for local and regional seismic hazard assessments (e.g., Burke et al., 2001) as well as geodetic models of current deformation in the western United States (e.g., Sauber et al., 1994).

This Technical Report for the National Earthquake Hazards Reduction Program (NEHRP) describes the results of our paleoseismic research near Lone Pine in light of previous investigations regarding the latest Quaternary OVF paleoearthquake history and fluctuations of pluvial Owens Lake. The original project and continuation proposals are by Burke et al. (2000; 2001). Preliminary results of this project's research were documented in a NEHRP project summary in 2001 (Bacon et al., 2001) and presented during meetings in December, 2000 at the American Geophysical Union Fall meeting in San Francisco, California (Bacon and Burke, 2000); in March, 2002 at the Geological Society of America, Rocky Mountain section meeting in Cedar City, Utah (Bacon et al., 2002a); and in October, 2002 at the Geological Society of America National meeting in Denver, Colorado (Bacon et al., 2002b). The data presented in this Technical Report is a synopsis of a Humboldt State University master thesis (Bacon, 2003).

Purpose and significance

The purpose of this research is to document the magnitude of displacement and timing of paleoearthquakes on the OVF near Lone Pine, in addition to characterizing the style of deformation associated with the historic 1872 earthquake. To do this, exploratory trenching techniques were applied at three different paleoseismic sites. After the first trench investigation, it became clear that to accurately interpret the stratigraphic context of deformed sediments at these two sites, a detailed study of the latest Pleistocene and Holocene Owens Valley lacustrine and fluvio-deltaic sequence stratigraphy would need to be initiated. In addition to the paleoseismic trench sites, ~1.5

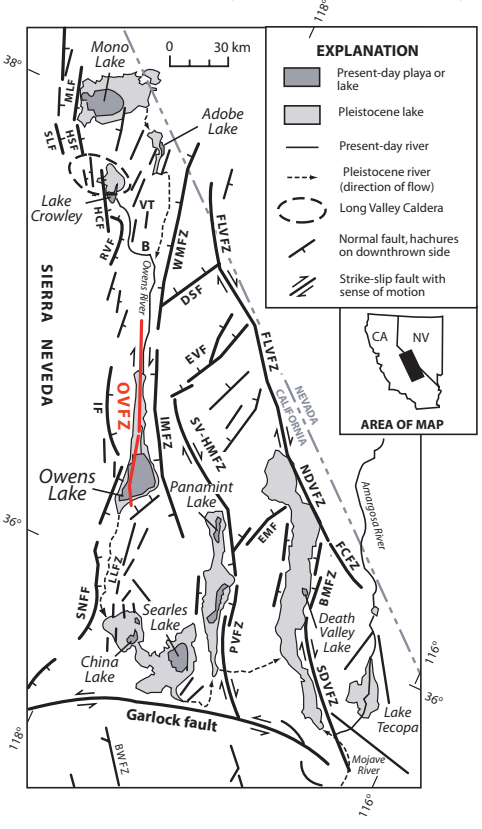

Figure 1. Map of major Quaternary faults in the southern Walker Lane belt / northern Eastern California shear zone and the locations of the Owens Valley Fault Zone, Owens Lake, and other lakes hydrologically connected upstream and downstream from it during pluvial periods of the Pleistocene. Faults are modified from Bryant (1984); dePolo et al. (1993); Dixon et al. (1995); Reheis and Dixon (1996); Machette et al. (2001). Pluvial lake figure modified from Smith and Bischoff (1997). Faults (F) and fault zones (FZ): MLF, Mono Lake; SLF, Silver Lake; HSF, Hartly Springs; HCF, Hilton Creek; RVF, Round Valley; IF, Independence; SNFF, Sierra Neveda Frontal, WMFZ, White Mountain; OVFZ, Owens Valley; IMFZ, Inyo Mountain; DSF, Deep Springs; EVF, Eureka Valley; SV-HMFZ, Saline Valley-Hunter Mountain; EMF, Emigrant; PVFZ, Panamint Valley; FLVFZ, Fish Lake Valley; NDVFZ, Northern Death Valley; FCFZ, Furnace Creek; BMFZ, Black Mountain; SDVFZ, Southern Death Valley; LLFZ, Little Lake; BWFZ, Black Water; B, Bishop; VT, Volcanic Tableland.

km of Owens River bluffs exposure was mapped to support the stratigraphy revealed at the paleoseismic sites (Bacon, 2003).

Following four years of investigating the latest Quaternary sediments near Lone Pine from both natural exposures and stratigraphic pits excavated during this project and in light of the work from previous studies, this study has documented the timing and magnitude of past lake-levels associated with pluvial Owens Lake. The knowledge of this stratigraphy will contribute to the understanding of paleoclimate in this part of the Basin and Range and to the chronology of the chain of lakes that were connected at different times down drainage of pluvial Owens Lake (Fig. 1). Furthermore, the paleoseismic results developed from this research are used to provide insight into the neotectonic and kinematic role that the OVF plays in distributing strain within the southern Walker Lane belt / Eastern California shear zone (ECSZ) and strain partitioning within Owens Valley (e.g., Wesnousky and Jones, 1994).

Methods

The logs of seven trenches and four deep exploration pits excavated at two sites, informally named the "Alabama Gates and Quaker paleoseismic sites", were created similar to the methods described in McCalpin (1996a). In addition to the paleoseismic sites, several exploratory trenches and soil pits were excavated at a site informally named the "Shattered Fan site". Stratigraphic and structural criteria used to document the occurrence and timing of past earthquakes at these sites is comparable to the indicators mentioned in Weldon et al. (1996) and Lettis and Kelson (2000). Stratigraphic facies models determined from trench and pit exposures at the sites were described using standard sedimentologic techniques (e.g., Adams and Wesnousky, 1998; Baucom and Rigsby, 1999; Einsele, 2000). The paleoseismic data presented in this study is based on sequence stratigraphic analysis of fluvio-deltaic and lacustrine sediments related to fluctuating pluvial Owens Lake. The erosive systems related to these depositional environments created erosional and depositional unconformities across and into earlier fault traces and landforms, which are collectively used in sequence stratigraphic analysis as paleoseismic indicators. These indicators are then applied in conjunction with geochronologic methods to determine the magnitude and timing of specific pluvial Owens Lake lake-levels that are in turn used to decipher the paleoearthquake history on the OVF.

Geomorphic analysis of survey-controlled topographic profiles from the sites in addition to existing geomorphic data from earlier investigations around the northern shore of Owens Lake (playa) aid in deciphering between tectonically produced fault scarps from constructional and erosional landforms created by lacustrine, fluvial or mass-wasting processes. Both geologic and geomorphic mapping and identification of fault-related features were mapped using Slemmons (1968) 1:12,000 scale low-sun-angle black and white aerial photographs and 1977-BLM and 1990-LADWP 1:12,000 scale colored aerial photographs. Detailed fault zone strip maps by Bryant (1988) and Beanland and Clark (1994) were supplemented with field mapping. Geographic Information System (GIS) analysis of mapped features within the field area was used to provide topographic control. Site-specific topographic control at the Alabama Gates paleoseismic site is from CalTrans (1993) construction plans. Topographic control at the Quaker paleoseismic site is from a Topcon total station that was surveyed from bench marks set for this study, which were controlled by a differential global position system (GPS). Topographic control at the Shattered Fan site is from a total station that was controlled from the area of a bench mark shown on the USGS 7.5' Union Wash quadrangle map.

Geochronologic methods used to provide numerical age control at the Alabama Gates and Quaker paleoseismic sites include radiometric and accelerator mass spectrometry (AMS) techniques on charcoal, organic sediment, and tufa materials of 15 samples by Beta Analytical Inc. (Table 2), in addition to tephrochronology of 3 tephra samples by A.M., Sarna-Wojcicki, U.S. Geological Survey, Menlo Park, California (Table 3 in Bacon, 2003). Relative dating techniques used at the Shattered Fan site are after the methods of Burke and Birkeland (1979).

Previous fault studies in Owens Valley

Nearly 100 years after the 1872 earthquake and the initial descriptions and observations by Whitney (1872) and Gilbert (1884), work by Slemmons and Cluff (1968) started a series of detailed investigations on the OVFZ. Hill (1972) published mapping by D.B. Slemmons and his students in a special centennial issue of *California Geology* on the 1872 Owens Valley earthquake. Carver (1970) produced the first detailed and thorough study up until that time that focused on Quaternary tectonism and surface faulting on the southern end of the OVFZ in Owens

Lake basin. Later, Lubetkin and Clark (1988), Beanland and Clark (1994), and Bierman et al. (1995) determined slip rate and average recurrence interval estimates on the Lone Pine fault of the OVFZ near Lone Pine (Fig. 3). In addition, Martel et al. (1987) and Zehfuss et al. (2001) calculated numerically controlled late Quaternary slip rate estimates on the Fish Springs fault on the northern end of the OVFZ near Big Pine. In addition, a paleoseismic investigation by Lee et al. (2001b), presents an estimate for the time of one interseismic interval on the northern end of the OVFZ near Big Pine (Fig. 2).

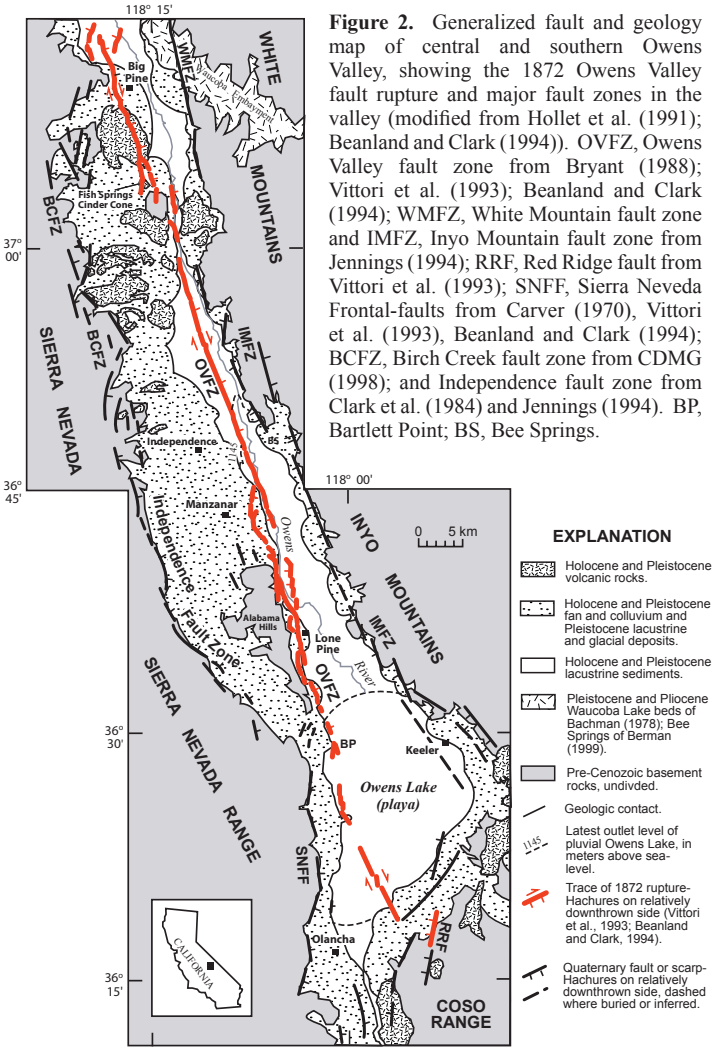

Figure 2. Generalized fault and geology map of central and southern Owens Valley, showing the 1872 Owens Valley fault rupture and major fault zones in the valley (modified from Hollet et al. (1991); Beanland and Clark (1994)). OVFZ, Owens Valley fault zone from Bryant (1988); Vittori et al. (1993); Beanland and Clark (1994); WMFZ, White Mountain fault zone and IMFZ, Inyo Mountain fault zone from Jennings (1994); RRF, Red Ridge fault from Vittori et al. (1993); SNFF, Sierra Neveda Frontal-faults from Carver (1970), Vittori et al. (1993), Beanland and Clark (1994); BCFZ, Birch Creek fault zone from CDMG (1998); and Independence fault zone from Clark et al. (1984) and Jennings (1994). BP, Bartlett Point; BS, Bee Springs.

Furthermore, there have been many investigations north of the OVFZ in Owens Valley near Bishop. Investigations northwest of Bishop by Pinter (1995) studied faulting within the volcanic tableland. Pinter and Keller (1995) performed a geomorphic analysis of neotectonic deformation in northern Owens Valley (Fig. 1). Investigations on the White Mountain fault zone (WMFZ) east of Bishop by dePolo and Ramelli (1987) and by Lienkaemper et al. (1987), soon after the 1986 Chalfant Valley earthquake, both document dextral displacement on the WMFZ. After the Chalfant Valley earthquake, a seismotectonic investigation by dePolo (1989) characterized the entire WMFZ. Recently, Kirby et al. (2002) and Schroeder et al. (2002) present data that corroborate with these earlier investigations and refine lateral slip rate estimates on the WMFZ.

The most extensive investigations along the entire OVFZ occurred during reconnaissance mapping for the State of California and for the U.S. Geological Survey as described in Bryant (1988) and Beanland and Clark (1994), respectively. The most comprehensive study along the entire OVFZ is by Beanland and Clark (1994) who assessed fault slip rates on the basis of horizontal to vertical average displacement per event ratio (6:1), and who interpreted possibly 2 paleoearthquakes of this size in Holocene time (3 including the historic 1872 event). The assessment was under the assumptions of uniform recurrence and that the oldest valley fill deformed by the fault is as old as 10 k.y. Our study has refined the results made by Beanland and Clark (1994) on the OVFZ by utilizing site-specific paleoseismic trench sites and detailed mapping of latest Quaternary fluvio-deltaic and lacusrine stratigraphy near Lone Pine.

STRATIGRAPHIC AND GEOMORPHIC INVESTIGATION ON THE OWENS VALLEY FAULT

To document the paleoearthquake history and characterize deformation on the OVFZ, seven exploratory fault trenches and four exploratory pits were excavated across and adjacent to the OVF at the Quaker (36°38’23”N,118 04’57”W) and Alabama Gates (36°39’55”N,118°05’35”W) paleoseismic sites. The Quaker site is ca. 4 km and the Alabama Gates site is ca. 7 km north of Lone Pine (Fig. 3). In addition to these new paleoseismic sites, the Lone Pine fault of Lubetkin and Clark (1988) and Beanland and Clark (1994; their Site 9), is located ca. 3 km south of the Quaker site and ca. 1.2 km west of Lone Pine, which is informally referred to in this study as the “Lone Pine paleoseismic site” (Fig. 3). Furthermore, Site 14 of Bryant (1988) and Beanland and Clark (1994) is located nearly halfway between the Alabama Gates and Quaker sites (Fig. 3). Collectively, all four sites cover ~7% of the total 1872 surface rupture and share common fault sections, thereby enabling stratigraphic and structural correlation between the sites with a high degree of confidence.

Elevation of paleoseismic sites

The Lone Pine paleoseismic site (Fig. 3) is near an elevation of 1160 m and Site 14 is near 1140 m, ~15 m above and 5 m below the sill elevation of 1145 m, respectively. The Alabama Gates site covers an elevation of 1116-1140 m with trenches and a pit between 1120 and 1128 m. The elevations at the Quaker site range from 1115-1125 m with trenches and pits between 1113.5 and 1122.5 m. The difference of ca. 17-31 m in elevation between the Alabama Gates and Quaker sites in relation to the 1145 m sill elevation has exposed the areas of the trenches and pits to fluctuating Owens Lake water-levels and fluvial modification, whereas the Lone Pine site and Site 14 are above the latest overflow lake-levels and fluvial modification.

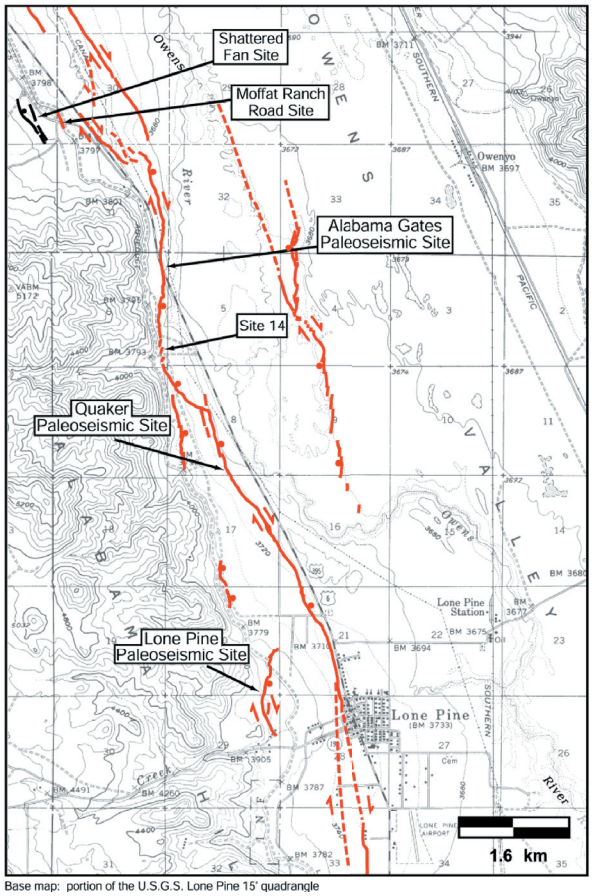

Base map: portion of the U.S.G.S. Lone Pine 15' quadrangle

Figure 3. Map of field area and location of paleoseismic and stratigraphic study sites in relation to the Owens Valley fault zone (shown in red) near Lone Pine. Sites identified refer to discussions in text. Faults are mapped from 1:12,000 aerial photographs, Bryant (1988), and Beanland and Clark (1994).

Scarp and shoreline profile methodology

The profiles developed from the paleoseismic sites are used to distinguish between scarps generated by earthquakes from scarps created by erosional and constructional shoreline or fluvial processes. Recognizing the differences between fault scarps, shorelines, or fluvial features enable the comparison or correlation to similar features documented in other parts of the valley with a high level of confidence. Shoreline features identified at the two trench sites consist of wave-cut notches, also referred to as shoreline scarps, beach ridges or berms, and tread surfaces.

Shoreline development is controlled by many factors such as local slope, the amount and characteristics of sediment available for transport, the availability of accommodation space, and the length of time a lake-level resides at a particular shoreline elevation (Adams and Wesnousky, 1998). In addition to shoreline features, fluvial processes produced geomorphic scarps along and adjacent to the trend of the OVF. Features identified at the two trench sites that are interpreted to be associated with a meandering fluvial system have the morphology of tread and risers.

For this study, the elevations of wave-cut notches and meander risers are taken at the distinct break-in-slope that significantly deviates from the rest of the slope. Elevations of tread surfaces are taken from well defined and prominent relatively flat surfaces that slope <3°. Shoreline and fluvial features were distinguished by aerial photographic interpretation, followed by field verification in conjunction with trench and natural exposures. The break-in-slope identified as a wave-cut notch is similar in morphology to what is also referred to as a shoreline angle. The elevation of a beach ridge or berm is determined from the crest of the landform. Wave-cut notches generally form at or below mean water level, whereas the crests of beach ridges or berms form above mean water level (e.g. Oviatt, 2000). The elevation of tread and risers associated with a fluvial system are determined in the same manner as shoreline features.

Alabama Gates Paleoseismic Site

Three exploratory fault trenches (T1-T3) and one deep exploratory pit (P1) were excavated in March 1999 at the Alabama Gates paleoseismic site (Figs. 3 and 4). The Alabama Gates paleoseismic site is equivalent to Site 15 of Beanland and Clark (1994). Trenches are oriented obliquely to the trend of the fault scarp and are located in a road-cut on the westside of "old" U.S. Highway 395 or the westside of "new" north bound U.S. Highway 395 (Figs. 4 and 5). The trenches nearly extend the entire fault zone. Excavations in T2 and T3 revealed a 12-inch

corrugated subdrain pipe that was assembled parallel to the scarp along the upper to middle scarp slopes during during initial highway construction. Portions of the ground surface and uppermost deposits at the trench site were benched into, graded, and removed to construct the road-cut.

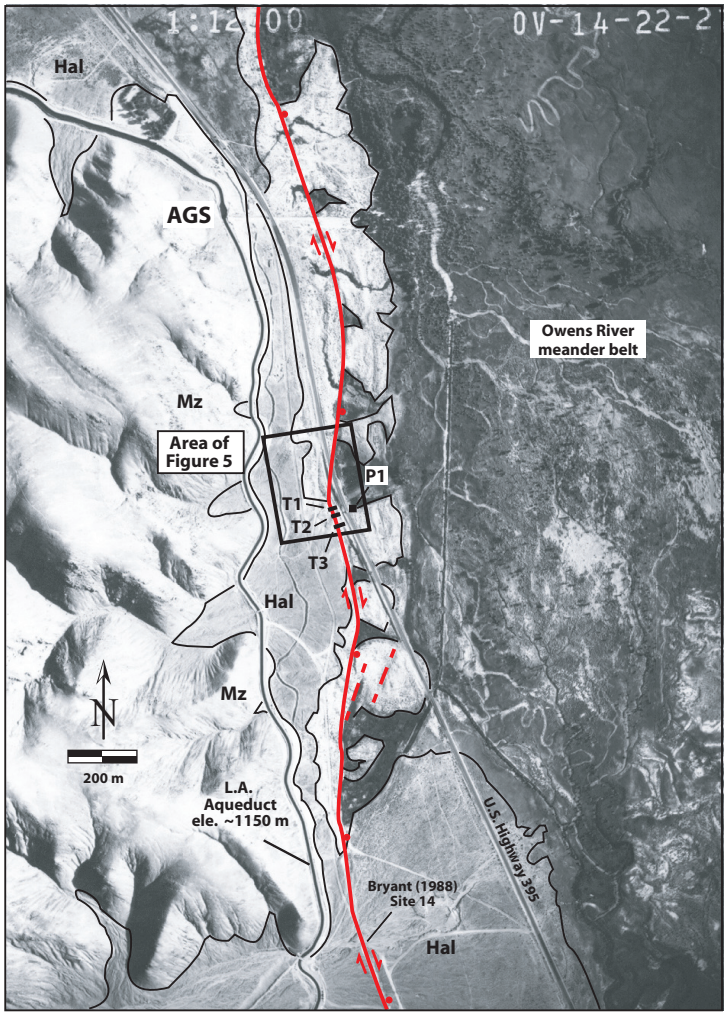

Figure 4. Black and white low-sun-angle aerial photograph of the Alabama Gates paleoseismic site. Fault trenches (T1-T3), exploritory pit (P1), and Bryant (1988) Site 14 are shown in relation to the 1872 Owens Valley fault trace (shown in red), the Alabama Hills (Mz) and Holocene alluvium derived from the Alabama Hills (Hal). Stratigraphy in trenches reveal that the 4-10 m geomorphic scarp contains a ca. 1.0 m single-event scarp formed by the 1872 earthquake. All three trenches show evidence for only the 1872 event at the surface. T1 is the only trench that contains subsurface evidence for a paleoearthquake, the penultimate event. AGS, Alabama Gates Spillway. (photo from Slemmons, 1968)

The initial road construction into the scarp provides deep exposures of faulted stratigraphy observed using relatively shallow trenches (2-2.5 m deep). The use of long and deep trenches at this site was not feasible, because at this particular site U.S. Highway 395 is ca. 5-7 m to the east, making it impossible to excavate a deep trench across the entire scarp. Nevertheless, the trenches expose relatively deep strata that provide data on fault mechanics, by displaying a complex distribution of faulting and offsets, as well as a slip rate estimate and evidence for a paleoearthquake, observations which are uncommon in most exposures in southern Owens Valley.

Geomorphology at the Alabama Gates paleoseismic site

The OVF in the area of the Alabama Gates paleoseismic site is expressed as a prominent east facing geomorphic scarp. Scarp heights range between 4 and 10 m, having slopes of 18-35° (Beanland and Clark, 1994). Runoff originating from the Alabama Hills, in addition to springs directly related to the fault, have produced numerous channels that are incised into and across the geomorphic scarp along with the ~1 m vertical fault scarp generated by the 1872 earthquake (Fig. 4). Incised channels that drain the Alabama Hills and cross the geomorphic scarp exhibit a sinuous morphology in contrast to the channels that are related to springs along the middle to lower slopes that are incised normal to the scarp. Well-formed channels north of the trench site appear to show evidence for deformation by exhibiting complex channel morphologies, but likely indicate base-level changes with as much as 7 m of incision across the scarp. It is not clear whether the sinuous patterns are related to recurrent deformation or if the total measured incision is natural. It is likely that the channels were enhanced by outbursts related to dynamiting the L.A Aqueduct-Alabama Gates spillway (AGS; Fig. 4) by angry citizens of Owens

Valley on November 23, 1924 and again in the Spring of 1927 (Schumacher, 1962). The western boundary of the Owens River meander belt has truncated and eroded into the lower scarp slopes in areas east of the trench site.

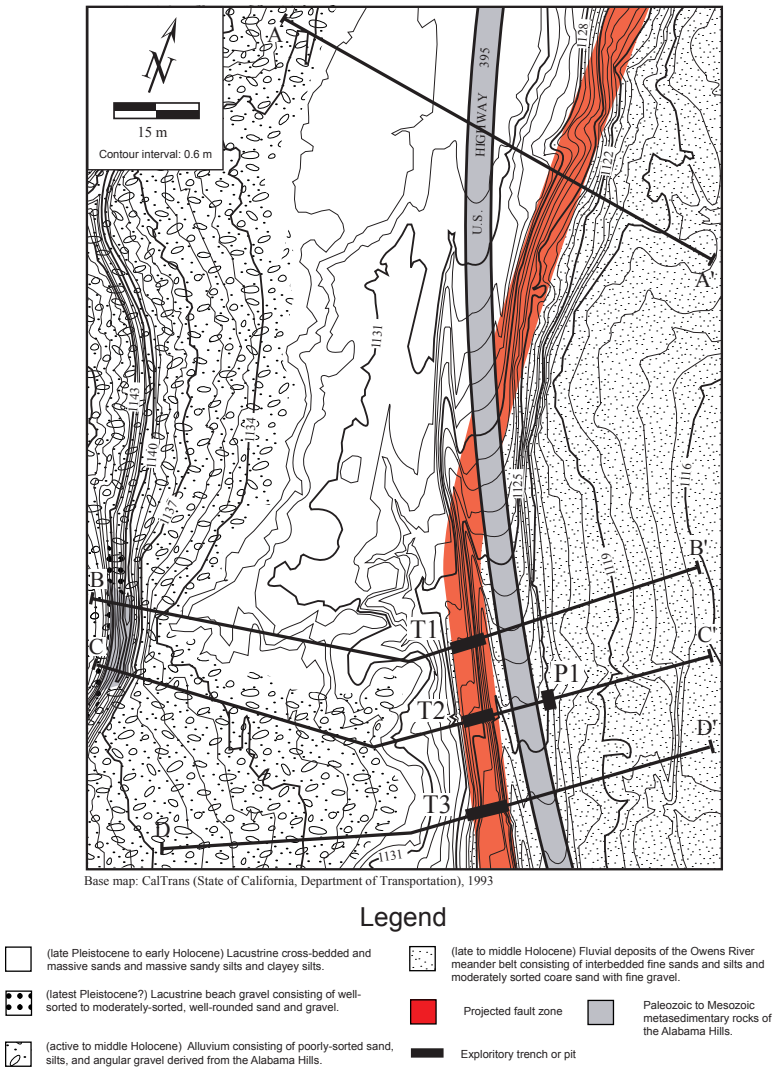

Figure 5. Geologic map of the Alabama Gates paleoseismic site showing location of trenches (T1-T3) and exploritory pit (P1) excavated across and adjacent to the 1872 Owens Valley fault rupture (fault zone shown in red). The fault and geomorphic scarp was benched into during initial highway construction for U.S. highway 395, removing the upper portions of the scarp. Transects (A-A' through D-D') show the location of profiles shown in Bacon, 2003.

Scarp profiles

The profiles from the Alabama Gates site provide evidence that the trace of the OVF is along a geomorphic scarp, which is interpreted to contain preserved tread surfaces, wave-cut notches, and meander risers that formed prior to the 1872 earthquake. Four profiles were constructed and show 2 to 3 significant breaks-in-slope (Bacon, 2003). Figure 6 is an example of one of the four profiles. The highest geomorphic feature at the site is a tread surface at an elevation between 1132-1134 m that is attributed to shoreline erosion (Figs. 5 and 6). There are two wave-cut notches at two different elevations at the site. The higher of the two is exposed along a cut related to construction of the L.A. aqueduct. The notch is at an elevation of 1135-1136 m. The lower wave-cut notch is at an elevation of 1128 m, which is also present along undisturbed portions of the scarp south of the trench site. Meander risers associated with the western boundary of the Owens River meander are located along the lower scarp slope at an elevation near 1116 m (Figs. 5 and 6).

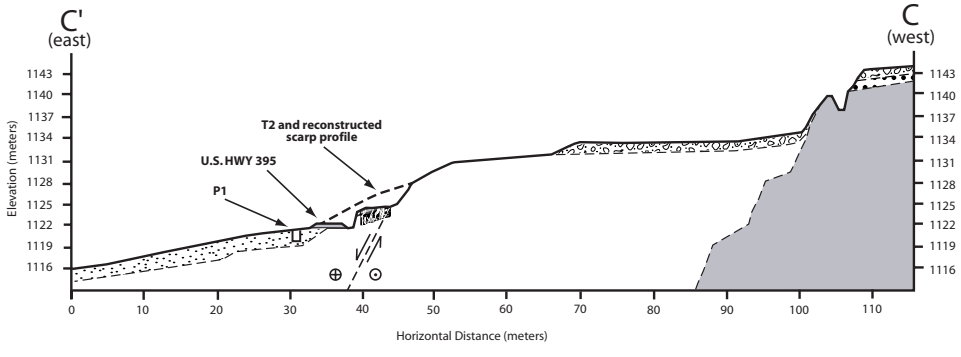

Figure 6. General geologic cross-section along transect C-C' showing T2 and P1 in relation to U.S. Highway 395 and the projection of the Owens Valley fault at depth. Reconstructed scarp profile provides an estimate of how much the scarp was benched into during initial highway construction. Reconstructed scarp profile is based on the unmodified portion of the scarp along transect A-A'. Legend to geologic units is presented in Figure 5.

Alabama Gates Trench Investigation

The three fault trenches (T1-T3) excavated across the trace of the OVF range between 5-7 m in length and 2-2.5 m in depth with an exploratory pit (P1) having a depth of ~2 m (Figs. 7-10). The trenches expose stratigraphy consistent with lithofacies attributed to at least two transgressive and regressive lake-cycles of pluvial Owens Lake and subsequent erosion and deposition from a meandering stream system. Stratigraphy is primarily late Pleistocene to early Holocene lacustrine nearshore facies and Holocene alluvium in the footwall, against latest Pleistocene lacustrine deep water facies, and shore facies that are in turn overlain by terrestrial spring/marsh sediments. The spring/marsh sediments in the hanging wall are unconformably overlain by middle to early Holocene lacustrine nearshore facies forming an erosional contact (sequence boundary) that truncates fault strands associated with a paleoearthquake. All three trenches expose structural evidence related to the 1872 earthquake, whereas two trenches (T1 and T2) contain structural and stratigraphic evidence for the penultimate event.

Trench stratigraphy

Alabama Gates lithofacies and facies associations

The sequence stratigraphy exposed in the three trenches contains lithofacies that are laterally continuous and correlatable between the trenches (T1-T3; Figs. 7-9). In addition, the lithofacies and facies associations (FAs) used to describe the units exposed in the trenches are also common to natural exposures described in other locations of the field area, which are collectively shown in Table 1. The three FAs include: (1) delta front (FA-A); (2) delta plain (FA-B); and (3) lacustrine (FA-C). The specific lithofacies that are associated with each FA are classified on the basis of grain size, sedimentary structure, biological components, and lateral and vertical stratigraphic position (e.g., Baucom and Rigsby, 1999; Einsele, 2000). As a result of the same sedimentologic characteristics and processes that often occur in different depositional environments, the different FAs often include the same lithofacies.

Within all the trench exposures, there are sequence boundaries (SBs) that are used to determine the number of transgressive or regressive sequences (lake-cycles). Typically, SBs are generated by a relative fall in water-level (i.e., change in base-level). This relative fall in water-level may be influenced by changes in the rate of tectonic subsidence, uplift, changes in climatic conditions and associated sedimentation, or a combination of all these factors, as long as there are changes that result in a net loss of accommodation space (Emery and Myers, 1996; Einsele, 2000).

Stratigraphy

The sediment exposed in the trenches are mostly lacustrine (FA-C; Table 1). The oldest sediment observed in the Alabama Gates trenches is a stiff, green clayey silt that is only exposed in T2 and is mapped into lithofacies 1a or 1b (Fig. 8; Table 1). Lithofacies 1a or 1b has a sharp upper erosional boundary, interpreted as an abrasion platform representing sequence boundary SB1. The depositional environment of lithofacies 1a or 1b is interpreted to be offshore because it is massive and fine grained (lacustrine FA-C; Table 1). The abrasion platform exposed in T2 is overlain by a massive, moderately sorted, well rounded fine to coarse sand with minor amounts of fine pebbles that contain lithologically heterogeneous sediment derived from up valley source areas, consisting of scoria, basalt, tuff, and pumice. This massive sand is placed into lithofacies 7b, lacustrine FA-C (Table 1). It is exposed at the bottom of all three trenches (T1-T3; Figs. 7-9). Lithofacies 7b likely was deposited in a shore (beach) depositional environment, based on its sedimentologic characteristics and stratigraphic position above the abrasion platform in T2. Stratigraphically overlying lithofacies 7b is a 10-40 cm thick silty sand to sandy silt deposit (T1-T3; Figs. 7-9). It has a conformable lower contact with lithofacies 7b. The stratigraphy defines a fining upward sequence and is in lithofacies 3b. The facies association of this deposit is interpreted to be lacustrine FA-C characteristic of a nearshore depositional environment (Table 1). Overlying lithofacies 1a or 1b, 3b, and 7b are sediments that were deposited in a terrestrial environment. Collectively, the sediment is mapped into lithofacies 4b and includes thinly interbedded (0.25-0.4 m) diatomaceous silts with a reworked tephra, organic rich silts with detrital charcoal, and non-organic silts and fine sands. The same lithofacies in T1 and T2 is relatively thicker and primarily composed of a fining upward sequence of ~0.3 m of charcoalized plant fibers to 0.25-1.75 m thick organic silts and fine sands (Figs. 7 and 8). The plant fibers have a morphology similar to bull rushes, which are exposed in the bottom eastern portion of T2. The charcoalized plant fibers form a 0.3 m soft silty peat deposit that was sampled for ^{14}C age dating (Fig. 8). Sediment of lithofacies 4b was deposited in a marsh and/or spring terrestrial environment within the delta plain FA-B (Table 1). In addition, a massive, 0.25-

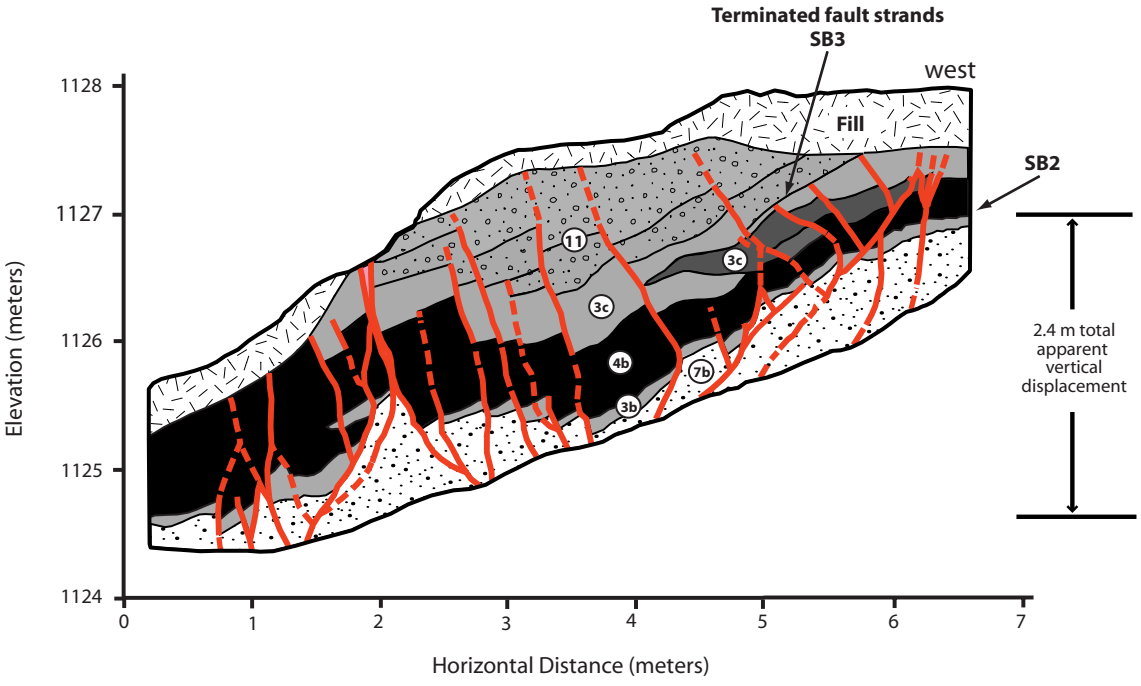

Figure 7. Trench log for the south wall of the Alabama Gates paleoseismic site T1. Lithofacies 3b, 7c, and 11 are within lacustrine FA-C. Lithofacies 4b is within delta plain FA-B. Lithofacies numbers and facies associations are described in Table 1. Figure 21 is a stratigraphic column. Lower contacts of lithofacies 4b and 11 define sequence boundaries SB2 and SB3, respectively.

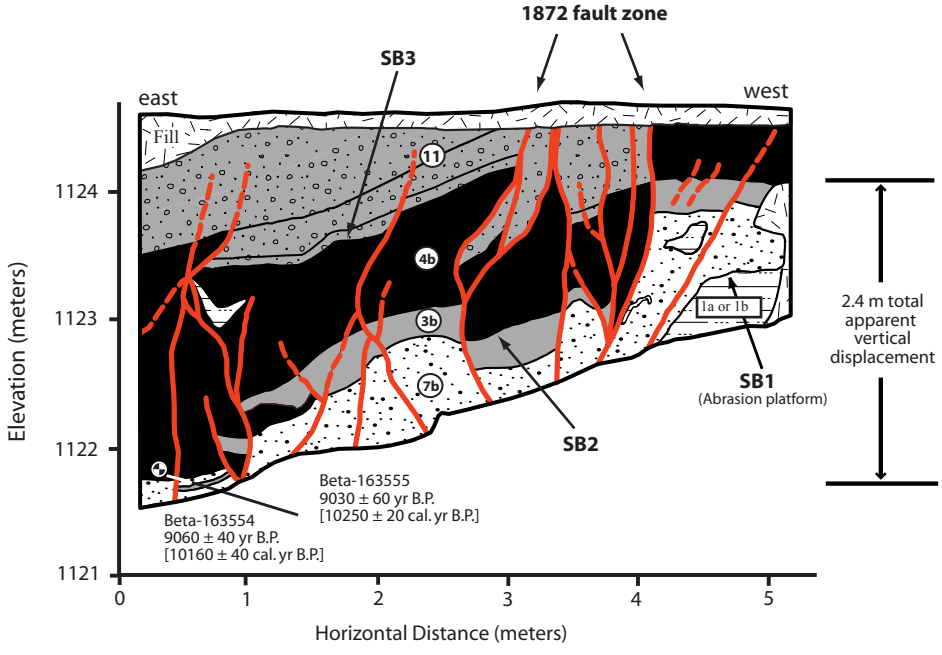

Figure 8. Trench log for the south wall of the Alabama Gates paleoseismic site T2. Lithofacies 1a, 1b, 3b, 7c, and 11 are within lacustrine FA-C. Lithofacies 4b is within delta plain FA-B. Lithofacies numbers and facies associations are described in Table 1. Figure 21 is a stratigraphic column. The location of the two radiocarbon samples is shown with a line and circle and listed in Table 2. The abrasion platform formed into lithofacies 1a or 1b defines sequence boundary SB1. Lower contacts of lithofacies 4b and 11 define sequence boundaries SB2 and SB3, respectively.

0.70 m thick poorly-sorted silty sand with trace fine pebbles unconformably overlies lithofacies 4b in T3 (Fig. 9). This poorly-sorted silty sand differs significantly from lithofacies 7b by its degree of sorting. It possesses characteristics of a colluvial apron across the scarp, thereby is placed in lithofacies 9a, alluvium FA-B (Table 1). Collectively, lithofacies 3b, 4b, and 7b mark SB2. The sediment mapped as lithofacies 3b, 4b, and 9a for this study was described earlier by Beanland and Clark (1994) in the U.S. 395 highway roadcut to represent a nearshore beach and backbar depositional environment. The sediment in this study and that of Beanland and Clark (1994) are similar.

Overlying lithofacies 4b and 9a is a 0.1-0.5 m thick sandy silt deposit that is similar in sedimentology to lithofacies 3b. This deposit is mapped as lithofacies 3c; lacustrine FA-C (Table 1). Lithofacies 3c has a sharp lower contact with lithofacies 4b in T1 and T3 (Figs. 7 and 9). In addition, lithofacies 3c contains a relatively

thin (0.1-0.2 m) sandy silt bed in the western portions of T1 and T3, which is truncated by faults in T3 and pinches out to the east in T1 (Figs. 7 and 9). Lithofacies 3c in T1 and T3 is overlain by another massive sandy silt deposit, but differs in that it contains 10-15% angular fine to medium pebbles. The lower boundary of this deposit with lithofacies 3c is sharp and interpreted to be an erosional contact and defines SB3 (Figs. 7 and 9). This same deposit is also underlain by lithofacies 4b in T2, having an erosional contact as well (SB3; Fig. 8). Because this massive silt deposit contains angular pebbles with lithologies of the Alabama Hills, it is assigned to a new lithofacies, lithofacies 11 (Table 1). The depositional environment of lithofacies 11 is interpreted to be nearshore and assigned to the lacustrine FA-C, likely related to a regressive lake-level. Evidence to suggest deposition during a regressive lake-level is indicated by the occurrence of angular pebbles that are poorly-sorted within a silty matrix, and the erosional lower contact with underlying lithofacies 3c and 4b (SB3). The upper boundary of lithofacies 11 in all three trenches is sharp and related to excavation into the scarp to construct a bench for the U.S. Highway 395 road-cut. Above this boundary is fill and disturbed sediment.

Stratigraphy east of U.S. Highway 395 is significantly different from stratigraphy exposed in natural and trench exposures west of the highway. Exploratory pit (P1) is located ca. 10 m east of T2 at an elevation of 1122.5 m (Fig. 5). Stratigraphy exposed in the pit includes 1.5 m of alternating fine sand and silt that is moderately sorted, moderately rounded, and soft to slightly hard (Fig. 9). This deposit is mapped as lithofacies 12 and has sedimentologic characteristics of a meandering stream, similar to flood plain silts and fine sands (e.g. Baucom and Rigsby, 1999; Einsele, 2000). Lithofacies 12 is placed within the delta plain FA-B (Table 1). Lithofacies 12 is underlain by poorly- to moderately-sorted and subangular to well rounded fine to coarse sand and fine gravel at the bottom ~40 cm of the pit (Fig. 9). This deposit contains lithologically heterogeneous sediment derived from up valley source areas that consist of scoria, basalt, tuff, and pumice. The contact between this deposit with lithofacies 12 is wavy, with sandy discontinuous lenses over ~20 cm long. The contact is conformable and indicates that the sandy deposit is likely the facies of a distributary channel of a meandering stream. This deposit is mapped as lithofacies 5c; delta plain FA-B (Table 1).

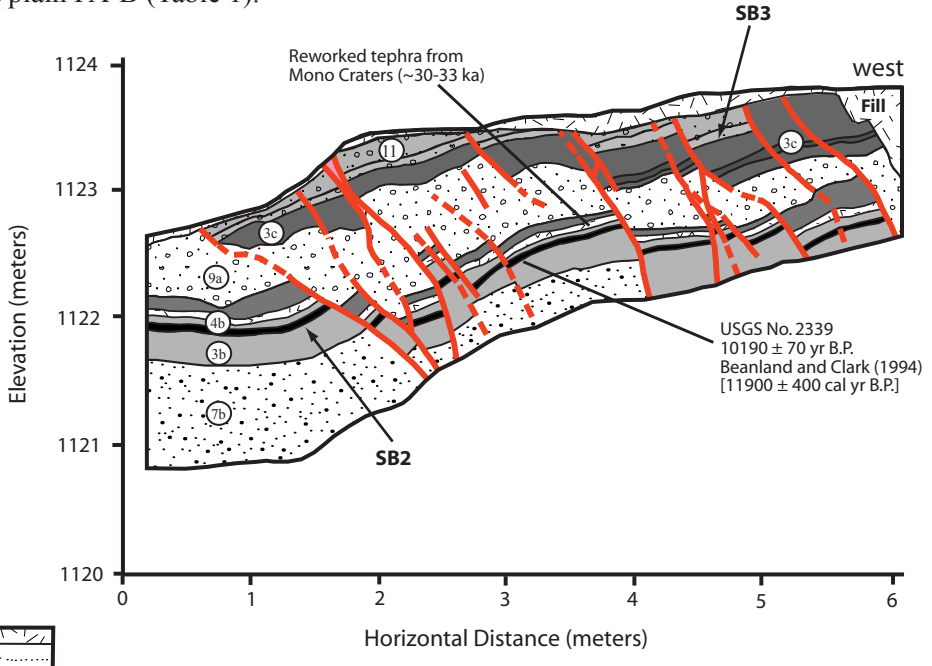

Figure 9. Trench log for the north wall of the Alabama Gates paleoseismic site T3. Log is transposed to reflect a south wall orientation. Lithofacies 3b, 7c, and 11 are within lacustrine FA-C. Lithofacies 4b is within delta plain FA-B and lithofacies 9a is within alluvium FA-B. Lithofacies numbers and facies associations are described in Table 1. Figure 21 is a stratigraphic column. The location of the radiocarbon age correlated to the sample site of Beanland and Clark (1994) is shown with a line. Lower contacts of lithofacies 4 and 11 define sequence boundaries SB2 and SB3, respectively. The location of the reworked Mono Crater tephra is shown with a line and discussed in Bacon, 2003.

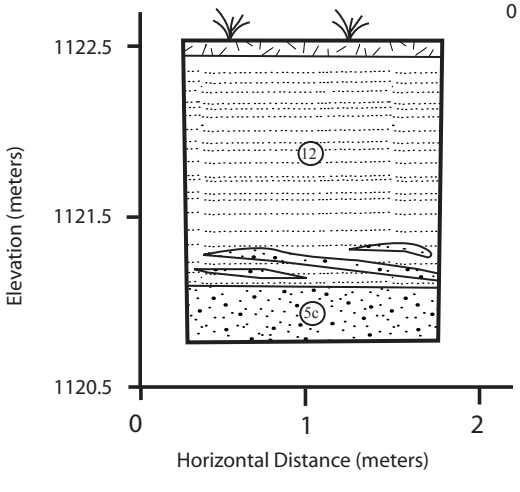

Figure 10. Log for the south wall of the Alabama Gates paleoseismic site P1. Lithofacies 5c and 12 are within delta plain FA-B. Lithofacies numbers and facies associations are described in Table 1 and mentioned in text. Figure 2 is a stratigraphic column.

TABLE 1. LITHOSTRATIGRAPHIC FACIES, DESCRIPTIONS, AND FACIES ASSOCIATIONS OF STRATIGRAPHY LOCATED AT PALEOSEISMIC SITES AND IN NATURAL EXPOSURES NEAR LONE PINE, EASTERN CALIFORNIA

Lithostratigraphic facies	Description	Facies association	Depositional environment
1a,b 	Clayey silt, massive, firm, plastic, green with minor interbeded of silty sand.	Lacustrine (FA-C)	offshore (deep water)
2a,b 	Alternating sand (fine to coarse), clayey silt, silty sand, moderately-sorted to well-sorted coarse sand, slightly hard to hard, convolute bedding, wavy and planar laminated; oxidation along bedding.	Delta front (FA-A)	distributary mouth bar
3a-d 	Sandy silt, massive, hard; contains localized vertical oxidation root casts.	Delta front (FA-A; 3a) Lacustrine (FA-C; 3b-d)	distal mouth bar nearshore
4a,b 	Alternating, thinly bedded (3-10 cm), light brown, silt; organic rich silt and charcoalized plant detritus; diatamecous silt; massive (15-250 cm), black peaty to organic rich silt and clay with woody debris.	Delta plain (FA-B)	marsh and mud flat
5a-c 	Alternating sand (fine to coarse), pebble (fine to coarse), gravel, (fine), poorly-sorted to moderately-sorted, subangular to well-rounded, loose to slightly hard; contains cross-bedding and localized foreset bedding.	Delta front (FA-A; 5a) Delta plain (FA-B; 5b,c)	distributary mouth bar distributary channel
6a,b 	Alternating sand (fine to coarse), pebble (fine to coarse), gravel, (fine), poorly-sorted to moderately-sorted, subangular to well-rounded, loose to slightly hard; contains cross-bedding and localized foreset bedding, and Alabama Hills derived lithology sand and gravel.	Delta front (FA-A; 6a) Delta plain (FA-B; 6b)	distributary mouth bar distributary channel
7a-e 	Alternating sand (fine to coarse) and silty sand, moderately-sorted to well-sorted, loose to slightly hard; contains cross-bedding, climbing ripple and planar lamination, and localized pebble and fine gravel; lithofacies 7e locally cemented by tufa.	Delta front (FA-A;7a) Lacustrine (FA-C; 7b-e)	distributary mouth bar shore
8 	Alternating sand (fine to coarse) and silty sand, moderately-sorted to well-sorted, loose to slightly hard; contains cross-bedding, and climbing ripple and planar lamination; localized pebble and fine gravel. Alabama Hills derived lithology sediment.	Delta front (FA-A) Lacustrine (FA-C)	distributary mouth bar shore
9a-c 	Pebbly, silty, sand, massive, poorly-sorted, slightly hard to hard; contains Alabama Hills lithology sand and pebble.	Alluvium (FA-B)	alluvial fan colluvial apron
10a-c 	Sand (fine to medium), well-sorted, well-rounded, loose; contains foreset-bedding.	Eolian (FA-B)	sand dune
11 	Silty sand to sandy silt, massive, slightly hard to hard; contains 10-15% angular pebbles (fine to medium) derived from the Alabama Hills.	Lacustrine (FA-C)	nearshore
12 	Alternating sand (fine) and silt, moderately- to well-sorted, moderately rounded, loose to soft.	Delta plain (FA-B)	meandering stream
13a,b 	Sand (fine to medium), massive, well-sorted, well-rounded, slightly hard; locally contains platy sheets of tufa along upper boundary; lithofacies initially deposited as eolian dunes and subsequently submerged by lacustrine environment; lithofacies 13b is locally reworked.	Lacustrine (FA-C)	shore to nearshore
14a-c 	Sand (fine to medium), massive, well-sorted, well-rounded, slightly hard; contains subrounded to angular pebble and fine gravel size tufa fragments.	Lacustrine (FA-C)	shore (regressive facies)
15 	Alternating sand (fine to coarse), moderately-sorted to well-sorted, loose to slightly hard; contains cross-bedding, and climbing ripple and planar lamination; localized pebble and fine gravel that grades into massive, hard, sandy silt; contains subrounded to angular pebble and fine gravel size tufa fragments.	Lacustrine (FA-C)	shore to nearshore
16 	Silt (fine to coarse), massive, well-sorted, soft to slightly hard.	Eolian (FA-B)	loess

Age estimates at the Alabama Gates paleoseismic site

Age estimates for the sediment exposed in trenches at the Alabama Gates paleoseismic site are from two AMS ages on charcoal and bulk organic sediment recovered from T2, and one radiometric age on charcoal by Beanland and Clark (1994) that is correlated to sediment in T3 (Figs. 8 and 9). In addition to the radiocarbon ages, a reworked tephra within a thin diatomaceous bed of lithofacies 4b is exposed in T3 (Fig. 9). The two AMS radiocarbon samples from T2 were recovered during this study. The radiometric age for T3 is correlated from the location of where it was sampled along the roadcut of U.S. Highway 395 during the investigation of Beanland and Clark (1994) (S. Pezzopane, personal comm., 1999). The sample locality is at the location where T3 was excavated. As a result, correlation of the sample is considered to have a high degree of confidence. The sample recovered by Beanland and Clark (1994) has a radiometric ^{14}C age of 10,190 ± 70 ka. [11,560 to 12,350 cal. yr B.P.]. Two AMS radiocarbon samples of charcoal and bulk organic sediment were recovered from the silty peat deposit in the bottom eastern part of T2 (lithofacies 4b; Fig. 8). The AMS ^{14}C age on the charcoal is 10,160 ± 20 cal. yr B.P. (Table 2). The AMS age on the bulk organic sediment is 10,250 ± 20 cal. yr B.P. (Table 2). The two samples were located less than 10 cm from each other in the trench and have essentially the same ^{14}C age within error.

The interbedded tephra in T3 was identified after applying the tephrochronologic methods as described in Sarna-Wojcicki (2000) by A. Sarna-Wojcicki. The tephra is a heterogeneous mixture of old glass shards that are derived from the 0.76 Ma Bishop and/or the some what older Glass Mountain ash beds from the Long Valley Caldera along with glass shards that are as young as the Wilson Creek ash beds from Mono Craters (A. Sarna-Wojcicki, written comm., 2002) (Table 3 in Bacon, 2003). Chemically, the younger glass shards best match Wilson Creek ash beds numbers 8-15. Wilson Creek ash beds numbers 8-15 have a correlative age of 28.0-25.3 ^{14}C ka [33.2-30.0 cal. ka after Bard et al., 1993] (A. Sarna-Wojcicki, written comm., 2002). Tephra exposed in T3 is reworked, based on the occurrence of a heterogeneous mixture of glass shards. In addition, the maximum age of the deposit that contains the reworked tephra is ca. 12 cal. ka, because it is stratigraphically underlain by the organic silt horizon dated by Beanland and Clark (1994) (Fig. 9) and has a minimum age of ca. 10 cal. ka based on the age of lithofacies 4b from T2. Therefore, the reworked tephra was deposited between ca. 12-10 cal. ka. A schematic composite stratigraphic column for sediments exposed at the Alabama Gates paleoseismic site is presented as Figure 21.

Quaker Paleoseismic Site

Four exploratory fault trenches (T4-T7) and three deep exploratory pits (P2-P4) were excavated in March of 2001 and June of 2002 at a site informally known as "Quaker paleoseismic site" (Figs. 3 and 11). The Quaker paleoseismic site is on the Diaz Lake section of the OVFZ (Figure 3) and is equivalent to Site 12 of Beanland and Clark (1994). The Quaker site is located ca. 3.0 km south of the Alabama Gates site, 4.0 km north of Lone Pine, and ca. 200 meters west of U.S. Highway 395 (Figs. 3 and 11). The four trenches and three pits cross the OVF at elevations between 1115-1124 m, which is similar in elevation and age to the stratigraphy exposed in the trenches at the Alabama Gates site (T2-T3 and P1). As a result, the stratigraphy and paleoseismic relations exposed at both paleoseismic sites are correlatable with a high degree of confidence.

Geomorphology at the Quaker paleoseismic site

The trend of the OVF at the Quaker paleoseismic site is expressed as a prominent east facing geomorphic scarp. The trace of the 1872 rupture trends along the top or at the base of the scarp. Scarp heights range between 1 and 4 m, having slopes of 13-25° (Beanland and Clark, 1994). Runoff originating from the scarp and from the Alabama Hills has produced many small channels that are incised into and across the geomorphic scarp and the ~1 m 1872 fault scarp (Fig. 11). There is no unequivocal evidence at the surface to indicate that any of the many small channels were horizontally displaced by the 1872 earthquake or to paleoearthquakes at the Quaker site.

The Quaker site is 20-30 m below the sill elevation of Owens Lake basin. The only deposits associated with the sill elevation that are near the site are ca. 21 ka tufa-cemented beach gravel at an elevation near 1155 m (Lubetkin and Clark, 1988) (Fig. 12). The lower elevations and geomorphic relations observed at the surface of the Quaker site, in addition to observations at the Alabama Hills site, indicate that the older OVF scarps were modified by fluctuating shorelines and associated fluvial-lacustrine burial or erosion. The erosional processes enhanced,

obscured, or removed evidence of pre-1872 scarps, as well as older latest Pleistocene(?) shorelines. Furthermore, Bryant (1988) recognized the occurrence of eroded fault scarps at the Quaker site (Site 12). The Owens River has generated prominent tread and riser morphology that formed into the geomorphic scarp. A remnant landform interpreted to be a shoreline feature (beach berm) is preserved adjacent to the scarp. The berm is deformed only by the 1872 earthquake, with the trace of the rupture located ca. 12 m east of the scarp near T4 (Figs. 20 and 21). Since construction of the beach berm, the Owens River eroded into the eastern portion of the berm and into areas located to the north and south, defining the western boundary of the Owens River meander belt (Figs. 11 and 12).

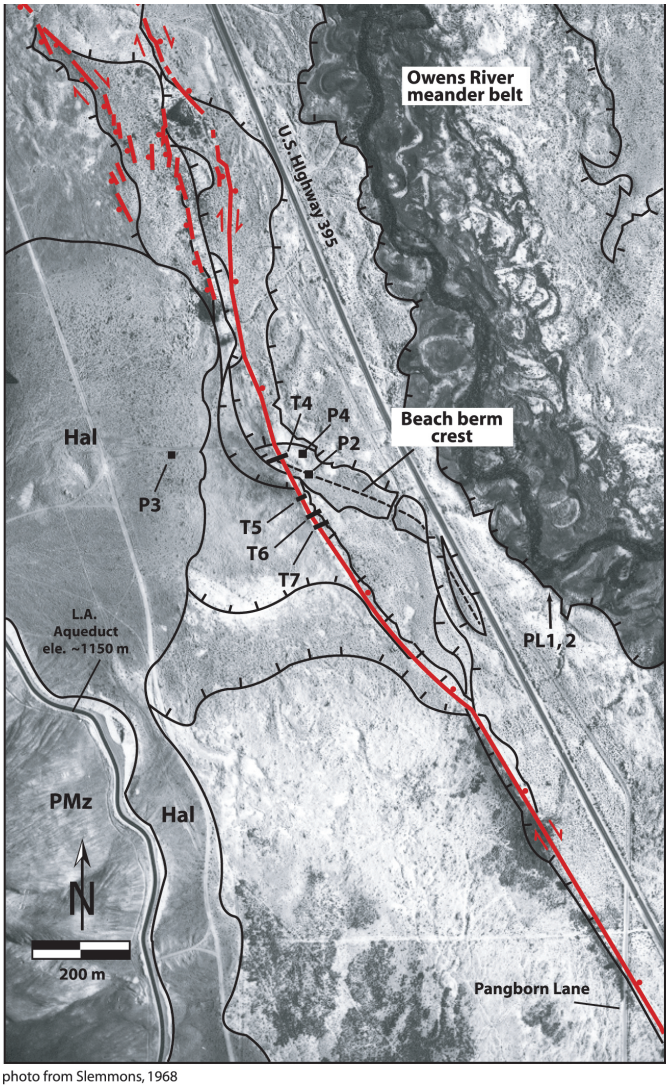

photo from Slemmons, 1968

Figure 11. Black and white low-sun-angle aerial photograph of the Quaker paleoseismic site (ele. 1116-1125 m). Exploritory fault trenches (T4-T7) and pits (P2, P3, and P4) are shown in relation to the 1872 Owens Valley fault trace (shown in red), the Alabama Hills (PMz), Holocene alluvium derived from the Alabama Hills (Hal), and prominent tread and risers (hachures). Shoreline and fluvial processes produced the tread and riser morphology. The 1872 Owens Valley fault scarp is located along a 1 to 4 m geomorphic scarp that contains shoreline and fluvial erosional and constructional features. Figure 12 is the geologic and geomorphic map of the site.

Scarp profiles

Five profiles were surveyed perpendicular to the local trend of the scarp with many survey lines diverging in orientation to survey other geomorphic features of interest (Fig. 12). The profiles provide evidence that the trace of the Owens Valley fault is located along a scarp that is interpreted to contain tread surfaces, wave-cut notches, meander risers and a constructional landform (beach berm) that all formed prior to the 1872 earthquake (Bacon, 2003). Profile 2 of the 5 profiles is presented to show the geomorphic scarp and beach berm (Fig. 13).

The highest identified geomorphic feature at the Quaker site is a tread surface at elevation >1123.5 m attributed to a higher lake-level. Below 1123.5 m are two flights of tread surfaces and associated risers. The risers are evident in aerial photographs as arcuate risers and different tread surface morphologies (Figs. 11 and 12). The higher tread surface is at an elevation between 1122 and 1123 m. The lower tread surface is located at an elevation of 1121 m. In addition to the tread and riser morphology, there are wave-cut notches at an elevation of 1118-1119.5 m (Fig. 13). The shoreline that formed the wave-cut notch also constructed the berm east of the geomorphic scarp, having a berm crest elevation that ranges between 1118.5 and 1119 m (Fig. 13). Meander risers that formed after the construction of the berm are below 1116.5 m and define the western boundary of the Owens River meander belt (Fig. 13). The meander belt eroded most of the berm north and south of Profiles 1 and 5, with a relatively small preserved remnant ca. 240 m north of Profile 1 (Figs. 11 and 12).

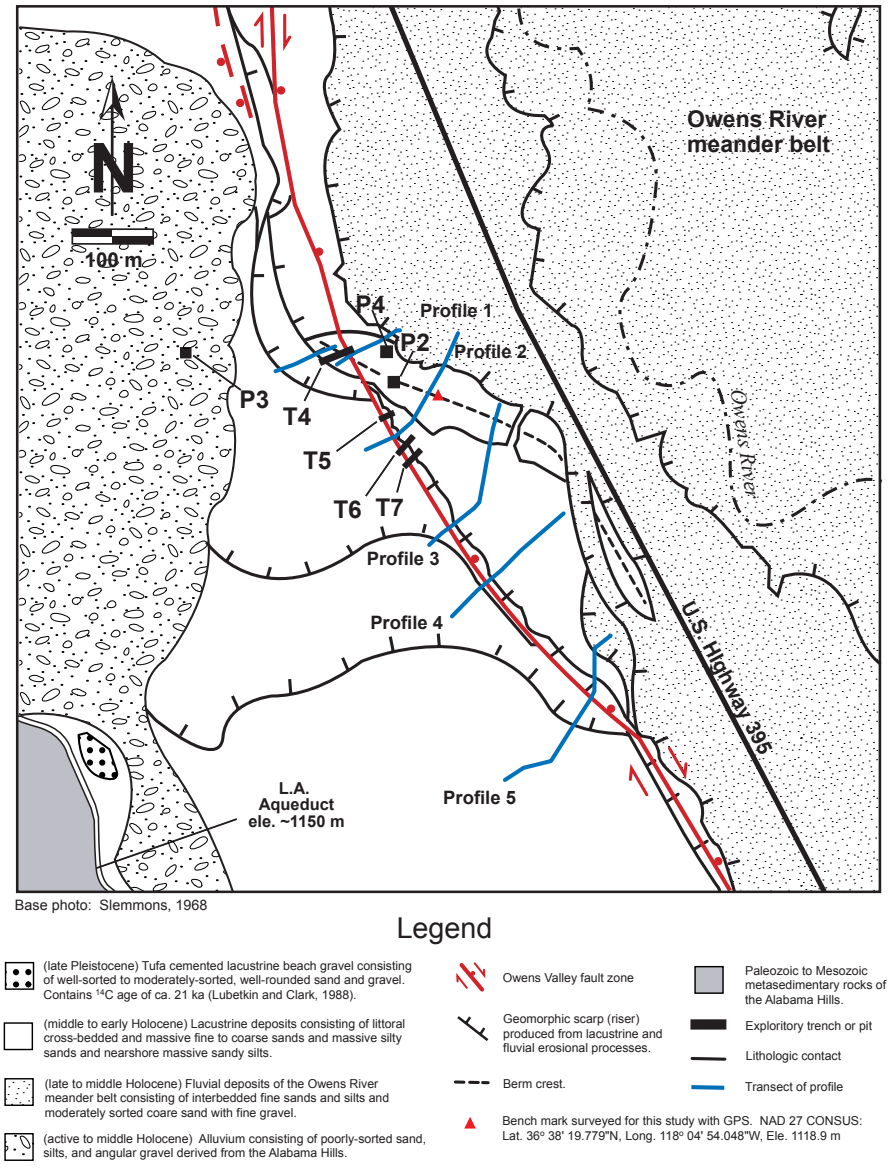

Figure 12. Geologic and geomorphic map of the Quaker paleoseismic site showing the location of trenches (T4-T7) and exploritory pits (P2-P4) excavated across and adjacent to the 1872 Owens Valley fault rupture. Transects of Profiles 1-5 are oriented across a geomorphic scarp that has been modified by shoreline and fluvial erosional processes in Bacon, 2003.

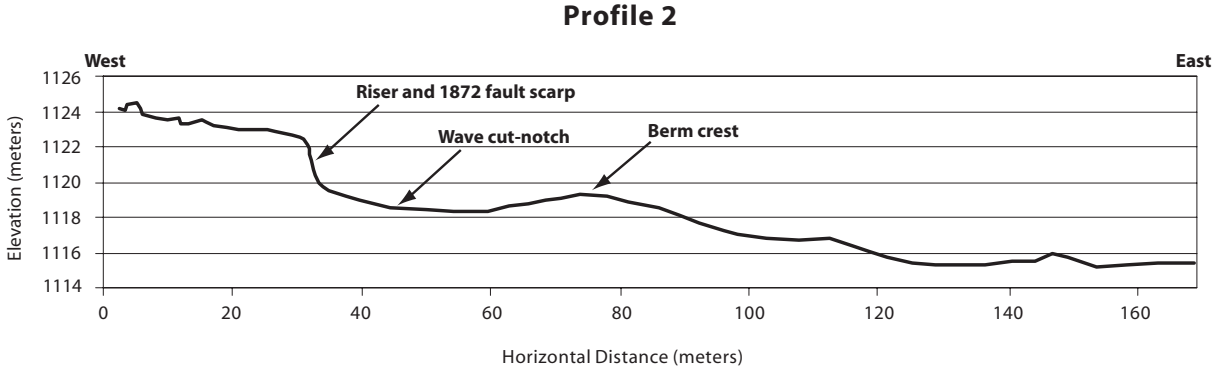

Figure 13. Scarp profile 2 at the Quaker paleoseismic site located between trenches T5 and T6 (3.5x vertical exaggeration). Profile 2 was surveyed perpendicular to the local trend of scarp. The trend of the survey is shown in Figure 12. The geomorphic scarp has been modified by fluvio-deltaic and shoreline erosional processes. The ~1 m single-event scarp related to the 1872 rupture is located along a geomorphic scarp (riser).

Quaker Trench Investigation

The four fault trenches (T4-T7) excavated across the trace of the OVF are 13-33 m in length and 2-4 m in depth, with exploratory pits (P2-P4) having depths of 3-4 m (Figs. 14-20). Trench T5 contains the best example of the stratigraphy and structure at the Quaker site. Trenches expose stratigraphy consistent with lithofacies that are attributed to at least four transgressive and regressive lake-cycles punctuated by erosion and deposition from a fluvio-deltaic system. Stratigraphy is primarily composed of latest Pleistocene lacustrine deep water sediment overlain by early Holocene marsh and/or mud flat sediments that are in turn overlain by early to middle Holocene lacustrine shore to nearshore sediment in the footwall. The sediments are juxtaposed against a sequence of latest Pleistocene lacustrine deep water sediment overlain by marsh and/or mud flat and fluvio-deltaic sediment, which is in turn overlain by early to middle Holocene interbedded lacustrine shore to nearshore and eolian sediments in the footwall. There are as many as five sequence boundaries (SBs) that are correlatable between the trench and pit exposures. One SB truncates fault strands, sand dikes, and liquefaction features attributed to a paleoearthquake. All four trenches expose structures related to the 1872 earthquake, whereas two trenches (T4 and T5) contain structural and stratigraphic evidence for the penultimate event.

Trench stratigraphy

Quaker lithofacies and facies associations

The sequence stratigraphy exposed at the Quaker site contains lithofacies that are laterally continuous and correlatable between the trenches and pits (T4-T7 and P2-P4; Figs. 14-20). In addition, the lithofacies and facies associations used to describe the units in the trenches are also common to the Alabama Gates paleoseismic site, which are collectively shown in Table 1. Because of the large horizontal component of displacement generated on the OVF, only five lithofacies units are exposed in the trenches that correlate across the fault zone, but most of the lithofacies are time stratigraphic equivalent. As a result, the lithofacies descriptions are grouped into footwall and hanging-wall stratigraphic sections.

Footwall Stratigraphy

The oldest sediment observed in the footwall and exposed at the base of the trenches is a firm, plastic, green clayey silt that is exposed in T5 and P3 and is grouped into lithofacies 1b (Figs. 15 and 19; Table 1). The depositional environment of lithofacies 1b is interpreted to be offshore lacustrine FA-C related to sedimentation in a relatively deep water column (Table 1). Lithofacies 1b has a clear to gradual upper contact with an organic rich brown and firm clayey silt that contains 5% disseminated charcoal and detrital charcoal that range between 1-3 mm in length. The organic rich deposit is exposed in T4-T7 and P3-P4 (Figs. 14-17 and 19-20). It is 0.25-1.25 m thick and mapped into lithofacies 4b and forms SB1. Lithofacies 4b is interpreted to represent a terrestrial depositional environment, specifically a marsh and/or mud flat of the delta plain FA-B (Table 1). Lithofacies 4b is overlain by a massive, silty, fine sand that has grains which are well-rounded, well-sorted, and is slightly hard. The lower contact of the massive deposit with lithofacies 4b is abrupt. This deposit is mapped as lithofacies 13a and interpreted to represent a transition between nearshore and shore depositional environments of lacustrine FA-C (Figs. 15, 16, and 19; Table 1). Lithofacies 13a has sedimentologic characteristics that are similar to eolian deposits that contain no sedimentary structures. It is plausible that lithofacies 13a was originally deposited by eolian processes that accumulated above lithofacies 4b within the delta plain and then was subsequently reworked by nearshore to shore lacustrine processes during a transgression in lake-level.

Lithofacies 13a has a clear upper boundary with a 5-20 cm thick very hard sandy tufa sheet that marks the boundary between the two deposits in T5 and T6, which defines SB2 (Figs. 15 and 16). The sandy tufa sheet is also exposed in natural channels and along the 1872 fault scarp between T4 and T7 as discontinuous broken plates. The sandy tufa sheet grades into poorly-sorted, well-rounded to subangular pebble and fine gravel sized tufa fragments supported by a slightly hard to hard, massive, well-sorted silty fine sand. This tufa rich deposit is mapped into lithofacies 14a and is interpreted to be the result of subaqueous precipitation of $CaCo_3$ on a sandy substrate in a nearshore to shore depositional environment in the form of a tufa sheet (Figs. 15, 16, and 19; Table 1). The tufa precipitated from a time of a relatively stable water column that was deep enough to form and preserve the tufa sheet prior to sedimentation during fluctuating lake-levels, lacustrine FA-C (Table 1). Evidence to suggest sedimentation during fluctuating lake-levels is the presence of well rounded to subangular pebble and fine gravel sized tufa fragments that are derived from the 5 to 20 cm thick tufa sheet. Changes in wave base related to fluctuating lake-levels eroded and reworked the existing tufa sheet into angular to subangular pebble

and gravel sized clasts. These relations are similar to what is observed in the Pyramid Lake basin by Benson (1994), with the presence of isolated patches of tufa that formed on flat-lying unconsolidated lake sediments. In addition, Mono Lake, ca. 200 km to the north of this study, contains lacustrine shore sediment consisting of subangular pebble and gravel tufa fragments along the margin of the lake. The sediment exposed along the shoreline of Mono Lake appears to have been deposited when recessional lake-level fluctuations reworked existing *in situ* tufa during LADWP water diversions (S. Bacon, pers. obs., 1996-2001).

Other cemented sediment exposed at the Quaker site is exposed in T4 and P4, which consists of well rounded, well sorted, medium sand to fine gravel that is cemented with $CaCo_3$ interpreted as tufa. This deposit is very hard and contains prominent cross-bedding and foreset (lakeward dipping), sedimentary structures that are common in barrier ridges or berms (Adams and Wesnousky, 1998). The tufa rich deposit is mapped in lithofacies 7e, lacustrine FA-C and is interpreted to represent sediment deposited at a beach (shore) adjacent to and into an existing scarp (Figs. 14 and 20; Table 1). Lithofacies 7e contains lithologically heterogeneous sediment derived from up valley source areas that consist of scoria, basalt, tuff, and pumice. Lithofacies 7e has an erosional lower contact with lithofacies 2b, 4b and 13a that defines SB5 and has an upper surface that reflects the original surface morphology near T4. The strata exposed in the upper sections of T4 and P4 is within the berm mapped in Figures 11 and 12 that is truncated to the west by the scarp (Profile 1; Fig. 12). T4 shows an erosional contact and interfingering relation between the berm and older sediments that comprise the scarp in the western portion of the trench (Fig. 14). The erosional contact consists of many discontinuous lenses and rotated blocks of older sediment that are composed of fine sand, faintly bedded silty sand, fine sand with tufa fragments, and organic clayey silt that are grouped into lithofacies 13b (Table 1). Lithofacies 13b interfingers with lithofacies 7e, therefore they are time-stratigraphic equivalents.

Overlying the strata of the footwall block is a 0.3-0.5 m thick massive well-sorted coarse silt. This silt unit is exposed in all trenches and is mapped as lithofacies 16 (Figs. 14-17). Lithofacies 16 is interpreted as a loess sheet, eolian FA-B (Table 1). In addition, a poorly-sorted and slightly hard, pebbly, silty, sand deposit that contains lithologies derived from the Alabama Hills is located on slopes that are nearly flat. This deposit is mapped into lithofacies 9b in P3 and 9c in T4 (Figs. 14 and 19). Lithofacies 9b is interpreted to be mudflow depositon from the Alabama Hills and 9c is from a colluvial apron, derived locally from the scarp and sand dunes (alluvium FA-B; Table 1).

Hanging-wall Stratigraphy

Sediment exposed in the hanging-wall at the Quaker paleoseismic site is generally coarser grained, well stratified, and has more sequence boundaries compared to stratigraphy exposed in the footwall. The oldest sediment at the Quaker site exposed in the hanging-wall is in P4 (Fig. 20). At the base of the trench is a 0.25-0.4 m thick clayey silt that contains well preserved charcoalized woody twigs that are 1-8 cm in length and 0.5-2.0 cm in diameter. This organic rich deposit is mapped as lithofacies 4a and defines SB0. Lithofacies 4a represents terrestrial deposition in a marsh or mud flat (FA-B). Lithofacies 4a is overlain by interbedded clayey silts (lithofacies 1b) and alternating sequences of sands and silts (lithofacies 2a) that reflect fluctuating lake-levels, with the deposition of both lacustrine and deltaic facies associations (Table 1). Lithofacies 1b is also exposed in T4, T5, and P2-P4 (Figs. 14, 15, and 18-20; Table 1). Lithofacies 2b is exposed only in T4, T5, and P4 (Figs. 14, 15, and 20). Lithofacies 2b has an erosional contact with lithofacies 7e in T4 (SB5) and erosional contact with lithofacies 7d in T5 (SB1) (Figs 14 and 20; Table 1). In addition, P2 exposes a contact between lithofacies 7d and 7e that represents SB5 (Fig. 18). Lithofacies 4b has been completely or partially eroded in the areas of T5 and P2 and the western half of T4 (SB1). Lithofacies 2b is exposed in T5 and preserved within the graben in T4. Lithofacies 2b represents an upward-fining sequence of soft, moderately sorted, medium to coarse sand with faint and discontinuous wavy and planar laminations that grade into interbedded to structureless, loose, well-sorted fine sand and silt to a slightly hard, massive silt (Fig. 15). The interbedded fine sand and silt exhibit prominent soft sediment deformation structures and thin 0.2-0.4 cm thick sand dikes. The entire deposit is interpreted as fluvio-deltaic sedimentation in delta front FA-A, and specifically at a distributary mouth bar (Table 1). Lithofacies 2b has lower and upper contacts that are abrupt. The upper contact forms SB2 that truncates zones of soft sediment deformation and sand dikes (Fig. 15).

Sequence boundary SB2 is overlain by alternating 10-30 cm thick fine to coarse sand with climbing ripples, planar laminations, and cross-bedding that are mapped as lithofacies 7d in T5 (Fig. 15). Lithofacies 7d is also present in T6, T7, and P2 (Figs. 16-18). Lithofacies 7d is interpreted to represent deposition in a lacustrine (FA-C), shore depositional environment (Table 1). The relation of SB2 with lithofacies 7d suggests that SB2 defines an abrasion platform, which is similar to the abrasion platform observed at the Alabama Gates site, discussed earlier in text (T2; Fig. 8). Along the surface of the abrasion platform and at the base of lithofacies 7d are 0.5-1.5 cm thick and 2-4 cm long hard to very hard subangular cemented fine sand fragments interpreted as platy tufa exposed only in T5 (Fig. 15). Overlying lithofacies 7d is a 0.4 m thick massive sandy silt mapped as lithofacies 3d. Lithofacies 3d conformably overlies lithofacies 7d in T5 and is correlated to an eroded block situated within a matrix of lithofacies 7d in T6 (Figs. 15 and 16). Lithofacies 3d is interpreted to represent sedimentation in a nearshore depositional environment, lacustrine FA-C (Table 1). Exposed in T5, lithofacies 3d and 7d forms an angular unconformity. Both lithofacies 3d and 7d are overlain by lithofacies 10b above this contact (Fig. 15). Lithofacies 10b is 0.4-1.5 m thick and consists of well-rounded and well-sorted fine to medium sand that displays prominent foreset sedimentary structures. The upper half of the deposit contains ~30% well-rounded pebble sized pumice clasts that are correlated to the 0.76 Ma Bishop and/or Glass Mountain ash (A. Sarna-Wojcicki, written comm., 2002), in addition to 1.0-3.0 cm thick and up to 10.0 cm wide discontinuous *in situ* tufa cemented sand fragments, and pumice along foreset bedding planes that are hard to very hard. Lithofacies 10b has sedimentary characteristics similar to eolian dune sands and is placed in eolian FA-B (Table 1). The angular unconformable contact of lithofacies 10b with lithofacies 3d and 7d defines SB3 (Fig. 15).

The upper boundary of lithofacies 10b is an unconformable contact with a 0.4-2.2 m thick massive sandy silt deposit that has sedimentologic characteristics similar to lithofacies 3d mentioned earlier. This massive sandy silt has a subtle upward-fining characteristic and is mapped into lithofacies 3d, lacustrine FA-C (Table 1). Lithofacies 3d is exposed in T5-T7 (Figs. 15-17). Exposed in the southern most trench (T7) and within sediments that resemble both lithofacies 3d and 7d are well-rounded to subangular tufa fragments that are similar to the tufa fragments within lithofacies 14a. The 0.75 m thick tufa fragment-rich fine and coarse grain sediments in the hanging-wall are mapped into lithofacies 15 (Fig. 17). The coarser facies of lithofacies 15 depositional environment is the same as lithofacies 7d, whereas the finer facies of lithofacies 15 is similar to lithofacies 3d, shore to nearshore facies, respectively (Table 1).

The presence of the tufa fragments is likely related to fluctuating lake-levels that laterally transported the tufa fragments to the east in the area of T7, incorporating the fragments into different lithofacies. These relations are similar to what is exposed in T5 (Fig. 15) with the platy tufa fragments observed above SB2 within lithofacies 7d. The tufa fragments grade upward to massive sandy silts, interpreted to represent nearshore sedimentation (Fig. 17). The relatively thick sandy silt deposit of lithofacies 3d is overlain by lithofacies 14b. The contact between lithofacies 3d and 14b is conformable, indicating a depositional boundary that is only observed in T5 (Fig. 15). The sequence of lithofacies 3d overlain by lithofacies 14b suggests that lithofacies 14b was deposited during an overall regressive but fluctuating lake-level. The stratigraphic position between the two lithofacies defines SB4 (Fig. 15).

Capping the entire package of strata in the hanging wall is sediment deposited in a terrestrial environment. Lithofacies 16 (loess sheet) correlates across the fault and is exposed only in T5 (Fig. 15; Table 1). In addition, lithofacies 9c (colluvium) and lithofacies 10c (eolian sand dune) are exposed in T4 and T7 (Figs. 14 and 17).

Age estimates at the Quaker paleoseismic site

Age estimates for the sediment exposed in trenches and pits at the Quaker paleoseismic site are from six AMS ^{14}C ages on charcoal and bulk organic material and one radiometric age on bulk organic sediment recovered from T4 and P4 (Figs. 14 and 20). In addition to the radiocarbon ages on charcoal and organic sediment, three radiometric ages are from tufa recovered from T4, T5, and P4 (Figs. 14, 15, and 20). The oldest sediment at the Quaker site is determined from three AMS ^{14}C radiocarbon samples of charcoalized twigs from lithofacies 4a in P4 (Fig. 20). The AMS ^{14}C ages of selected twigs are 12,580 ± 60, 12,590 ± 60, and 12,730 ± 60 yr B.P. [14,970 ± 690 cal. yr B.P] (Table 2). Three AMS radiocarbon samples and one radiometric sample were selected from lithofacies 4b in the eastern part of T4 (Fig. 14). The AMS ^{14}C age on the bulk organic sediment is 9,160 ± 50 yr B.P. [10,330 ± 110 cal. yr B.P.] (Table 2). The radiometric ^{14}C age on the bulk organic sediment is 9,680 ± 50 yr B.P. [11,130 ± 70 cal. yr B.P.] (Table 2). The AMS ^{14}C age on the charcoal is 9,920 ± 50 yr B.P. [11,280 ± 70 cal. yr B.P.] (Table 2).

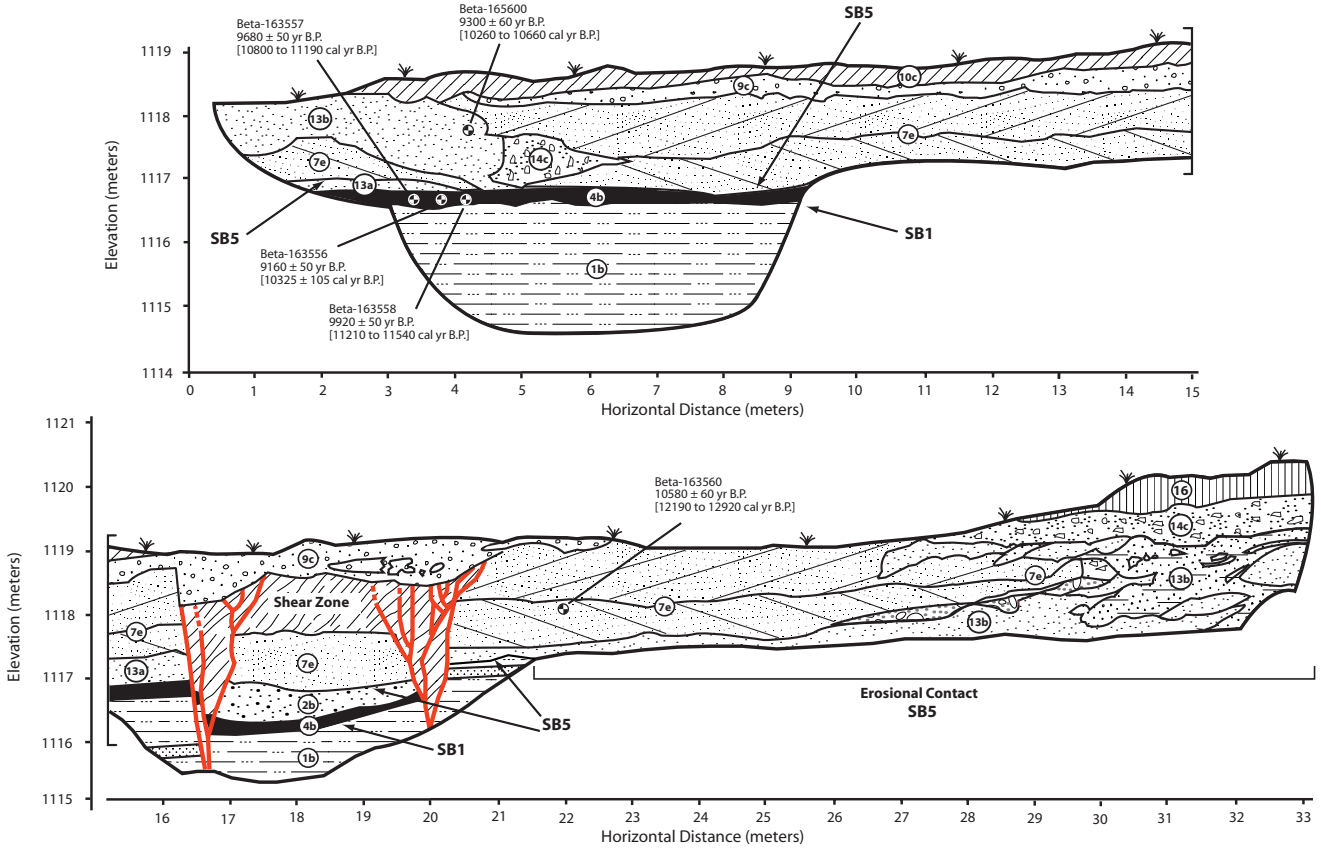

Figure 14. Trench log for the south wall of the Quaker paleoseismic site T4. Lithofacies 1b, 7e, 13b, and 14c are within lacustrine FA-C. Lithofacies 2b is within delta front FA-A. Lithofacies 4b is within delta plain FA-B, lithofacies 9c is within alluvium FA-B, and lithofacies 10c and 16 are wihtin eolian FA-B. Lithofacies numbers and facies associations are mentioned in text and described in Table 1. Figure 21 is a stratigraphic column. The location of four radiocarbon samples are shown with a line and circle and listed in Table 2. Lower contacts of lithofacies 4b and 7e define sequence boundaries SB1 and SB5, respectively. The erosional contact of 7e into lithofacies 2b, 4b, 13b, Reworked 13, and 14c also define sequence boundary SB5.

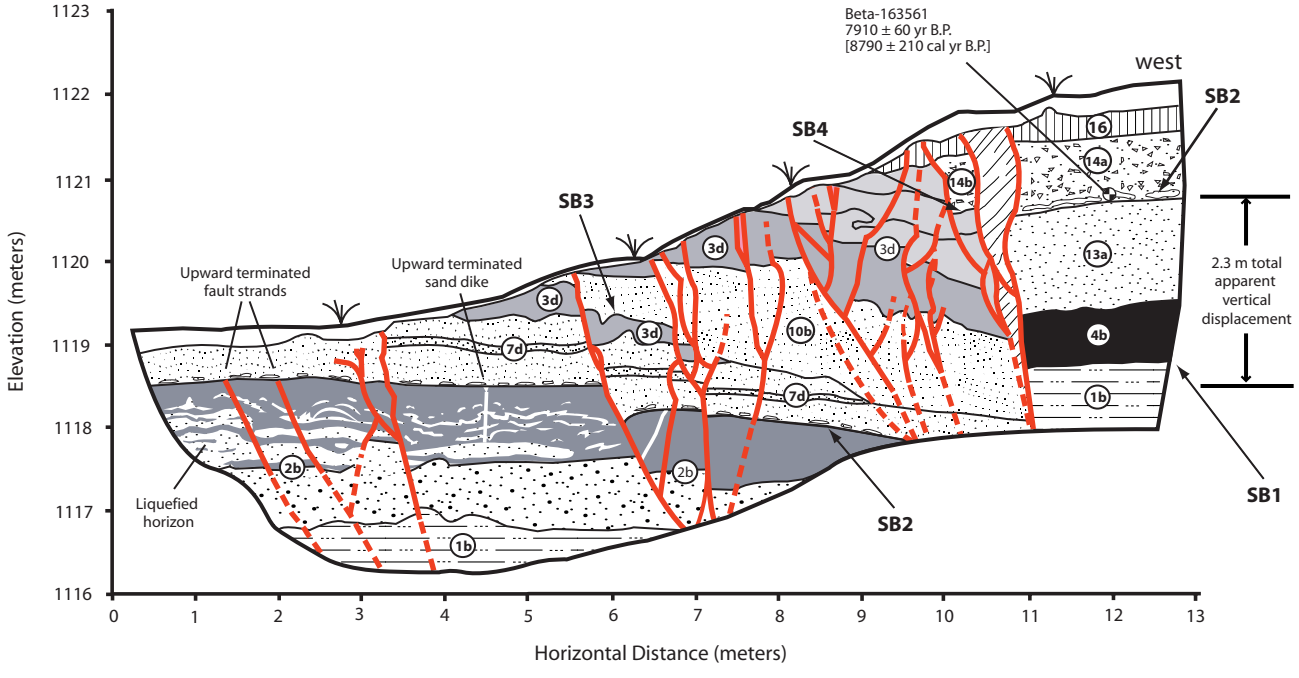

Figure 15. Trench log for the south wall of the Quaker paleoseismic site T5. Lithofacies 2b is within delta front FA-A. Lithofacies 4b is within delta plain FA-B and lithofacies 10b and 16 are within eolian FA-B. Lithofacies 1b, 3d, 7d, 13a, and 14a,b are within lacustrine FA-C. Lithofacies numbers and facies associations are mentioned in text and described in Table 1. Figure 21 is a stratigraphic column. The location of one radiocarbon sample is shown with a line and circle and listed Table 2. The abrasion platform formed into lithofacies 2b and 13a defines sequence boundary SB2. Lower contacts of lithofacies 4b, 10b, and 14b define sequence boundaries SB1, SB3, and SB4, respectively.

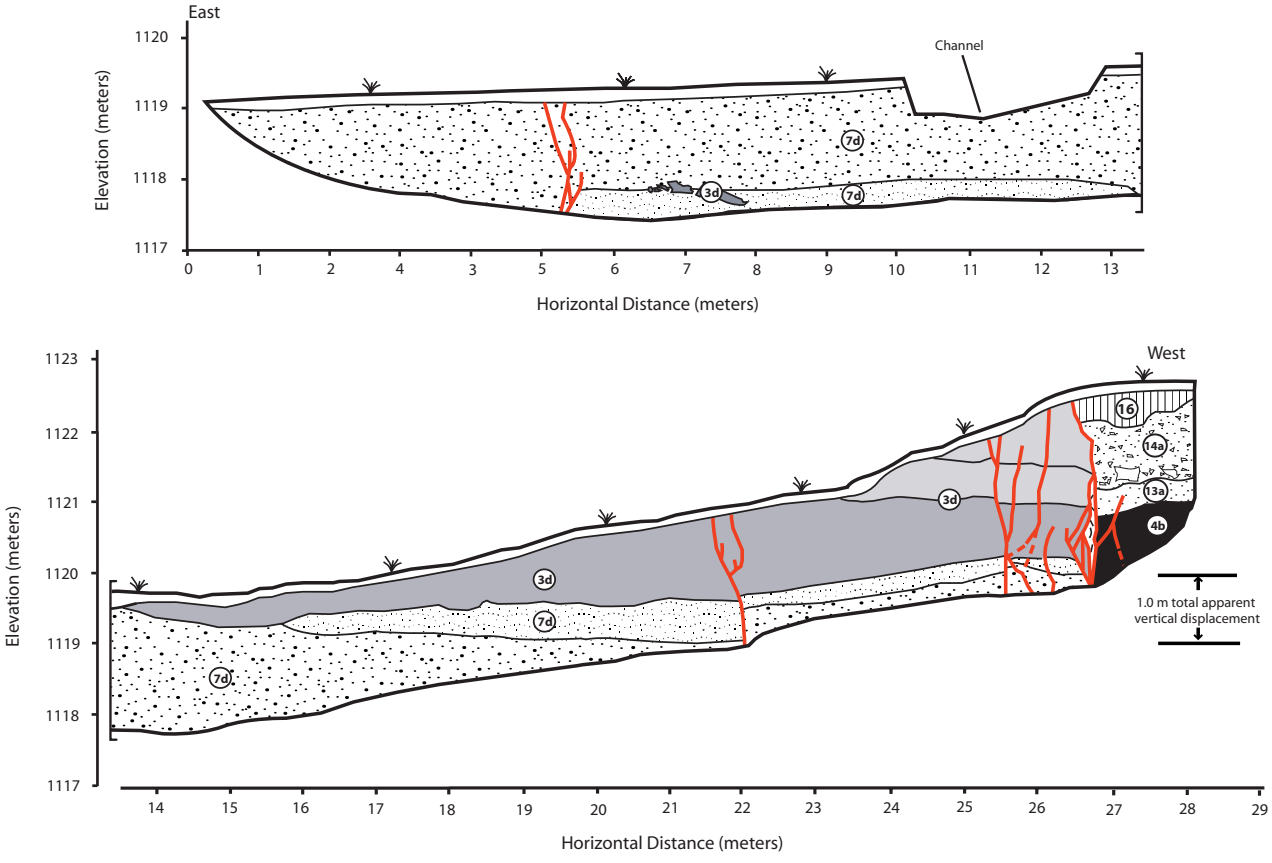

Figure 16. Trench log for the south wall of the Quaker paleoseismic site T6. Lithofacies 4b is within delta plain FA-B. Lithofacies 3d, 7d, 13a, and 14a are within lacustrine FA-C. Lithofacies 16 is within eolian FA-B. Lithofacies numbers and facies associations are mentioned in text and described in Table 1. Figure 21 is a stratigraphic column.

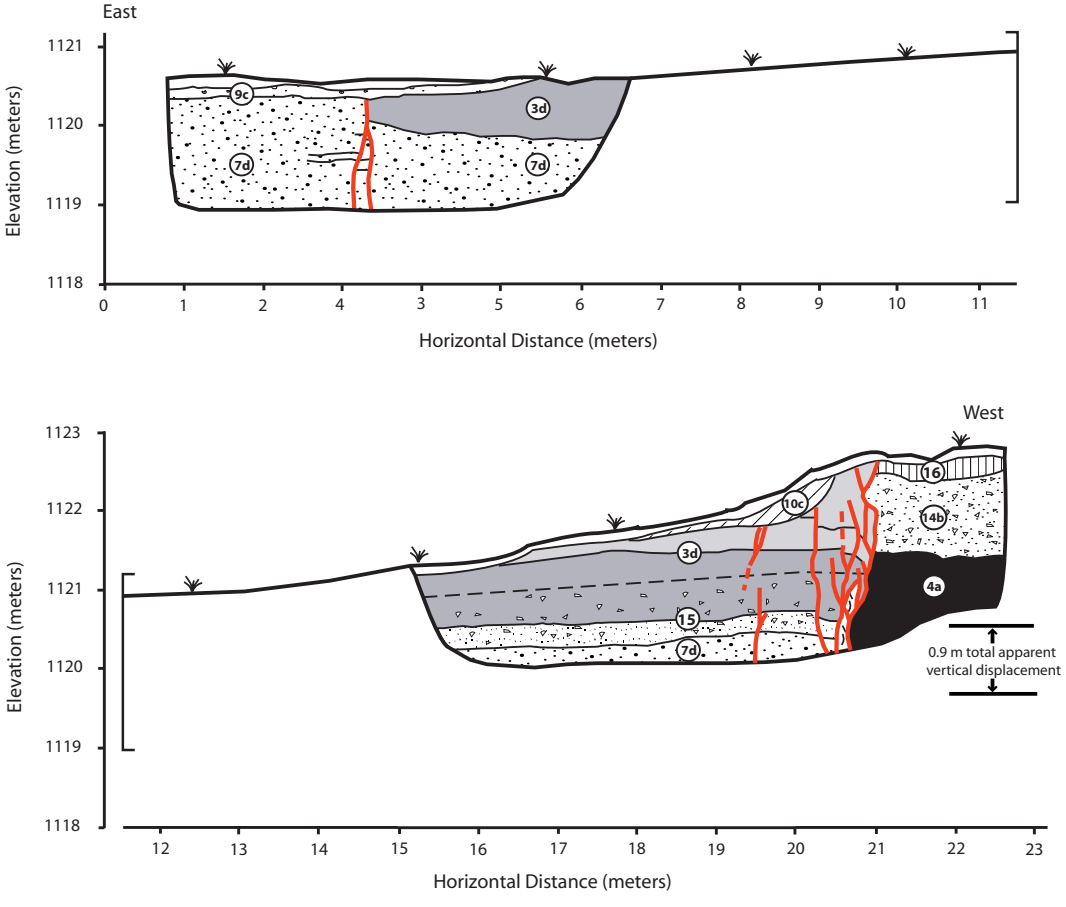

Figure 17. Trench log for the south wall of the Quaker paleoseismic site T7. Lithofacies 4b and 9c are within delta plain FA-B. Lithofacies 3b, 7d, 14b, and 15 are within lacustrine FA-C. Lithofacies 10c and 16 are within eolian FA-B. Lithofacies numbers and facies associations are mentioned in text and described in Table 1. Figure 21 is a stratigraphic column.

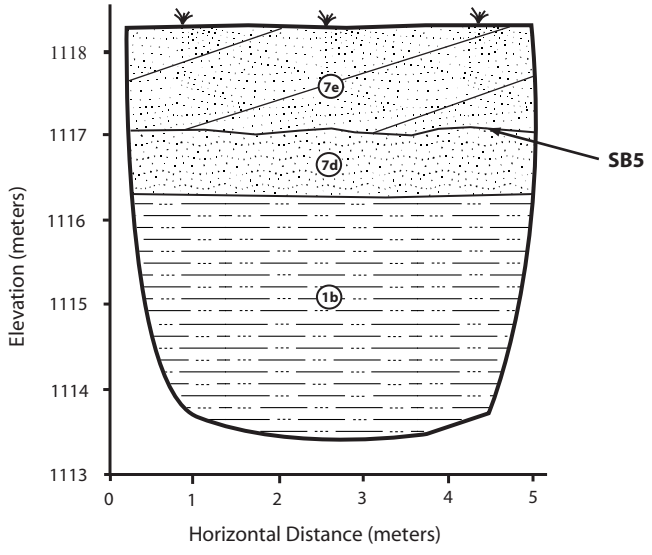

Figure 18. Trench log for the north wall of the Quaker paleoseismic site P2. Lithofacies 1b, 7d, and 7e are within lacustrine FA-C. Lithofacies numbers and facies associations are mentioned in text and described in Table 1. Figure 21 is a stratigraphic column. Lower contact of lithofacies 7e defines sequence boundary SB5.

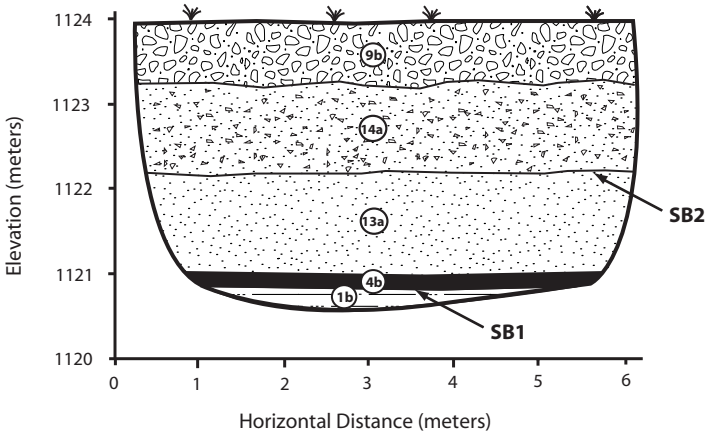

Figure 19. Trench log for the east wall of the Quaker paleoseismic site P3. Lithofacies 4b is within delta plain FA-B and lithofacies 9b is within alluvium FA-B. Lithofacies 1b, 13a, and 14a are within lacustrine FA-C. Lithofacies numbers and facies associations are mentioned in text and described in Table 1. Figure 21 is a stratigraphic column. Lower contacts of lithofacies 4b and 14a define sequence boundaries SB1 and SB2, respectively.

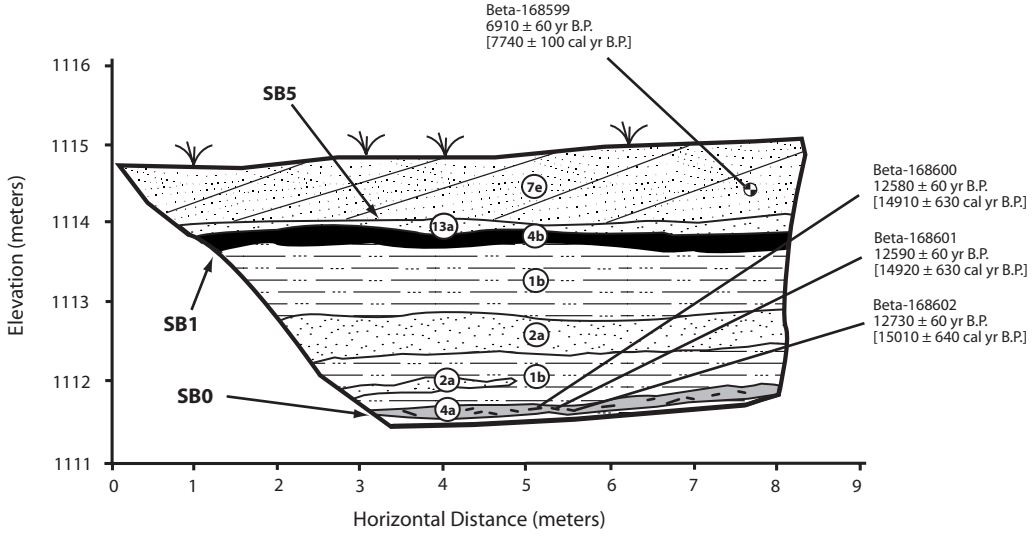

Figure 20. Trench log for the south wall of the Quaker paleoseismic site P4. Lithofacies 2a is within delta front FA-A. Lithofacies 4a,b are within delta plain FA-B. Lithofacies 1b, 7e, and 13a are within lacustrine FA-C. Lithofacies numbers and facies associations are mentioned in text and described in Table 1. Figure 21 is a stratigraphic column. Lower contacts of lithofacies 4a and 4b define sequence boundaries SB0 and SB1, respectively. Lower contact of lithofacies 7e defines sequence boundary SB5.

The radiocarbon tufa sample recovered in T5 is from the very hard, fine to medium sandy tufa sheet at the base of lithofacies 14a (Fig. 15). The radiometric ^{14}C age on tufa from T5 is 7,910 ± 60 yr B.P. [8,790 ± 210 cal. yr B.P.] (Table 2). One radiocarbon tufa sample recovered from the beach berm in the central portion of T4 has cemented, well-rounded, well-sorted, medium sand to fine gravel (lithofacies 7e; Fig. 14). The radiometric ^{14}C age on the tufa from T4 is 10,580 ± 60 yr B.P. [12,190-12,920 cal. yr B.P.] (Table 2). In addition, one radiocarbon tufa sample of lithofacies 7e was recovered in P4 (Fig. 20). This sample is similar in sedimentology and morphology to the tufa sampled in T5. The radiometric ^{14}C age on the tufa from P4 is 6,910 ± 60 yr B.P. [7,740 ± 100 cal. yr B.P.] (Table 2).

The ^{14}C age of the tufa from T4 is not in stratigraphic agreement with the other ages and is in conflict with geomorphic relations. The tufa sample form T4 is ca. 1-3 k.y. older than the ca. 11-10 cal. ka lithofacies 4b that is stratigraphically below it. In contrast, the ca. 8.8 cal. ka age of the tufa from T5 is in good stratigraphic agreement with lithofacies 4b and 13b, which has a correlated ^{14}C age (avg.) of ca. 11-10 cal. ka. and ca. 10.5 cal. ka, respectively (Figs. 14 and 15; Table 2). The erosional boundary (SB5) in the western portion of T4 represents shoreline erosion with the incorporation and reworking of older lacustrine sediments (13a and 14a) within the younger tufa-cemented beach berm sands and fine gravel (lithofacie 7e) and lithofacies 13b and 14c. The tufa age from P4 (Fig. 14) of lithofacies 7e is in stratigraphic agreement. Therefore, the radiometric tufa age of ca. 13-12 cal. ka sampled from T4 does not represent the age of the beach berm, based on an understanding of the stratigraphic and geomorphic context of the radiocarbon samples, and because it conflicts with two different numerical age constraints. The tufa sample from P4 is considered to represent accurately the age of lithofacies 7e.

It has been demonstrated that tufas in certain environmental conditions are unsuitable for numerical dating by the radiocarbon method (e.g., Bischoff et al., 1993). The tufa sample from T4 appears to reflect this. Also, Benson (1994) explains how a reservoir correction needs to be applied to radiocarbon ages from tufa. In addition, evidence to support the ages of the tufa samples from P4 and T5 of ca. 7.7 and 8.8 cal. ka, respectively, comes from the proxy indicator of total inorganic carbon (TIC) from Owens Lake sediment cores. Benson et al. (1997) present data to show that the amplitude of TIC variability increases between 8.8 and 6.7 cal. ka. They suggest that the maxima in TIC were caused by carbonate precipitation in shallow lakes. The TIC data in the sediment core and the ^{14}C ages of ca. 7.7 and 8.8 cal. ka on tufa from P4 and T5 is collaborative evidence to support that the ^{14}C ages closely approximates the true age of the tufa, thereby providing a high level of confidence in ^{14}C age. See Figure 21 for the stratigraphic column.

Discussion of the Stratigraphic and Geomorphic Relations at the Quaker Paleoseismic Site

The sequence stratigraphy and geomorphic relations observed at the Quaker paleoseismic site indicate that the scarp has been constructed and the trace of the OVF has been modified and eroded by at least four transgressive and regressive lake-cycles of pluvial Owens Lake. These lake-cycles were punctuated with episodes of cut-and-fill from fluvio-deltaic erosional and depositional systems. To illustrate the sequence stratigraphy and structural relations at the Quaker paleoseismic site one event at a time, trench T5 is retrodeformed, because it contains a more complete stratigraphic sequence then the other fault trenches. Retrodeformation analysis of T5 takes into consideration a large horizontal component of displacement and incorporates other stratigraphic and paleoseismic relations exposed in adjacent fault trenches (T4, T6, and T7), stratigraphic pits (P2-P4), and the Owens River bluffs exposure in Bacon (2003) located ca. 600 m to the east. Four schematic depictions are developed to represent the stratigraphy prior to the paleo and historic earthquakes (Fig. 22). The sequence stratigraphy and paleoseismic indicators observed in T5 (Depiction F) were used to develop depictions A-E.

11,000-10,000 cal. yr B.P.

The stratigraphic relations in the trenches suggest that SB1 (lithofacies 4b) represents a terrestrial delta plain environment in this part of Owens Valley between an elevation of 1117-1121 m during a regressive lake-cycle of pluvial Owens Lake at ca. 11-10 cal. ka. The sediment of the delta plain is interbedded between older deep water facies clayey silts and massive eolian sands (Depiction A; Fig. 22). Erosion and incision by a fluvio-deltaic system

deltaic system during the lower lake-level occurred and was followed by subsequent deposition related to a relative rise in lake-level after ca. 11-10 cal. ka, which produced cut-and-fill stratigraphic relations into existing delta plain sediments (Depiction B; Fig. 22).

10,000-9,300 cal. yr B.P.
Depiction C illustrates deformation related to a paleoearthquake that occurred after ca. 11-10 cal. ka with an apparent 1.4 m of vertical displacement (Fig. 22). This depiction shows an upward-fining sequence of medium to coarse sand that grade into interbedded fine sand and silt, overlain by massive silts that cap prominent soft sediment structures. These soft sediment structures are interpreted to be liquefaction-induced features related to the penultimate event at the site.

~9,300-8,000 cal. yr B.P.
The liquefaction-induced features, sand dikes, and fault strands are truncated by SB2, which represents a relative lake-level rise that occurred just prior to ca. 8.8 cal. ka. Sequence boundary SB2 defines an abrasion platform that beveled portions of the fault scarp related to the penultimate event, followed by deposition of a package of interbedded lacustrine and eolian strata (Depiction D; Fig. 22). The strata shown in depiction D include three sequence boundaries (SB2-SB4) that indicate two different lake-cycles after ca. 8.8 cal. ka at an elevation above 1120 m. Sequence boundary SB2 is the lower boundary of a fining upward sequence of shore to nearshore lacustrine depositional environments. A relative lake-level lowering generated terrestrial conditions as indicated by SB3. Sequence boundary SB3 is in part a disconformity with an angular boundary and is interpreted to have been formed by fluvial processes. This angular boundary into older sediments appears similar in morphology to a thalweg of a paleodistributary channel. Additional evidence to suggest terrestrial conditions is the presence of the eolian sand deposit that overlies SB3. It appears the incision that generated SB3 eroded into older lacustrine sediments and across the trace of the fault. Soon after channel abandonment, sand dunes accumulated atop a ravinement surface and within the former thalweg and against channel walls (risers). Deposition of the sand dune was followed by a rise in relative lake-level, which submerged the sand dune deposit, precipitated $CaCO_3$ (tufa), deposited nearshore sediments, and reworked and deposited shore lacustrine sediments during a period of fluctuating lake-levels.

8,000 cal. yr B.P.-present
The last sequence of lacustrine sedimentation in the area near T5 is indicated by SB4, which marks a conformable depositional contact between nearshore and shore sediments that contain reworked tufa fragments. The stratigraphic relation of shallow water sediment underlain by relatively deep water sediment indicates a regressive sequence (Depiction D; Fig. 22). Similar to what occurred during the two prior regressive lake-cycles, the area of T5 was cut into by a paleoOwens River meander belt soon after the lake lowered below an elevation of 1120 m (Depiction E; Fig. 22). The fluvial system generated prominent fluvial features (treads and risers) west of the fault trace into the footwall stratigraphy (Figs. 11 and 12) and laterally eroded and removed existing lacustrine strata to form a ~3 m geomorphic scarp (riser) (Figs. 13-17). In addition to the fluvial system, subsequent erosion into the base of the scarp occurred during a rise in lake-level that reached a maximum elevation of 1118.5-1119 m that created wave-cut notches along the scarp near T5, and constructed the ca. 8 cal. ka beach berm in the area of T4 and P4 (Figs. 14 and 20).

The last phase of deposition and scarp modification occurred after the latest lake-level lowered below an elevation of 1116 m. Reoccupation of older fluvial and lacustrine erosional and constructional features, and the creation of new features along the western boundary of the Owens River meander belt below 1116 m is indicated on aerial photographs, Profile 2, and T4 (Figs. 11, 13, and 14). Since the latest ca. 8 cal. ka lake-level that reached an elevation of ca. 1119 m, the Owens River meander belt has modified the landscape in response to lower base-levels related to falling Owens Lake water-levels. During the late to middle Holocene the river was entrained within the area of the active meander belt east of U.S. Highway 395 below an elevation of ~1114 m. Depiction F shows ~1 m of apparent vertical deformation of post ~8.8 cal. ka bedded strata from the 1872 Owens Valley earthquake.

Figure 22. Schematic depiction of stratigraphy at the Quaker paleoseismic site prior to the penultimate and 1872 earthquakes (A-E). The stratigraphic and paleoseismic depictions were developed by retrodeforming the stratigraphy exposed in trench T5 (Depiction F) one event at a time, in light of other stratigraphic and paleoseismic relations exposed in adjacent fault trenches (T4, T6-T7) and stratigraphic pits (P2-P4) and the Owens River bluffs exposure in Bacon (2003) located ca. 600 m to the E-SE. The location of sequence boundaries (SB1-4) are shown.

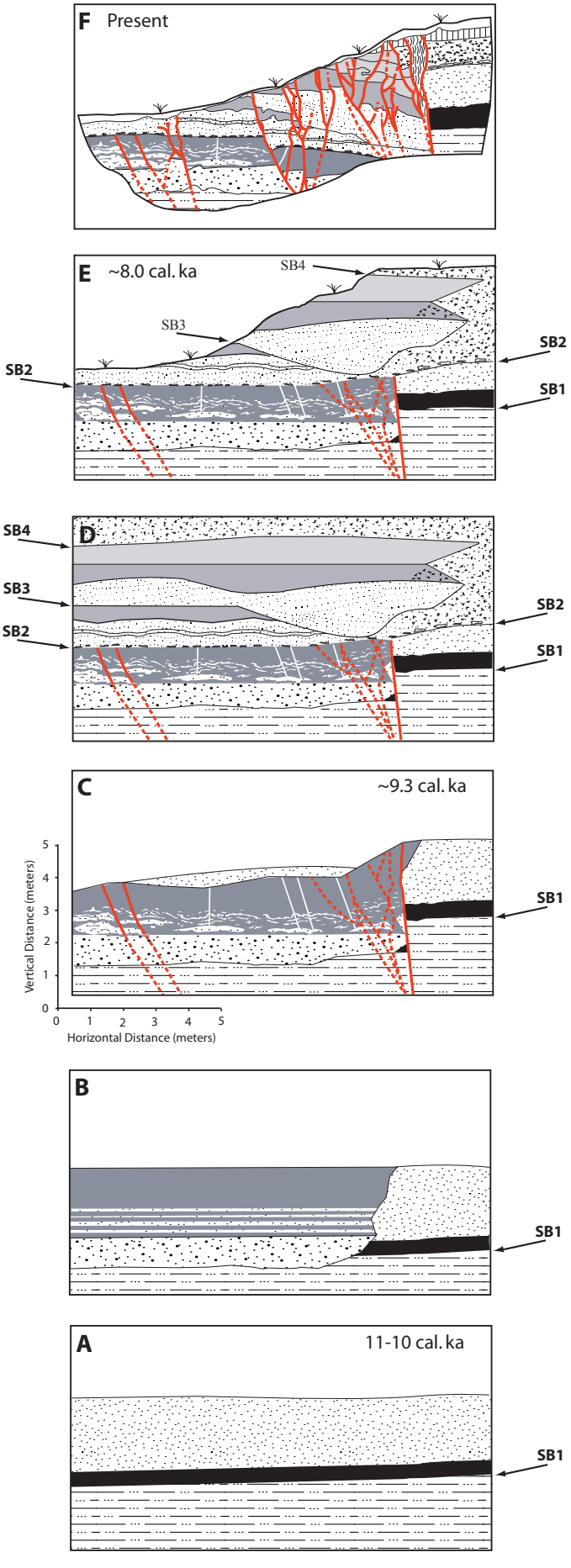

Figure 21. Schematic composite stratigraphic column developed from stratigraphic and geochronologic relations exposed at the Owens River bluffs exposure (Bacon, 2003) and the Alabama Gates and Quaker paleoseismic sites near Lone Pine. The stratigraphic column shows the positions of the penultimate and most recent event horizons from exposures in fault trenches T1-T7 and paleoliquefaction features attributed to the penultimate event exposed in T5 and along the Owens River bluffs exposure. Relative thickness of lithofacies is schematic and does not represent relative time.

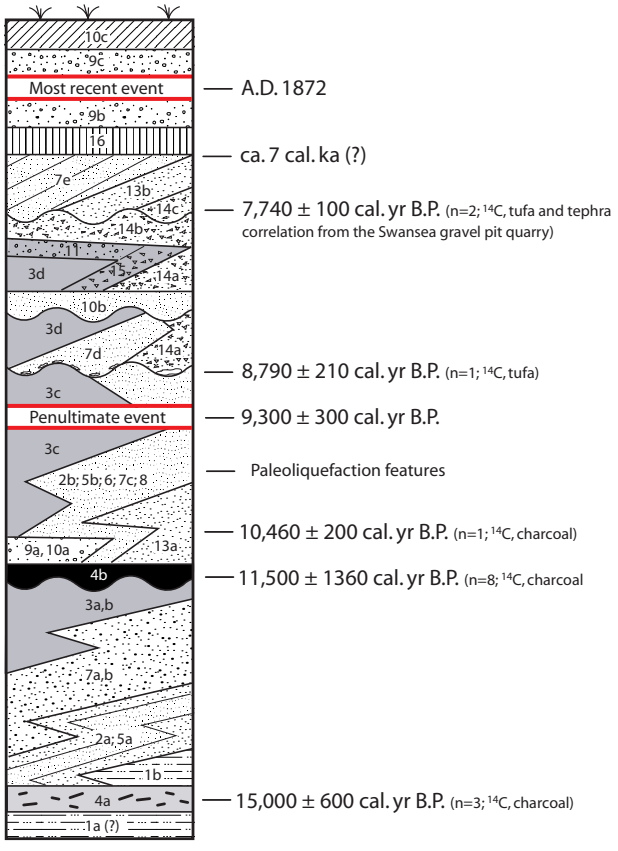

TABLE 2. RADIOMETRIC AND ACCELERATOR MASS SPECTROMETRY RADIOCARBON AGES ON CHARCOAL, ORGANIC SEDIMENT, AND TUFA FROM SITES NEAR LONE PINE, EASTERN CALIFORNIA

Sample number and material dated	Sample location and stratigraphic unit	^{14}C age* (yr B.P. $\pm$ 1σ)	$\delta^{13}C/\delta^{12}C$ (‰)	Calibrated age range** (cal. yr B.P. $\pm$ 2σ)
Beta-163551 (AMS-charcoal)	OR-2B## lithofacies 4b	9990 $\pm$ 40	-22.1	11410 $\pm$ 160
Beta-163552 (AMS-organic sediment)	OR-2A## lithofacies 4b	10480 $\pm$ 40	-26.1	12570 $\pm$ 280
Beta-163553 (AMS-organic sediment)	OR-4## lithofacies 4b	9560 $\pm$ 40	-25.4	10910 $\pm$ 200
Arithmetic mean of sample ages $\pm$2σ (95% C.L.)		10010 $\pm$ 300		
Beta-163554 (AMS-charcoal)	T2 lithofacies 4b	9060 $\pm$ 40	-23.9	10160 $\pm$ 20
Beta-163555 (AMS-organic sediment)	T2 lithofacies 4b	9030 $\pm$ 60	-25.4	10250 $\pm$ 20
Arithmetic mean of sample ages $\pm$2σ (95% C.L.)		9045 $\pm$ 60		
Beta-163556 (AMS-organic sediment)	T4 lithofacies 4b	9160 $\pm$ 50	-25.2	10330 $\pm$ 110
Beta-163557 (Radiometric-organic sediment)	T4 lithofacies 4b	9680 $\pm$ 50	-25.1	11130 $\pm$ 70
Beta-163558 (AMS-charcoal)	T4 lithofacies 4b	9920 $\pm$ 50	-24.7	11280 $\pm$ 70
Arithmetic mean of sample ages $\pm$2σ (95% C.L.)		9590 $\pm$ 260		
Beta-165600 (AMS-charcoal)	T4 lithofacies 13b	9300 $\pm$ 60	-25.3	10460 $\pm$ 200
Beta-163560 (Radiometric-tufa)	T4 lithofacies 7e	10580 $\pm$ 60#	-2.9	12760 $\pm$ 180
Beta-163561 (Radiometric-tufa)	T5 lithofacies 14a	7910 $\pm$ 60	-3.2	8790 $\pm$ 210
Beta-168599 (Radiometric-tufa)	P4 lithofacies 7e	6910 $\pm$ 60	-1.2	7740 $\pm$ 100
Beta-168600 (AMS-charcoal)	P4 lithofacies 4a	12580 $\pm$ 60	-27.8	14910 $\pm$ 630
Beta-168601 (AMS-charcoal)	P4 lithofacies 4a	12590 $\pm$ 60	-28.2	14920 $\pm$ 630
Beta-168602 (AMS-charcoal)	P4 lithofacies 4a	12730 $\pm$ 60	-27.7	15010 $\pm$ 640

Note : Radiometric and accelerator mass spectrometry (AMS) ages provided by Beta Analytical Inc., Miami, Florida.

*Sample ages are uncalibrated conventional radiocarbon ages using Libby meanlife of 8033 years.

**Conventional radiocarbon age is calibrated using Talma and Vogel (1993) and Stuiver et al. (1998).

#Radiocarbon age on tufa is not in stratigraphic agreement with other radiocarbon ages and is in conflict with geomorphic relations at the site where sampled, therefore the age estimate is considered inaccurate because it is to old.

##AMS ages from the Owens River bluffs exposure of Bacon (2003)

PALEOSEISMIC RESULTS ON THE OWENS VALLEY FAULT NEAR LONE PINE

The Alabama Gates and Quaker paleoseismic sites record evidence for recurrent deformation attributed to the 1872 earthquake and the penultimate event at both sites. The stratigraphic and structural criteria of fault-related features are used to determine the number of events. The criteria used in this investigation include: (1) offset of stratigraphic units; (2) abrupt upward termination of fault strands or sand dikes by an unconformity; (3) lithologic variation across faults; (4) variation in thicknesses of stratigraphic units; (5) fissure-fill structures; (6) liquefaction deformation horizons underlain and overlain by undeformed horizons; and (7) systematic increase in displacement down section (e.g., Weldon et al., 1996; Lettis and Kelson, 2000).

Displacement at the Alabama Gates paleoseismic site

Trenches T1 and T2 expose deformation that is interpreted to be the result of two earthquakes since 10,210 ± 60 cal. yr B.P. The 1872 event is recorded in all 3 trenches as near vertical fault strands and fissure fills that likely extended to the surface, but evidence was removed when the scarp was benched into during initial highway construction (Figs. 7-9). Trench T1 shows 1.0 ± 0.1 m total offset of lithofacies 11 above sequence boundary SB2 that abruptly terminates fault strands interpreted to be directly related to the penultimate event (Fig. 7; Table 3). The principal fault zone is exposed in T2 between 2.5 and 4 m horizontal distance (Fig. 8). This zone offsets lithofacies 3b, 4b, 7c, and 11 1.0 ± 0.1 m, using SB2 as a piercing point (Fig. 8; Table 3). The principal fault zone displays the same amount of apparent vertical offset as T1, but displacement is mostly across a single fault that is attributed to the 1872 event. T3 records only hanging wall deformation related to the 1872 event, with fault strands and a fissure fill displacing all exposed sediment 1.1 /-0.4 m (Fig. 9; Table 3). The total cumulative apparent vertical displacement across all faults in T1 and T2 is 2.4 ± 0.2 m. (Figs. 7 and 8; Table 3). Subtracting the vertical offsets of 1.0 ± 0.1 m attributed to the 1872 event in T1 and T2 from their corresponding cumulative vertical displacement, provides a vertical displacement for the penultimate event of 1.4 ± 0.2 m in T1 and T2 (Table 3).

Displacement at the Quaker paleoseismic site

All 4 trenches (T4-T7) at the Quaker paleoseismic site document faulting related to the 1872 event as near-vertical fault strands and fissure fills (Figs. 14-17). T4 and T5 are the only trenches at the site that record direct evidence for recurrent deformation. Deformation attributed to the 1872 event in T4 displaces all lithofacies above an abrasion platform (SB5). The abrasion platform is interpreted to be related to basal erosion from a pluvial Owens Lake transgression just prior to 7,740 ± 100 cal. yr B.P. (Fig. 14). Deformation attributed to the 1872 event in T5 displaces lithofacies 3d, 7d, 10b, and 14b above the abrasion platform (SB2) in the hanging-wall. The abrasion platform is interpreted to be related to basal erosion from a pluvial Owens Lake transgression just prior to 8,790 ± 210 cal. yr B.P. that truncates near-vertical fault strands and sand dikes in addition to liquefaction-induced features (Fig. 15).

The apparent vertical displacement from the 1872 event, measured in T4-T7, ranges from 0.5 ± 0.1 m in T4 and 1.0 ± 0.1 m in T7 using between 1 and 6 piercing points observed in trench walls (Table 3). The total apparent offset attributed to the 1872 event in T5 is 0.7 +0.1 m, measured using 6 piercing points across all faults above the abrasion platform (SB2). The total cumulative apparent vertical displacement in T5 from the 1872 and penultimate events is 2.3 ± 0.2 m, measured from the elevation difference between the lower contacts of lithofacies 7d in the hanging-wall and lithofacies 14a in the footwall that are interpreted to be time-stratigraphic equivalent (SB2; Fig. 15). Subtracting the apparent vertical displacement related to the 1872 event in T5 from the corresponding total apparent vertical displacement provides an apparent vertical displacement for the penultimate event of 1.6 /-0.3 m (Table 3). The total cumulative apparent vertical displacement in T4 from the 1872 and penultimate events is 1.2 ± 0.2 m, measured from the elevation difference across the graben between a sandy unit within lithofacies 1b (Fig. 14). Subtracting the apparent vertical displacement related to the 1872 event in T4 of 0.5 ± 0.1 m, based on the elevation difference across the graben of SB5, from the corresponding total cumulative vertical displacement, provides an apparent vertical displacement for the penultimate event of 0.7 ± 0.2 m (Table 3). T4 crosses the OVF at a right-step; as a result, the measured amount of apparent vertical displacement for both the 1872 and penultimate earthquakes is considered a minimum and not used in determining average displacement.

Applying a cumulative distribution function (CDF) to the displacement data of the 1872 and penultimate events, and assuming the data represent a Gaussian distribution, the average displacement per event can be estimated at 2σ (95% confidence level). The total cumulative vertical displacement measured in T1, T2, and T5 from the 1872 and penultimate events is 2.3 ± 0.3 m (2σ) (Table 3). The average vertical displacement for the 1872 event, as measured confidently in five trenches (T1, T2, T5, T6, and T7) is 0.9 ± 0.3 m (2σ) (Table 3). The average vertical displacement for the penultimate event measured from T1, T2, and T5 is 1.4 +0.3/-0.4 m (2σ) (Table 3). Interestingly, the vertical displacement of the penultimate event is ca. 60% greater than that of the vertical displacement of the 1872 event. These relations imply that the magnitude of the penultimate event may have been larger than the 1872 event.

TABLE 3. APPARENT VERTICAL TRENCH DISPLACEMENT DATA FROM THE ALABAMA GATES AND QUAKER PALEOSEISMIC SITES NEAR LONE PINE, EASTERN CALIFORNIA

Trench	1872 earthquake		Penultimate earthquake**		Total displacement	
	meters	±	meters	±	meters	±
1	1.0*	0.1	1.4*	0.2	2.4*	0.2
2	1.0*	0.1	1.4*	0.2	2.4*	0.2
3	1.1	-0.4				
4##	0.5	0.1	0.7	0.2	1.2	0.2
5	0.7*	+0.1	1.6*	-0.3	2.3*	0.2
6	1.0*	0.1				
7	0.9*	0.1				
Arithmetic mean ± 2-sigma (95% C.L.) #	0.9	0.3	1.4	+0.3/-0.4	2.3	0.3

Note: Data is apparent vertical displacement that is assumed to represent a Gaussian distribution.

*Displacement data used in cumulative density function (CDF).

**Penultimate earthquake vertical displacement determined by subtracting the vertical displacement of the 1872 earthquake from the total vertical displacement measured in each trench, except for trench T4.

#Determined from (CDF) for the 1872 and penultimate earthquakes.

##T4 crosses the Owens Valley fault at a right-step, as a result, the measured amount of apparent vertical displacement for both the 1872 and penultimate earthquakes is considered a minimum.

Style of deformation

Trench exposures reveal deformation that is distributed across a 5-6 m wide fault zone along more northerly trending fault scarps at the Alabama Gates site, in contrast to a 5-23 m wide fault zone along more northwesterly trending fault scarps at the Quaker site. Both sections of the fault zone consist of numerous near-vertical to west-dipping antithetic fault strands and near-vertical to east-dipping principal fault strands. Collectively, the faults form a half graben that is structurally similar to a negative flower structure as described by Sylvester (1988). In particular, the massive cohesive clayey silt lithofacies overlain by bedded and less cohesive silt and loose sand lithofacies in T2, T4, and T5 reflects this style of deformation. These structural relations are a result of a vertical to near-vertical fault at depth as described by Carver (1970). Normal oblique displacement in trench exposures is confirmed by noting the style and variation in thicknesses of stratigraphic lithofacies across individual fault strands.

Faulting at the paleoseismic sites and fracturing at natural exposures appear to be partitioned on north-northwest and north-northeast striking and east dipping primary, and west dipping secondary near-vertical faults and fractures. More northerly striking faults and fractures generally have steeper dips than do the more northwesterly striking faults and fractures. The measured attitude of fractures exposed in an active channel along Moffat Ranch Road (~2.7 km north of the Alabama Gates site; Fig. 3) are attributed to the 1872 event because the fractures extend to the surface of a geomorphically young alluvial fan surface estimated to be late Holocene in age after relative dating methods. The fractures range from N40W 81SW - N36E 86SE to N2E 88NW - N9E 85SE (Fig. 23). The attitudes of faults measured in six trenches (T1-T3 and T5-T7) from the paleoseismic sites attributed to the 1872 and penultimate events range from N30W 44SW - N2W 85SW to N26W 58-74NE - N8W 76 NE, with one attitude measured to be N85W 76NE (Fig. 23).

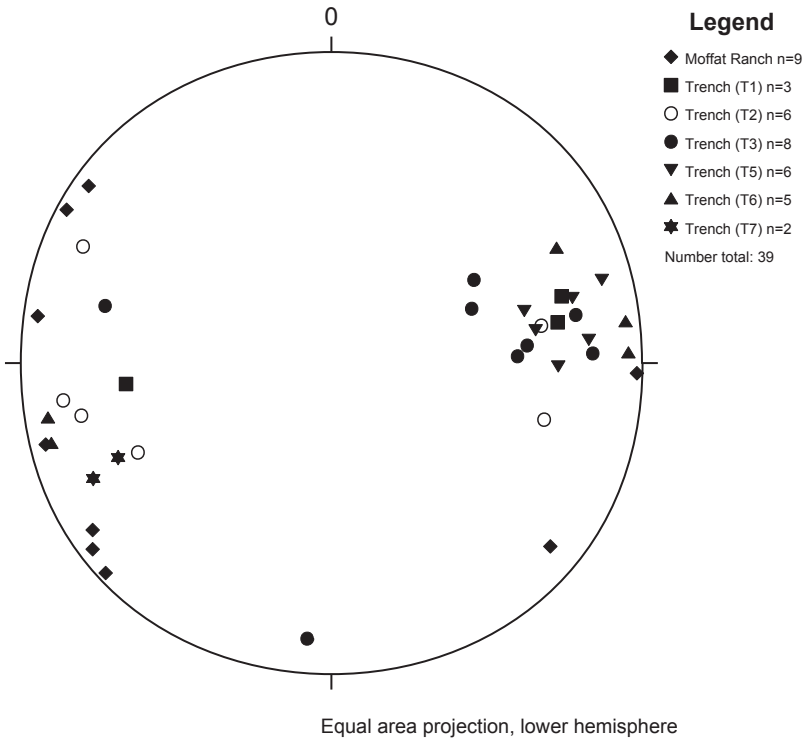

Figure 23. Structural data for faults measured in trenches (T1, T2, T3, T5, T6, and T7) at the Alabama Gates and Quaker paleoseismic sites and fractures exposed in a channel along Moffat Ranch Road located ca. 2.7 km north of the Alabama Gates paleoseismic site (Fig. 3). Symbols are poles to planes. Stereonet represents an equal area projection in the lower hemisphere.

Interseismic interval estimates

Direct evidence of deformation related to the penultimate event is exposed in T2 at the Alabama Gates and T4 and T5 at the Quaker paleoseismic sites, respectively (Figs. 7, 14, and 15). Lithofacies 4b in T2 provides a maximum age constraint for the penultimate event of 10,210 ± 60 cal. ^{14}C yr. B.P. (Tables 2 and 4). Lithofacies 14a in T5 provides a minimum age constraint for the penultimate event of 8,790 ± 210 cal. ^{14}C yr B.P. based on the correlation of SB2 (Tables 2 and 4).

The age of the penultimate event is estimated to be 9,300 ± 300 cal. yr B.P. on the basis of the event horizon position with respect to the location of the ^{14}C ages and sedimentation rates (Table 4). Sedimentation rates are determined from the thickness of sediment that was deposited in T5 between ca. 11-10 and 8.8 cal. ka (SB1 and SB2) and in P4 between ca. 15 and 11-10 cal. ka (SB0 and SB1). Early Holocene sedimentation rates measured from T5 and P4 range between 70 and 100 cm/k.y. The sedimentation rate from this study is similar to a latest Quaternary sedimentation rate of ~80 cm/k.y. from the Owens Lake core (Bischoff et al., 1997). The sedimentation rate is applied to the event horizon stratigraphy in T2 and T4 to estimate the age of the penultimate event.

Recurrence intervals cannot be calculated from the Alabama Gates and Quaker paleoseismic sites because evidence for only two events is recorded. Data from the trench investigations do provide an estimate of the time of one interseismic interval between the penultimate and 1872 events (Table 4). Using the age of the penultimate event and accounting for the elapsed time between the 1872 earthquake and 1950, because ^{14}C ages are referenced from 1950, the interseismic interval between the two earthquakes is ca. 9,500 to 8,900 yrs (Table 4).

In addition to determining the age of the penultimate event, data from P4 at the Quaker paleoseismic site provides a minimum age constraint for the antepenultimate event (APE). The oldest sediment in P4 that is not deformed by the APE is ~15,000 ± 600 cal. yr B.P. This ca. 15 cal. ka ^{14}C age provides a minimum constraint for the APE. The maximum age of sediment deformed by the APE is 21,000 ± 1,300 ^{14}C yr B.P. (Lubetkin and Clark, 1988). Using the range of constraining ^{14}C ages of sediment that bound the APE, the event occurred 18,400 ± 4,000 cal. yr B.P. Given the poor age constraint of the APE, the interseismic interval estimate between the PE and APE is 12,800 to 5,400 yrs (Table 4).

TABLE 4. SUMMARY OF LATEST QUATERNARY INTERSEISMIC INTERVALS RECORDED ON THE OWENS VALLEY FAULT ZONE FROM THIS STUDY AND PREVIOUS INVESTIGATIONS NEAR LONE PINE, EASTERN CALIFORNIA

Age constraints	This study		Lubetkin and Clark (1988)	Beanland and Clark (1994)	Bierman et al. (1995)
	Calibrated ^{14}C age* (cal. yr B.P.)	Calibrated ^{14}C age[S] (cal. yr B.P.)	Conventional ^{14}C age (yr B.P.)	Conventional ^{14}C age (yr B.P.)	Cosmogenic ^{10}Be and ^{26}Al age (yr)
Maximum	10,210 ± 60 [§]	21,000 ± 1,300[¤]	21,000 ± 1,300[¤]	10,200 ± 70 [#]	17,400**
Minimum	8,790 ± 210	15,000 ± 600[†]	10,000 [‡]	N/A	8,000 [§§]
Age estimate of the Penultimate event [¤¤]	9,300 ± 300	N/A	N/A	N/A	N/A
Age range for the Antepenultimate event [##]	N/A	18,400 ± 4,000	N/A	N/A	N/A
Number of events	2	2	3	3	3
Number of interseismic intervals	1	1	2	2	2
Average recurrence interval	N/A	N/A	10,500 to 5,000	5,000 to 3,300	8,000 to 5,800
Interseismic intervals from numerical dating methods	PE - MRE	APE - PE	N/A	N/A	APE - PE PE - MRE
Age range	9,300 ± 300 - A.D. 1872	18,400 ± 4000 - 9,300 ± 300	N/A	N/A	17,400 - 8,000 8,000 - 0
Interseismic interval (duration in years)***	9,500 to 8,900	12,800 to 5,400	N/A	N/A	9,400 to 8,000

Note: Most recent event (MRE); penultimate event (PE); antepenultimate event (APE); not applicable (N/A)

*Maximum and minimum calibrated age constraints for the PE are from trenches T2 and T5, respectively (Table 2)

[S] Maximum and minimum age constraints for the APE are from Lubetkin and Clark (1988) and pit P4, respectively (Table 2).

[§]Calibrated ^{14}C age of 10,210 ± 60 yr B.P. determined from the arithmatic mean (95% C.L.) of calibrated ^{14}C ages for the PE shown in Table 2; Beta-163554 and Beta-163555.

[†]Calibrated ^{14}C age of 15,000 ± 600 yr B.P. determined from the arithmatic mean (95% C.L.) of calibrated ^{14}C ages of sediment not deformed by the APE from P4 shown in Table 2; Beta-168600, -168601, and -168602.

[¤]Maximum ^{14}C age is from tufa located at an elevation of ca. 1150 m that constrains the age of an alluvial fan that is displaced by three earthquakes (APE - MRE) from Lubetkin and Clark (1988).

[#]Radiocarbon age is assumed to represent the oldest lacustrine sediments displaced by the Owens Valley fault below an elevation of ~1137 m at Site 15; same sample site is correlated at the Alabama Gates paleoseismic site at an elevation of 1122 m, this study.

**Average surface exposure age of alluvial fan that is displaced by 3 earthquakes (APE - MRE), same fan Lubetkin and Clark (1988) estimate is ca. 21 ka.

[‡]Assumed minimum age from Lubetkin and Clark (1988) based on pluvial Searles Lake stratigraphy of Smith and Street-Perrott (1983).

[§§] Average surface exposure age of alluvial fan that is displaced by 2 earthquakes (PE - MRE).

[¤¤]The age of the PE is estimated on the basis of the PE horizon position with respect to the location of the constraining ^{14}C ages and sedimentation rates.

[##]The range of constraining ^{14}C ages of sediment that bound the APE. The maximum age is ca. 21 ka and the minimum age is ca. 15 cal ka.

***The interseismic interval is determined by acounting for the elapsed time between A.D. 1872 and 1950 (ca. 100 yrs).

Slip rate estimates

The rationale of the characteristic earthquake model of Schwartz and Coppersmith (1984) is used to characterize oblique slip rates on the OVF near Lone Pine. The characteristic earthquake model simply assumes that ruptures are limited to primary segments, that displacement per event at a point is constant, and that slip rate along strike is variable, making no assumptions about recurrence (McCalpin, 1996b). Given the trench data from the two paleoseismic sites that show comparable amounts (within 60%) of apparent vertical displacement from the two most recent events, in addition to observations made by Lubetkin and Clark (1988) and Beanland and Clark (1994) at the Lone Pine paleoseismic site, the characteristic earthquake model for the latest two interseismic intervals is applicable. Using this model, a latest Quaternary oblique slip rate for the southern end of the OVFZ can be resolved with a high level of confidence. Table 5 shows a summary of geologic slip rate estimates on the OVF from this study and previous investigations in Owens Valley.

Vertical slip rate estimates

Three different apparent vertical slip rate estimates were calculated for this study, based on interseismic intervals between the PE-MRE, APE-PE, and APE-MRE. The PE-MRE vertical slip rate based on the average 1872 vertical displacement of 0.9 ± 0.3 m (2σ) and an interseismic interval of 9,200 ± 300 cal. yr B.P. is 0.10 ± 0.03 m/k.y. (Table 5). The APE-PE vertical slip rate based on the average penultimate event vertical displacement of 1.4 +0.3/-0.4 m (2σ) and an interseismic interval of 9,100 ± 3,700 cal. yr B.P. is 0.20 ± 0.08 m/k.y. (Table 5). The two interseismic interval (APE-MRE) vertical slip rate based on the average total vertical displacement of 2.3 ± 0.3 m (2σ) since 18,400 ± 4,000 cal. yr B.P. is 0.10 ± 0.03 m/k.y. (Table 5).

Oblique slip rate estimates

There is no unequivocal surface evidence at the Alabama Gates and Quaker paleoseismic sites for lateral offsets associated with the penultimate event or early events, because the landscape has been modified by fluctuating mid to early Holocene lake-levels and the Owens River below an elevation of ~1140 m. In addition, there is no unequivocal evidence for lateral offsets related to the 1872 event at both sites. To derive estimates of the average and maximum latest Quaternary oblique slip rates, individual vertical displacements of the MRE, PE, and the total cumulative displacement are scaled by the horizontal to vertical displacement ratios of 6:1 and 10:1 determined by Beanland and Clark (1994).

PE-MRE two-event slip rate: Scaling the average vertical displacement of the MRE (Table 5) with the displacement ratios provides an average (6:1) and maximum (10:1) oblique displacement of 5.4 ± 1.8 m and 9.0 ± 3.0 m, respectively. Dividing the average and maximum oblique displacement estimates by the PE-MRE interseismic interval of 9,200 ± 300 cal. yr B.P. results in slip rates of 0.6 ± 0.2 m/k.y and 1.0 ± 0.3 m/k.y., respectively (Table 5).

APE-PE two-event slip rate: Scaling the average vertical displacement of the PE (Table 5) with the displacement ratios provides an average (6:1) and maximum (10:1) oblique displacement of 8.4 ± 2.4 m and 14.0 ± 4.0 m, respectively. Dividing the average and maximum oblique displacement estimates by the PE-MRE interseismic interval of 9,100 ± 3,700 cal. yr B.P. results in slip rates of 0.9 ± 0.5 m/k.y. and 1.5 ± 0.8 m/k.y., respectively (Table 5).

APE-MRE three-event slip rate: Scaling the average total vertical displacement attributed to both the PE and MRE (Table 5) with the displacement ratios provides an average (6:1) and maximum (10:1) oblique displacement of 13.8 ± 1.8 m and 23.0 ± 3.0 m, respectively. Dividing the average and maximum oblique displacement estimates by the age range that bounds the APE of 18,300 ± 4,000 cal. yr B.P., results in slip rates of 0.8 ± 0.2 m/k.y. and 1.3 ± 0.3 m/k.y., respectively (Table 7). Applying a cumulative distribution function (CDF) and assuming a Gaussian distribution to the three different 6:1 oblique slip rate estimates, results in a latest Quaternary average oblique slip rate that ranges from 0.4 to 1.3 m/k.y. (2σ) (Table 5).

TABLE 5. SUMMARY OF GEOLOGIC SLIP RATES ON THE OWENS VALLEY FAULT ZONE FROM THIS STUDY AND PREVIOUS INVESTIGATIONS IN OWENS VALLEY, EASTERN CALIFORNIA

Displacement ratio*	This study				Martel et al. (1987)	Lubetkin and Clark (1988)	Beanland and Clark (1994)	Zehfuss et al. (2001)
	PE-MRE slip rate † (cal. m k.y.$^{-1}$)	APE-PE slip rate # (cal. m k.y.$^{-1}$)	APE-MRE slip rate ¤ (cal. m k.y.$^{-1}$)	Average slip rate $ (cal. m k.y.$^{-1}$)	Slip rate § (m k.y.$^{-1}$)	Slip rate** (m k.y.$^{-1}$)	Slip rate ## (m k.y.$^{-1}$)	Slip rate ‡ (m k.y.$^{-1}$)
Vertical	0.10 ± 0.03	0.20 ± 0.08	0.10 ± 0.03		0.25 ± 0.03			0.24 ± 0.04
6:1 (average)	0.6 ± 0.2	0.9 ± 0.5	0.8 ± 0.2	0.8 +0.5/-0.4		1.5 ± 0.7	2 ± 1	1.4
10:1 (maximum)	1.0 ± 0.3	1.5 ± 0.8	1.3 ± 0.3					

Note: Most recent event (MRE); penultimate event (PE); antepenultimate event (APE).

*Displacement ratio represents the average (6:1) and maximum (10:1) oblique slip from the 1872 and prehistoric earthquakes determined by Beanland and Clark (1994).

†Slip rate based on the interseismic interval between the PE and MRE (9,300 ± 300 cal. yr B.P.; Table 4) and arithmatic mean (95% C.L.) of the MRE vertical displacement measured from trenches

#Slip rate based on the interseismic interval between the APE and PE (9,100 ± 3,700 cal. yr B.P.; Table 4) and arithmatic mean (95% C.L.) of the PE vertical displacement measured from trenches

¤Slip rate based on the interval of time between the APE and MRE (ca. 18,300 ± 4,000 cal. yr B.P.; Table 4) and arithmatic mean (95% C.L.) of the total vertical displacement measured from trenches

$Average slip rate (95% C.L.) based from cumulative density function (CDF) of slip rate estimates for the PE-MRE, APE-PE, and APE-MRE.

§Long-term vertical displacement rate over 314 ± 36 k.y. ± 2 standard deviation from ^{39}Ar/^{40}Ar numerical age on the Fish Springs cinder cone.

**Average and maximum latest Quaternary displacement rate over a time interval of 21-0 k.y. from ^{14}C age on tufa located at an elevation of ca. 1150 m.

##Average Holocene displacement rate.

‡Long-term vertical and 6:1 displacement rate over a time interval of 314-0 k.y. that integrates cosmogenic ^{10}Be and ^{26}Al modeled surface ages and soil development on fan surfaces and ^{39}Ar/^{40}Ar numerical age on the Fish Springs cinder cone.

SECONDARY EVIDENCE ATTRIBUTED TO SEISMIC EVENTS NEAR LONE PINE

Within the field area there is secondary evidence attributed to seismic events on the OVF. In addition to surface rupture, liquefaction-induced features related to the 1872 earthquake were documented soon after the event (e.g., Wills, 1996). Beanland and Clark (1994) document several conical accumulations of loose sand that they interpret as sand blow liquefaction-induced features. These liquefaction-induced features are all located near Independence at an elevation ~1145 m, which is the same elevation of the latest overflow level of pluvial Owens Lake. It is plausible that the source of sand from the sand blow features is related to a paleo-shoreline.

In addition to the sand blows, other liquefaction-induced features attributed to the 1872 earthquake occurred as large-scale lateral spreads forming grabens around Owens Lake (playa) below an elevation of 1145 m (Carver, 1970; Bryant, 1988). Furthermore, numerous mapped grabens and scarps are located in the northwest portion of the basin, south of Lone Pine, above an elevation of 1160 m (Carver, 1970; Bryant, 1988; Beanland and Clark, 1994). Carver (1970) map these features associated with the 1872 earthquake. Bryant (1988) and Beanland and Clark (1994) map the same features as Quaternary faults likely associated with the Sierran Nevada frontal fault system. Since these investigations, it is considered that these same features could be associated with the head scarp of a mega-landslide. This landslide is thought to have deformed sediments exposed at Point Bartlett in the northwest corner of Owens Lake (playa) (Fig. 2). The deformed sediments were interpreted by Carver (1970), Miller (1989), and by Beanland and Clark (1994) to be directly associated with the OVF, but now thought in stead to be associated with the toe region of a mega-slumb block (G. Carver, pers. com., 2000). These relations are similar to what is observed in Summer Lake basin, Oregon by Simpson (1990), Pezzopane (1993), and Langridge (1998) and in Dixie Valley, Nevada by Caskey (2002).

Shattered Fan Site

Possible secondary evidence for a paleoearthquake(s) from the OVF or from nearby capable faults is located at the Shattered Fan site. The Shattered Fan site is located ~10 km north of Lone Pine and ~3 km north of the Alabama Gates paleoseismic site (Fig. 3). The Shattered Fan site consists of a prominent graben near an elevation of 1160 m that is mapped as late Quaternary by Beanland and Clark (1994) and Stone et al. (2000). The graben is ~150 m in width and extends close to contour for 0.5-0.7 km across an alluvial/outwash fan surface. The scarp heights range from 2 m along the eastern boundary to ~8 m along the western boundary. Three exploratory trenches were excavated across the graben along with five soil pits on three different surfaces in June of 2002 to investigate the late Quaternary paleoseismic history on the OVFZ (Fig. 24A). Total station controlled profiles were surveyed across the graben and adjacent slopes of the fan (Fig. 24B).

The trenches excavated across the graben indicate it is filled with at least 2-3 m of alluvial interbedded sand and silt since its formation. The package of fill is likely underlain by moderately- to well-sorted and rounded gravel of the alluvial/outwash fan. The soil pits show clast supported moderately- to well-sorted and rounded gravel of the fan. Based on the relative age dating techniques after the methods of Burke and Birkeland (1979) three surfaces are differentiated at the Shattered Fan site.

(Qp≥ta) ≥*Tahoe-age fan*
The oldest surface that the graben deforms exhibits a similar degree of weathering and a surface morphology found on other aggradational fans in Owens Valley that are ≥140 ka (≥Tahoe glaciation) equivalent to oxygen isotope stage (OIS): ≥6 (e.g., Zehfuss et al., 2001). This surface is mapped as Qp≥ta based on preliminary data from 3 described soil pits and 3 exploritory trenches within the graben (Fig. 24A). The lower part of the Qp≥ta fan is modified by the ~20 ka shoreline near an elevation of ~1160 m of Lubetkin and Clark (1988) and Orme and Orme (2000).

(Qpti) *Tioga-age fan*
The graben does not cross a relatively younger surface that is geomorphically inset and located to the south of the Qp≥Ta surface. The southern surface exhibits a similar weathering profile and surface morphology to other surfaces in Owens Valley that are ~20 ka (Tioga glaciation; OIS: 2) (e.g., Lubetkin and Clark, 1988; and Zehfuss et al., 2001). This surface is mapped as Qpti based on preliminary data from 2 described soil pits (Fig. 24A).

At the lower and eastern portion of the Qpti fan surface, near the elevation of the ~20 ka shoreline, numerous cobbles and boulders at the surface and subsurface grade to sands, which suggests the occurrence of fan delta sedimentation. East and lower in elevation of the 1160 m shoreline, the delta fan is eroded and truncated by the ~15 cal. ka shoreline, which generated a prominent wave-cut notch and associated platform at an elevation of ~1145 m (Fig. 24A).

(Qh) *Holocene-age fan*

The graben does not cross surfaces that are geomorphically inset and located to the north and south of both the Qp≥ta and Qpti surfaces. These surfaces exhibit a similar weathering profile and surface morphology to other surfaces in Owens Valley that are <10 ka (Holocene) (e.g., Lubetkin and Clark, 1988; Stone et al. 2000; and Zehfuss et al., 2001). The Holocene surface is mapped as Qph based on preliminary data from numerous borrow pit, channel exposures, and three soil pits and trenches (Fig. 24A).

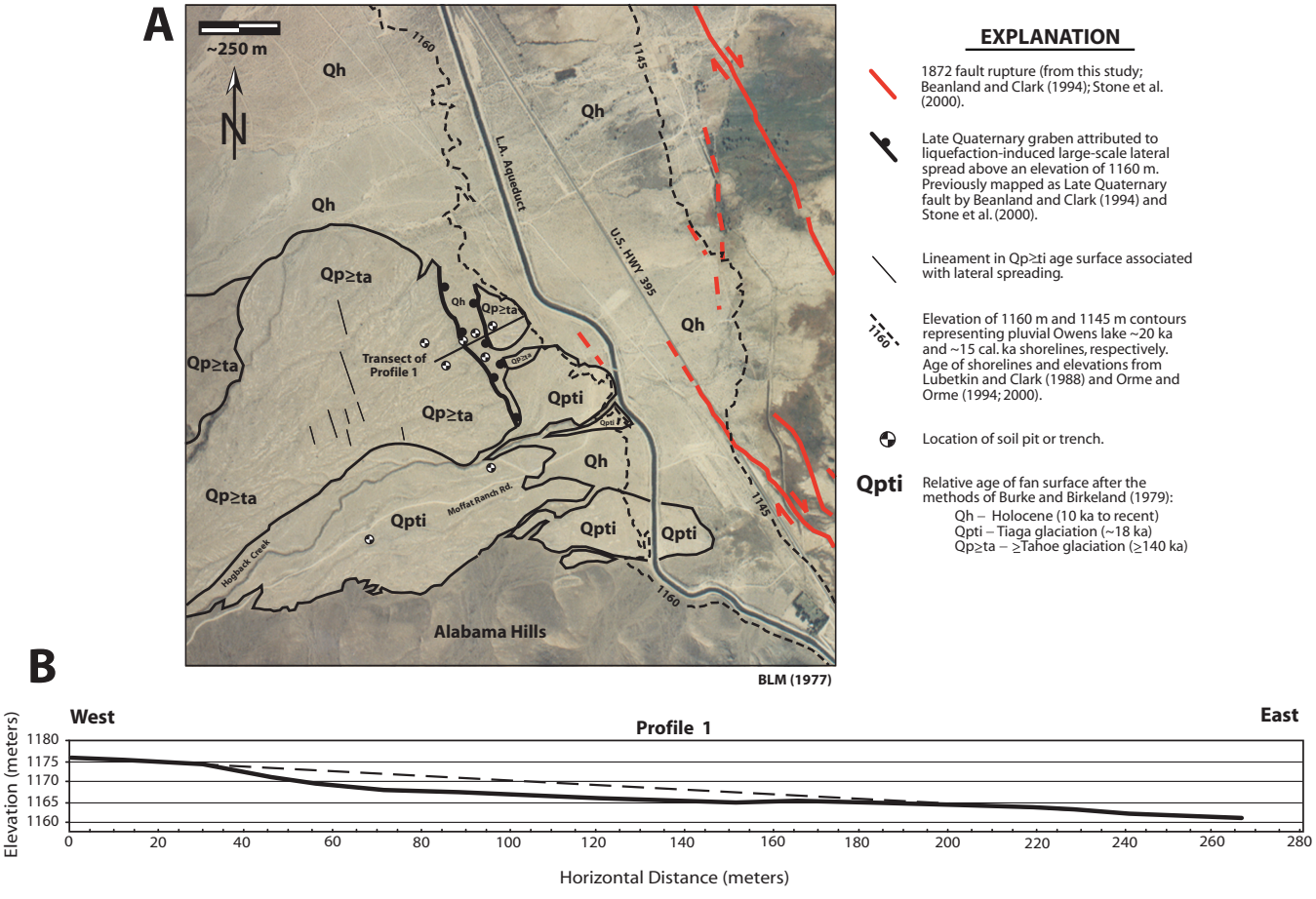

Figure 24. Geologic map showing fan units and a survey-controlled profile across a graben at the Shattered Fan site (A and B, respectively). Three fan surfaces are differentiated at the site based on 8 soil pits and trenches and the methods of Burke and Birkeland (1979). Profile 1 was surveyed perpendicular to the trend of the graben. The projected line across the graben indicates that there is no measurable vertical separation of the surfaces that bound the graben. East of the graben is a subtle break-in-slope near an elevation of ~1162.5 m that reflects modification associated with the ~20 ka pluvial Owens Lake shoreline of Lubetkin and Clark (1988) and Orme and Orme (2000). As a result of no measurable vertical separation across the graben, which is similar to other features attributed to mega-landsliding south of Lone Pine (Carver, 1970), the formation of the Shattered Fan graben is likely related to a large-scale lateral spread.

Preliminary results

Based on stratigraphy exposed in trenches, soil pits, and the structural relations shown on the survey profile, the graben likely formed during a large-scale lateral spread when ground water conditions were in phase with a pluvial Owens Lake level that was at an elevation of ≥1160 m. Structural evidence to support this is the lack of any significant vertical separation across the graben using the survey profile (Fig. 24B) and the methods of Caskey (1995) and descriptions in Keefer (1999) and Caskey (2002). The trench at the western scarp exposes a relatively narrow slide plane filled with $CaCO_3$ that dips ~65º within matrix supported gravel. Total vertical displacement could not be measured in the relatively shallow 2.5-2.7 m deep trench exposure. The trench exposed colluvial wedge stratigraphy that truncated the slide plane. There were no other observable truncated planes in the shallow

exposure. The scarp appears to be a single-event scarp that has been degraded and modified by mass-wasting and/or lacustrine erosional processes since the formation of the graben, which have generated nontectonic bevels into the scarp.

The lateral spread at the Shattered Fan site is located 15-16 km north of other similar geomorphic and structural features attributed to mega-landsliding near Bartlett Point (G. Carver, pers. com., 2000). A possible maximum age for the timing of the mega-landslide at Bartlett Point is 30-19 ^{14}C ka from shells in lacustrine sediments dated by Beanland and Clark (1994) and described by (Miller, 1989). Based on the reconnaissance-level relative dating and correlation of fan surfaces and the presence of the ~20 ka shoreline near the site, the formation of the graben is constrained between ~20 ka and ≥140 ka. The lower minimum age is based on the Qpti fan surface and the ~20 ka shoreline at the Shattered fan site. This lower minimum age of the graben is similar to the lower maximum age constraint of the mega-landslide at Bartlett Point.

This study has determined that the APE occurred between 22.4 and 14.4 cal. ka. The older range of the APE is within the range of constraining ages of the graben and the mega-landslide. Attributing the lateral spread and mega-landslide features to a seismogenic event(s) on the OVF is equivocal unless a refined age constraint of the formation of the features are determined and/or a more complete late Pleistocene paleoearthquake record in Owens Valley occurs.

DISCUSSION OF PALEOSEISMIC RESULTS ON THE OWENS VALLEY FAULT

Vertical slip rates

Previous studies along the northern portion of the OVFZ in areas near Big Pine provide late Quaternary vertical slip rates. Fish Springs cinder cone and surfaces of Tahoe-age and Tioga-age alluvial fans are vertically displaced by the Fish Springs fault splay of the OVFZ (Fig. 2). The cinder cone is directly dated by the ^{39}Ar/^{40}Ar method, and provides an average vertical slip rate of 0.25 ± 0.03 m/k.y. since 314 ± 36 ka (Martel et al., 1987). Later, Zehfuss et al. (2001) determined vertical slip rates on the Fish Springs fault that are deduced from integration of cosmogenic ^{10}Be and ^{26}Al methods and soil development on alluvial fan surfaces that are ~140 ka and using an age of ca. 300 ka from of the Fish Springs cinder cone. The slip rate of Zehfuss et al. (2001) is 0.24 ± 0.04 m/k.y., which is comparable with the slip rate determined by Martel et al. (1987).

The apparent vertical slip rate estimates from this study range between 0.10 ± 0.03 and 0.20 ± 0.08 m/k.y. (Table 5). The vertical slip rates from Martel et al. (1987) and Zehfuss et al. (2001) are derived from sites on the Fish Springs fault splay, nearly 45 km north of the paleoseismic sites of this study. This study presents a latest Quaternary vertical slip rate that is within 0.10 m/k.y. of the late Quaternary vertical slip rate from the Fish Springs fault splay of the OVFZ (Table 5).

Oblique slip rates

Lubetkin and Clark (1988) characterized the style of faulting on the Lone Pine fault splay of the southern OVFZ near Lone Pine. In addition, Beanland and Clark (1994) described the surface rupture related to the 1872 earthquake and geomorphic evidence for paleoearthquakes on the entire OVFZ, including the Lone Pine fault splay. Both of their paleoseismic trench investigations or information from trenches excavated south of Bartlett Point (Fig. 2) by Carver (1970) were unable to constrain the timing of paleoearthquakes, due to both the lack of direct evidence and lack of numerical age control on faulted deposits. What Lubetkin and Clark (1988) and Beanland and Clark (1994) did demonstrate qualitatively are approximately equal amounts of displacement in each event, which supports the characteristic earthquake model of Schwartz and Coppersmith (1984). They show that in the area of the abandoned Lone Pine Creek alluvial fan, the Lone Pine fault splay (Fig. 3) has a compound fault scarp across a Tioga-age (ca. 20 ka) alluvial fan above an elevation of 1160 m. They used channel and levee features on the fan as piercing points for lateral displacement. Alluvial fan surfaces at this site are displaced 6-6.5 m vertically and channels displaced 10-18 m right laterally, which they attribute to three 1872-style rupturing events.

The age of the Lone Pine fan was determined by using the relative age dating techniques after the methods of Burke and Birkeland (1979) in combination with a radiocarbon age of 21,000 ± 1,300 ^{14}C yr B.P. on lithoid tufa that formed in beach gravels at an elevation of ca. 1160 m, 3 km north of the Lone Pine fan (Fig. 12). The ca. 21 ka age estimate provides a maximum age for the alluvial fan. In addition, Lubetkin & Clark (1988) inferred a minimum age close to 10 ka based on the regional pluvial lake record and evidence from pluvial Searles Lake, with the assumption that Owens Lake overflowed between ~12-10 ka (Smith and Street-Perrott, 1983). Based on the average net displacement of 4.3-6.3 m for each earthquake and age estimates for the Lone Pine Creek fan, a latest Quaternary slip rate for the Lone Pine fault is 0.4 to 1.3 mm/yr. They then combined the 1872 lateral offsets of 2.7 and 4.9 m measured 1 km to the east along the main trace OVFZ, for a combined lateral slip rate of 0.7 to 2.2 mm/yr for the OVFZ (Lubetkin and Clark, 1988). Using the same age estimates for the fan and geomorphic and subsurface evidence for three earthquakes, the Lone Pine fault has an average recurrence interval between 5,000 and 10,500 yrs (Lubetkin and Clark, 1988) (Table 4).

Beanland and Clark (1994) characterize the style of deformation associated with 1872 event and paleoearthquakes by measuring scarp heights and geomorphic offsets along the entire OVFZ. They estimate a Holocene slip rate of 2 ± 1 mm/yr, using a non-calibrated radiocarbon age of 10.17 ± 0.07 ka from an elevation ca. 20 m below the 1145 m overflow level and infer 2 paleoearthquakes (3 earthquakes including 1872) to have occurred within this time. The ca. 10 ka age was inferred to represent the maximum age of the oldest Owens Valley sediments deformed by the fault at or below the elevation near 1125 m. Beanland and Clark (1994) noted that because they could not date individual paleoearthquakes, an average recurrence interval need not apply. But given their data, they estimated an average recurrence interval on the OVFZ of 5,000 to 3,300 years. Thus, their slip rate and earthquake average recurrence interval estimates were determined on the basis of an equivocal number of events and indirect age control (Table 4).

The average 6:1 (horizontal:vertical) slip rate estimates from this study based on two different single interseismic intervals and the time since the APE ranges from 0.6 ± 0.2 m/k.y. to 0.9 ± 0.5 m/k.y., respectively (Table 5). The maximum (10:1) slip rate estimates from this study based on two different single interseismic intervals and the time since the APE ranges from 1.0 ± 0.3 m/k.y. to 1.5 ± 0.8 m/k.y., respectively (Table 5). The average of the three 6:1 slip rate estimates using a CDF is 0.4-1.3 m/k.y. The average slip rate estimate from this study is the same as the Lubetkin and Clark (1988) slip rate estimate on the Lone Pine fault splay, which both are calculated over the same two interseismic intervals. The slip rates from this study are derived from the Alabama Hills and and main trace fault sections. Therefore, we did not add the Lubetkin and Clark (1988) slip from the Lone Pine fan to this studies slip rates. In addition, this study presents direct average and maximum latest Quaternary slip rates that are within the range of slip rate estimates determined from other earlier investigations (Table 5).

Previous evidence for the penultimate event on the OVFZ

Direct evidence for the penultimate event on the OVF using tectonic geomorphology is best expressed at the Lone Pine paleoseismic site (Fig. 3). The Lone Pine Creek alluvial fan that was faulted by three earthquakes since ca. 21 ka has an intermediate fan surface associated with a younger debris flow that is displaced 2.2 m vertically (2.3 ± 0.3 m (2σ), this study) and 12 m right laterally by the Lone Pine fault, indicating two events (Lubetkin and Clark, 1988; Beanland and Clark, 1994). Work done by Bierman et al. (1995) determined recurrence intervals on the Lone Pine fault by directly dating the different deformed surfaces on the alluvial fan. Using cosmogenic ^{10}Be and ^{26}Al age estimates from the surface of boulders of the alluvial fan, they estimate a maximum age of 17.4 ka for the alluvial fan that is faulted by 3 earthquakes and an age of 8 ka for the intermediate fan that is faulted by 2 earthquakes. Based on these data, they determine an average recurrence interval between 5,800 and 8,000 yrs on the Lone Pine fault. Their data are the first attempt to bracket the timing of pre-1872 ruptures on the OVFZ with numerical age dating techniques (Table 4).

In addition, Bryant (1988) worked on the OVFZ during a California Geological Survey (CGS), formerly known as California Department of Mines and Geology (CDMG), fault re-evaluation investigation. As a result of a new investigation on the OVFZ by Beanland and Clark (1994), the State of California re-evaluated the OVFZ around 1988 to meet current criteria for seismic zoning and to refine the mapping of previously zoned fault traces (Bryant, 1988). The fault evaluation report for the OVFZ contains additional new mapping, mapping by Beanland and Clark (1994), and a logged fault exposure on the northern Alabama Hills section, which is at Site

14 of Bryant (1988) and Beanland and Clark (1994) (Figs. 3 and 4). The trench at Site 14 was excavated prior to 1988 probably to sample for sand and gravel aggregate resources (W.A. Bryant, written comm., 2001). The trench crosses a compound fault scarp composed of coarse alluvium derived from the Alabama Hills that exhibits two distinct fault traces separated by ca. 4.6 m. The trench extends across the western trace, but does not reach the eastern trace. The western trace may not have ruptured during 1872, based on a gentle scarp (slope angle of 26°), ca. 1.5 m of scarp retreat, and colluvial wedge stratigraphy (Bryant, 1988). Although the trench did not extend across the eastern trace, based on a steeper scarp angle and morphology that is characteristic of 1872 fault scarps, the eastern fault trace probably did rupture in 1872 (Bryant, 1988). Site 14 is at an elevation close to 1140 m, 5 m below the overflow level, and exhibits evidence for 2 earthquakes at the surface. The morphologic setting, sedimentologic characteristics, and the inferred number of earthquakes observed at this particular site are similar to the 8 ka alluvial fan at the Lone Pine paleoseismic site that is also faulted by two events.

Recent paleoseismic results by Lee et al. (2000; 2001) for an area north of Lone Pine near Pangborn Lane, less than 1 km south of the Quaker paleoseismic site, contradict the findings of this study and the studies of both Lubetkin and Clark (1988) and Bierman et al. (1995), which has consequently been addressed in detail in an annual project summary for NEHRP by Bacon et al. (2001).

Paleoseismic data from this study have refined the slip rate and average recurrence interval estimates of Beanland and Clark (1994) and corroborate with the slip rate estimates and average recurrence intervals made by previous investigations on the OVF by Martel et al. (1987), Lubetkin and Clark (1988), Bierman et al. (1995), and Zehfuss et al. (2001).

LATEST QUATERNARY LAKE-LEVEL FLUCTUATIONS OF PLUVIAL OWENS LAKE

The Quaternary lacustrine stratigraphy in Owens Lake basin has attracted paleoclimate investigations in the past, with one of the earliest by Smith and Pratt (1957). More recently, sediment cores have documented the timing and qualitative changes of latest Pleistocene and Holocene lake-level fluctuations on the basis of $\delta^{18}O$, total inorganic carbon (TIC), ostracode, diatom, and pollen proxy climate indicators, in addition to lithologic changes in the form of unconformities (Newton, 1991; Benson et al., 1996; 1997; Smith et al., 1997; Lund et al., 1998; Smoot, 1998; Forester, 2000; and Li et al., 2000). Although sediment core data are useful in detecting chemical, biological, and sedimentological changes in a paleolake system, core data alone do not provide any indication of the surface elevation of a paleolake-level at any given period of time, except during a desiccation event when evaporitic minerals are observed.

Recent stratigraphic and geomorphic data of shoreline deposits and associated features presented by Orme and Orme (1993; 2000), Smith (1997a), and Stone et al. (2000), in combination with data presented in this study, indicate that pluvial Owens Lake water-levels fluctuated throughout the latest Pleistocene and Holocene, mostly within the basin at elevations much above the playa, yet below the latest overflow sill elevation of 1145 m. The majority of these studies occurred after the investigation of Beanland and Clark (1994), who in their Table 1 provide inferred Holocene ages of several individual strand lines with corresponding elevations below the sill. Their older range of inferred ages is in close agreement to the numerical ages and associated elevations presented in this study.

Methodology

In an effort to develop a latest Quaternary lake-level curve for pluvial Owens Lake in relation to the overflow elevation of 1145 m, utilization of both subsurface sediment core data and elevation-controlled surface stratigraphic and geomorphic data have been compiled and are shown in Figure 25. The figure covers the time interval from ~16 cal. ka to present. Ages are reported in calibrated ^{14}C yr B.P. after Bard et al. (1993). Elevations have a measured vertical accuracy within ±1 m. Landforms have been deformed as a result of tectonism within Owens Lake basin (e.g.. Carver, 1970). Most of the data points are located within the hanging-wall of the OVFZ and have been subjected to different degrees of seismic accelerations and coseismic deformation. We consider that an elevation correction factor of a minimum of 2.5 m could be applied to the stratigraphic and geomorphic data that were deposited or formed prior to the penultimate event, and a minimum of 1.0 m to the stratigraphic

and geomorphic data deposited or formed after the event at ca. 9.3 cal. ka determined form this study. These correction factors are considered a minimum, because it is not clear how much subsidence or uplift is distributed within Owens Lake basin during earthquakes on the OVFZ or on other faults that bound the basin, nor is it clear how much deformation has occurred due to isostatic rebound since the last significant highstand. In addition, the natural variability in the height of constructional beach features provides a ± 2.5 m difference in elevation when spatially compared to similar shoreline features (Adams and Wesnousky, 1998).

Age control

Age control of shoreline features, material formed subaqueously or subaerially is from AMS and radiometric ^{14}C on charcoal, tufa, shells, and bulk organic carbon. The ages reported in Orme and Orme (1993), Beanland and Clark (1994), and Bierman et al. (1995) are in conventional ^{14}C years. All the conventional ^{14}C ages, including the ages from this study, have been subsequently calibrated after Bard et al. (1993) in Figure 25. The calibrated ages after Bard et al. (1993) when compared to the ages after Stuiver et al. (1998), are the average ± 100-200 yrs.

Stratigraphic and geomorphic data in Figure 25 are from Orme and Orme (1993; 2000), Beanland and Clark (1994), Bierman et al. (1995), and this study. Solid circles represent shoreline data directly related to a lake-level from beach ridges that are numerically controlled by radiometric ^{14}C ages on shells (Orme and Orme, 1993), from archeological and historic data (Beanland and Clark, 1994; Li et al., 2000), and from radiometric ^{14}C ages on tufa that formed in a subaqueous environment from this study, Table 2. Open symbols denote ^{14}C ages of material or geomorphic features formed above a lake-level from Beanland and Clark (1994), Bierman et al. (1995), Smith et al. (1997), and Li et al. (2000) and this study, in addition to inferred ages based on numerical age control on stratigraphic and geomorphic relations from this study.

Sediment core data in Figure 25 are from Benson et al. (1997), Smith et al. (1997), and Li et al. (2000), which are all shown with a solid triangle. The elevation of each sediment core data point is approximated by comparing the reported age with a corresponding depth (elevation) using the graphic log of core OL-92 in Smith (1997). Age control of the sediment cores is derived from AMS ^{14}C on bulk organic carbon and carbonate. The reported ^{14}C ages in Benson et al. (1997) are in calendar years (calibrated age dates) using ^{230}Th-^{234}U and ^{14}C ages of corals after Bard et al. (1993), whereas, the ages in Li et al. (2000) were reported using a correlation to paleomagnetic secular variations because of uncertainties in the reservoir age estimation. The ^{14}C ages in Smith et al. (1997) were reported in conventional ^{14}C years. ^{14}C ages for cores in Figure 25 bound sediment hiatuses (unconformities) that are interpreted as proxy indicators of a change from the deposition of relative deep water facies to moderate to shallow water facies within a closed basin lake. The sediment hiatuses are marked by the presence of frosted quartz grains, coarse sand, and oolites (Benson et al., 1997; Smith et al., 1997).

Owens Lake Level Curve

15,000-11,300 cal. yr B.P.

Between ca. 15.0-11.6 cal. ka, pluvial Owens Lake significantly receded, with a drop in elevation of ~38 m (~1138-1100 m) in ca. 3-4 k.y. after it last overflowed (Fig. 25). During this time, shoreline data in the form of beach ridges and barriers indicate the occurrence of complex oscillations in lake-levels characterized as a disorderly regression that at times was punctuated by minor transgressions that were brief to long-term (Orme and Orme, 1993). Sediment core data during this same time interval reveal the presence of four unconformities (sand horizons) that suggest drops in lake-level that are synchronous with the five relative stable periods that are indicated by the shoreline data (Fig. 25). Soon after the lowest 1100 m lake-level at ca. 11.6 cal. ka, sediment core data record an unconformity around ca. 11.3 cal. ka that suggests a lake-level lower than 1100 m, before rising ca. 20-38 m during an early Holocene transgression.

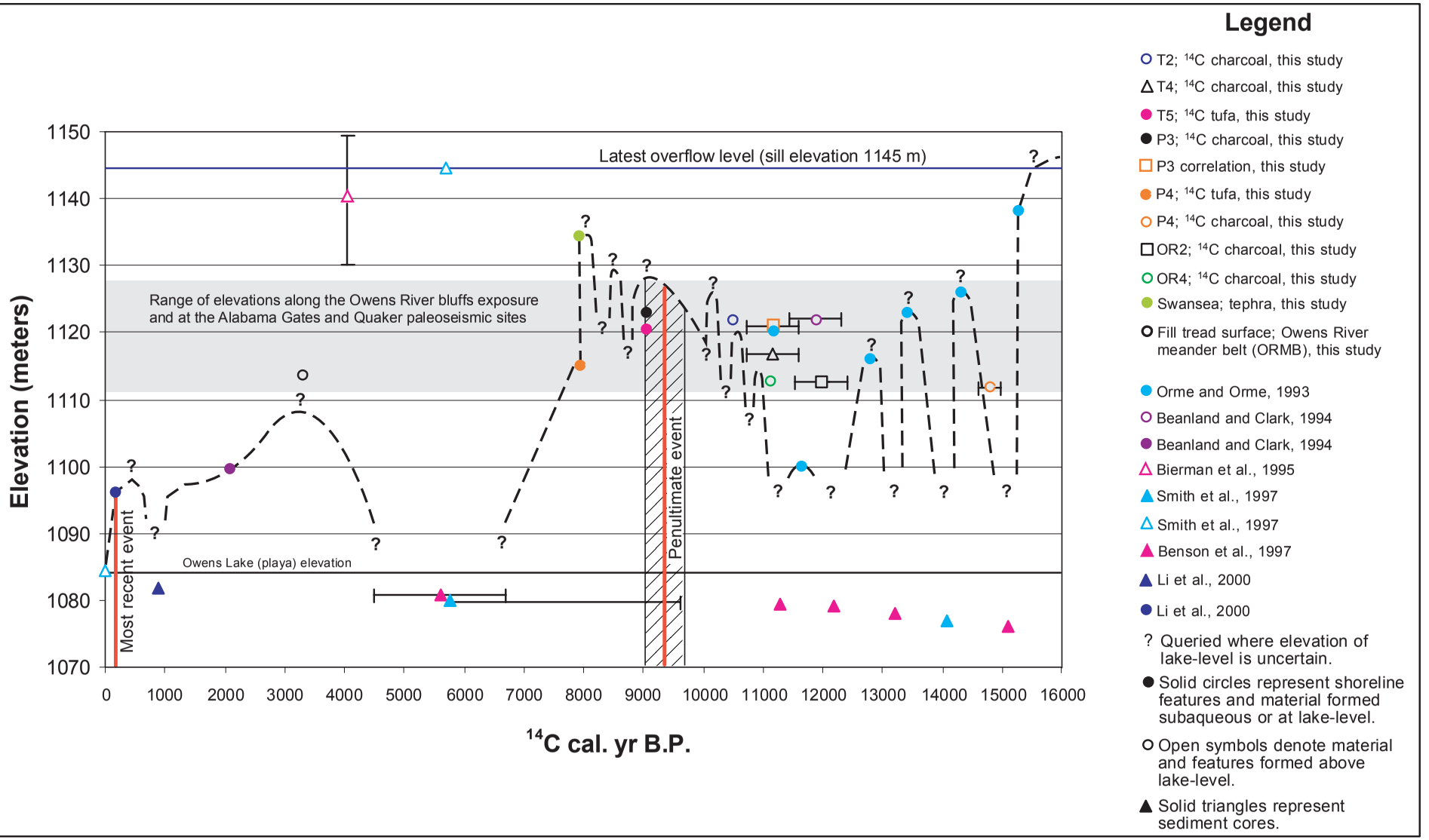

Figure 25. Lake-level curve of pluvial Owens Lake in relation to the Owens River bluffs exposure of Bacon (2003), the Alabama Gates and Quaker paleoseismic sites, and the latest overflow level of Owens Lake basin between 16 cal. ka and present. The Owens Lake level curve is a compilation of stratigraphic, geomorphic, and sediment core data from this study and previous investigations in southern Owens Valley and Owens Lake basin. The age of the most recent (A.D. 1872) and penultimate (9,300 ± 300 cal. yr B.P.) events on the Owens Valley fault are shown in relation to the relative lake-level curve. Calibrated radiocarbon ages are after the methods of Bard et al. (1993).

11,200-8,000 cal. yr B.P.

During this early Holocene transgression, pluvial Owens Lake had complex lake-level fluctuations that deposited shore, nearshore, and fluvio-deltaic facies over subaerial facies and constructed shoreline features between ca. 11.7-8.0 cal. ka. The lake-level curve shown in Figure 25 in this time interval is from sequence stratigraphy analysis at the Owens Bluffs exposure and at the Alabama Gates and Quaker paleoseismic sites of this study. Based on the stratigraphy and tephra chronology at the Swansea gravel quarry, the maximum Holocene pluvial Owens Lake highstand appears to have reached an elevation near 1135 m soon after ca. 8.0 cal. ka (Fig. 25). The Swansea gravel quarry is 5-15 km northwest of other shoreline features that are at an elevation near 1135 m (Beanland and Clark, 1994; Strandline C). Beanland and Clark (1994) infer that the wave-cut features near Keeler were formed between <7 to 2 ka (?).

In addition to the ~1135 m highstand localities at Swansea and near Keeler, geomorphic and stratigraphic evidence from the Alabama Gates and Quaker paleoseismic sites, ~17 km northwest of Swansea, provide evidence for relatively deep water conditions (nearshore depositional environments) between ca. 10 and 8 cal. ka. Geomorphic evidence at the Alabama Gates paleoseismic site indicates that wave-cut notches and tread surfaces are located at elevations between 1128 and 1136 m. Stratigraphy from this site supports the existence of a lake-level above ll27 m, with the presence of nearshore facies deposited after ca. 10 cal. ka. Stratigraphy at the Quaker site indicates lacustrine sedimentation and subaqueous tufa precipitation at an elevation as high as 1123 m after ca. 8.8 cal. ka. The ca. 8.0 cal. ka Holocene highstand appears to have been short lived, prior to a significant regression in lake-level, before stabilizing for a period of time when it eroded into existing sediments and constructed a well-developed beach berm at an elevation of ~1120 m at the Quaker paleoseismic site. The ^{14}C age of the beach berm is ca. 8 cal. ka, determined from tufa materials. Another tufa ^{14}C age in older lacustrine sediment and ^{14}C ages on charcoal support the tufa age of the berm.

An additional shoreline feature at an elevation of 1122 m is ca. 30 km to the south near Olancha (Beanland and Clark, 1994; Strandline D; Fig. 2). Beanland and Clark (1994) infer that this strandline formed between <7 to 2 ka (?). Their elevation of Strandline D is close to the elevation of the ca. 8 cal ka beach berm at the Quaker paleoseismic site of this study (Fig. 25). The ~3 m difference in elevation between the two features is within minimum error of deformation since ca. 9.3 cal. ka (±1 m; this study) and the natural variability in crest height of shoreline forms (±2.5; Adams and Wesnousky, 1998) that together total a minimum of ~3.5 m. It is plausible that the strandline at 1122 m documented by Beanland and Clark (1994) formed during the same relatively stable lake-level that constructed the ca. 8 cal. ka beach berm at the Quaker paleoseismic site.

8,000-4,500 cal. yr B.P.

Regression of pluvial Owens Lake continued after the construction of the ca. 8 cal. ka beach berm. Lake-level lowered to elevations that permitted subaqueous erosion of the lake bottom, causing discontinuities in the core, which is an indicator of near desiccation lake-levels. ^{14}C ages of oolites and bulk organic sediment that unconformably bound the oolites and sand horizons indicate near desiccation of pluvial Owens Lake between ca. 6.7-4.5 cal. ka (Benson et al., 1997; Smith et al., 1997). During this same period of time, alluvium was deposited in the overflow channel of pluvial Owens Lake at an elevation near 1145 m, south of Olancha (Fig. 3). The alluvium dammed the southern part of the channel to form Little Lake. Radiocarbon dates on basal sediment in a core from Little lake provide a minimum age of overflow from pluvial Owens Lake at ca 5.7 cal. ka (e.g., Smith et al., 1997) (Fig. 25).

4,500-present cal. yr B.P.

Lake-level is inferred to have increased after ca. 4.5 cal. ka, because the cores lack relatively shallow lake-level indicators between ca. 4.5-1.0 cal. ka. A maximum lake-level between this time interval below 1114 m is indicated by the sequence of cut-and-fill relations observed in the Owens River meander belt from the borehole site of Bacon (2003). The boreholes were drilled at the surface of a preserved fluvial tread at an elevation near 1114 m that is underlain by a 4 m package of bedded fluvial sands and silts in sharp contact with deep water lacustrine clayey silts. These relations suggest that the sharp contact is likely a ravinement surface formed in response to the lower lake-levels between ca. 6.7-4.5 cal. ka. During a subsequent change in base level, the Owens River north of Lone Pine apparently responded by aggradation of ca. 4 m, likely associated with a rise in lake-level after ca. 4.5 ka. The open circle shown in Figure 25 denotes the elevation of the tread surface and

and inferred age based on stratigraphic and geomorphic relations exposed at the Owens River borehole site, the Owens River bluffs exposure of Bacon (2003), and the Alabama Gates and Quaker paleoseismic sites, all of this study.

The fluvial tread surface elevation of ~1114 m likely formed in response to a transgression that stabilized at an elevation of 1107 m, suggested by the presence of a prominent beach ridge at the southern margin of Owens Lake (playa) that Beanland and Clark (1994) (their Strandline E) infer to be <7 to 2 ka(?). It is likely that the fluvial tread surface and strandline formed after ca. 4.5 cal. ka. The beginning of this transgression coincides with a ^{14}C age of ca. 4.5 cal. ka from Bierman et al. (1995) who dated a part of an alluvial fan that they mapped between 1150-1130 m elevation near Lone Pine (Fig. 25). The ^{14}C age on the fan is not considered a maximum age of the fan. Fan development at this time may be synchronous with aggradation of the Owens River and construction of a prominent beach ridge at Owens Lake during a time of relatively wetter conditions when compared to the earlier period between ca. 6.7-4.5 cal. ka (Fig. 25).

A regression after aggradation of the Owens River is implied by ca. 12 m of incision into fluvial and lacustrine deposits younger than ca. 8.0 cal. ka that are exposed along the western margin of the meander belt between the Alabama Gates paleoseismic site and north of Lone Pine (Figs. 3 and 11). This drop in lake-level is indicated by the lowest suite of prominent beach ridges and wave cut notches that encompass Owens Lake (playa) at an elevation of 1096-1100 m. These shoreline features are inferred to be <7 ka(?) to circa. 1872 (Beanland and Clark, 1994; Strandline F). An Indian artifact from one of the higher beach ridges at ~1100 m is estimated to be a few thousand years old, which provides a minimum age for the feature (Beanland and Clark, 1994) (Fig. 25). Between A.D. 950 and 1220, sediment core data provide evidence for highly saline and alkaline lake conditions that imply relatively low lake-levels. This was followed by a relative lake-level rise at A.D. 1220-1280. The period between A.D. 1280-1872 is characterized as fluctuating with lake depths that range from <10 m to the historical maximum of 14.9 m with a lake-level at 1096 m (Li et al., 2000) (Fig. 25). It wasn't until around 1921 when Owens Lake first began depositing salts onto the lake floor at an elevation of ~1086 m, because of stream diversions to the aqueduct system which began nearly eight years prior (Smith et al., 1997). Around 1931 Owens Lake had desiccated and become a playa (Li et al., 2000).

The ~1-2 k.y. intervals between the recorded oscillations of pluvial Owens Lake-levels shown in Figure 25 are similar to other studies in North America. For example, Viau et al. (2002) demonstrate wide evidence of 1,500 yr climate variability in North America during the past 14,000 yr, based on pollen records. The timing of 9 major transitions of vegetation communities identified by Viau et al. (2002) are nearly synchronous with transgressions and regressions of pluvial Owens Lake over the last ~15 cal. ka.

Comparison of latest Quaternary lake-level fluctuations in Owens Lake basin with Mono Lake basin

Based on stratigraphic and geomorphic data presented in Figure 25, pluvial Owens Lake last overflowed prior to ca. 15.5 cal. ka. It ceased to overflow because of a decrease in annual flow from the Owens River and an increase in evaporation that roughly coincides with the end of the Recess Peak glacial advance before ca. 13.1 ± 0.9 cal. ^{14}C ka (Clark and Gillespie, 1997) and probably with the end of overflow from pluvial Lake Russell in Mono basin (Smith and Street-Perrott, 1983; Reheis et al., 2002). In addition, pluvial Searles Lake had low lake-levels that were 180 m below its sill elevation between 16.5-14 cal. ka that imply relatively low to no overflow from pluvial Owens Lake (Smith and Street-Perrott, 1983).

The latest Quaternary lake-level curve for Owens Lake (Fig. 25) exhibits relative lake-level highs and lows that are similar to those documented for pluvial Mono Lake (Lake Russell), ca. 200 km to the north of Owens Lake basin and adjacent to the east side of the Sierra Nevada Range (Fig. 1). Sediment in the Wilson Creek Formation in Mono basin record a lowstand at 15.5-14.0 ^{14}C cal. ka that is nearly synchronous with a relative lowstand of pluvial Owens Lake (Benson et al., 1998). Before 10.5 cal. ka, pluvial Mono Lake was relatively deep with a surface elevation at ca. 1980 m (Stine, 1990). This surface elevation is ca. 30 m higher than the present surface of Mono Lake and ca. 208 m lower than the last overflow sill (Reheis et al., 2002). Pluvial Mono Lake water levels were high but fluctuating during the late Glacial and early Holocene from ca. 13.6-8.0 cal. ka (Davis, 1999), which is similar to pluvial Owens Lake during this time (Fig. 25). Pluvial Mono Lake during the middle Holocene from ca. 8.0-4.5 cal. ka had intermediate water levels between the elevations of 1980 and 1950 m

that are characterized as more constant than during the preceding interval (Stine, 1990; Davis, 1999). During this time, it appears pluvial Owens and Mono Lakes were not synchronous, because Owens Lake dropped as much as ~50 m in ~4.5 k.y. to near desiccation (Fig. 25). During the late Holocene from ca. 4.5 cal. ka to present, Mono Lake is characterized by shallow fluctuating lake-levels that had lowstands below the historic minimum of 1942 m at ca. 4.5, 2.5, and 1.0 cal. ka (Stine, 1990; Davis, 1999). The timing of the lowstands of Mono Lake at ca. 4.5 and 1.0 cal. ka are similar to the shallow lake-levels of Owens Lake indicated by the core data between ca. 6.7-4.5 cal. ka and at ca. 0.98 cal. ka (Fig. 25).

Comparison of pluvial lake-level fluctuations of Owens Lake basin with the Great Basin pluvial lake record

The lake-level curve for pluvial Owens Lake shows a similar regressive lake-level oscillation to pluvial Lake Lahontan from its highstand immediately prior to ca. 15.4 cal. ^{14}C ka (Adams and Wesnousky, 1998), in addition to the earlier studies in the Lahontan basin that place the last major highstand between about ca. 14.7-17.1 cal. ka (Adams and Wesnousky, 1998, and references therein). Similarly, pluvial Lake Newark in east-central Nevada, which was disconnected from pluvial Lake Lahontan during the last pluvial, began a regression from its highstand after ca. 15.0 cal. ka (Redwine, 2003). Likewise, pluvial Lake Chewaucan in southeastern Oregon had a highstand lake-level that lowered around ca. 15.3 cal. ka, which was followed by a significant rise and fall in lake-level at ca. 14.1 cal. ka (Licciardi, et al., 2001). The timing of regressive lake-level oscillations of pluvial Lake Lahontan, Lake Newark, and Lake Chewaucan are similar to the lake-level curve of pluvial Owens Lake.

CONCLUSION

This study incorporates the wealth of previous stratigraphic and paleoseismic investigations in Owens Valley. The results presented in this study have refined the stratigraphic and paleoseismic estimates determined by the most extensive investigation on the OVFZ by Beanland and Clark (1994). Detailed analysis of exploratory fault trenches and stratigraphic pits across the Owens Valley fault, in combination with over 1.5 km of described Owens River bluffs exposure in Bacon (2003) and other natural exposures, and mapping of surficial landforms in combination with existing Owens Lake sediment cores and stratigraphic data, have aided in the understanding of preserved geomorphic features and in the development of the associated lacustrine sequence stratigraphy. The sequence stratigraphy documents a complex interaction between fluctuating latest Pleistocene and early Holocene lacustrine and fluvio-deltaic systems and late to middle Holocene fluvial system that collectively have modified and reset the landscape and evidence of pre-1872 fault scarps below and near an elevation of ca. 1135 m near Lone Pine.

The complex distribution of geomorphic features and associated sediments have provided insight into the conceptual framework of scarp forming and modification processes in an arid, pluvial lake environment, which is used to distinguish between fault-related deposits and scarps from similar, but nontectonic, features produced by shoreline and fluvial modification. Based on these observations, this study presents a detailed stratigraphic facies model of latest Quaternary stratigraphy related to desiccation of pluvial Owens Lake, which in turn is used to determine the two interseismic intervals between the antepenultimate and 1872 events, thereby refining slip rate estimates on the OVF near Lone Pine.

Paleoseismic results on the Owens Valley fault

Paleoseismic results from this study are based on the chronology of fluvio-deltaic and lacustrine sequence stratigraphy associated with pluvial Owens Lake-level fluctuations, in combination with structural relations of offset sequence boundaries exposed in 7 trenches and 4 pit exposures. Measured in 3 trenches from two sites, the cumulative vertical offset from the historic and prehistoric earthquakes is 2.3 ± 0.3 m (2σ). All 7 trenches record faulting related to the 1872 event. The average vertical displacement for the 1872 event, as measured confidently in 5 trenches is 0.9 ± 0.3 m (2σ). In each trench, the vertical offset of the 1872 event is subtracted from the cumulative vertical offset to derive an average vertical offset for the PE of 1.4 +0.3/-0.4 m (2σ). Vertical displacement of the penultimate event is ~60% greater than the 1872 displacement. Analyses of ^{14}C in charcoal and tufa materials that bound the PE event horizon indicate the PE occurred between 10,210 ± 60 cal. yr B.P. and 8,790 ± 210 cal. yr B.P. The age of the PE is estimated at 9,300 ± 300 cal. yr B.P. on the basis of the PE

horizon position with respect to the location of the ^{14}C ages and sedimentation rates. Accounting for the elapsed time between 1872 and 1950, the interseismic interval between the two earthquakes is ca. 9,500 to 8,900 yrs. The oldest sediment in the trench exposures that is not deformed by the antepenultimate event (APE) is ~15,000 ± 600 cal. ^{14}C yr B.P. This ca. 15 cal. ka age provides a minimum constraint for the APE. The maximum age of sediment deformed by the APE is 21,000 ± 1,300 ^{14}C yr B.P. (Lubetkin and Clark, 1988). Using the range of constraining ages of sediment that bound the APE, the event occurred 18,400 ± 4,000 cal. yr B.P. Given the poor age constraint of the APE, the interseismic interval between the PE and APE is 12,800 to 5,400 yrs.

On the basis of tephra chronology, a Holocene highstand occurred after ~8 cal. ka and reached an elevation of ~1135 m, ~10 m below the latest overflow sill of Owens Lake basin. As a result, there is no unequivocal evidence of recurrent lateral offsets below this elevation, because this highstand and earlier lake-levels modified and reset the landscape and evidence of pre-1872 fault scarps near Lone Pine. To derive an estimate of the latest Quaternary slip rate on the OVF, the horizontal to vertical scaling ratios of 6:1 (avg.) and 10:1 (max.) determined by Beanland and Clark (1994) is used with the average individual vertical and total vertical cumulative offsets of the PE and MRE to estimate the average horizontal displacements. The average horizontal displacements, divided by their corresponding single interseismic intervals and age estimate of the APE, result in an average oblique slip rate estimate of 0.4-1.3 m/k.y. (2σ). Based on the maximum scaling ratio of 10:1 with the average total vertical cumulative offset and the age estimate for the APE, the three-event oblique slip rate estimate is 1.0-1.6 m/k.y.

Latest Quaternary pluvial Owens Lake level oscillations

Following an oscillating major regression from its latest Pleistocene highstand at an elevation of 1145 m after ca. 15 ka, pluvial Owens Lake dropped ~38 m around ca. 11.5 cal. ka. This lowstand was followed by a fluctuating transgression that had an early Holocene highstand near 1135 m after ca. 8 cal. ka, before dropping ≥45 m to near desiccation lake-levels between ca. 6.7 and 4.5 cal. ka. A minor transgression-regression of pluvial Owens Lake compared to earlier periods after 4.5 cal. ka is suggested by fluvial cut-and-fill relations in the Owens River meander belt in Bacon (2003) north of Lone Pine and two shoreline features described by Beanland and Clark (1994). This minor transgression was followed by alkaline conditions and fluctuating shallow lake-levels during the late Holocene (Li et al., 2000).

The stratigraphic and paleoseismic observations included in this NEHRP technical report will improve prior probabilistic seismic hazard assessments and provide insight for geodetic strain and kinematic models on the OVFZ, in addition to characterizing the magnitude of pluvial Owens Lake-level fluctuations during the early to middle Holocene.

ACKNOWLEDGEMENTS

This project would not be possible without permission and access to trench and work on City of Los Angeles, Department of Water and Power (LADWP) lands and with the local ranchers that lease the land. I acknowledge Paula Hubbard of LADWP who helped with making the permitting process enjoyable. We would like to thank Tom Noland of the Anchor Ranch who provided access to work on his land. We thank Srikanth Balasubramanian and personnel of the California Department of Transportation (CalTrans) for their gracious and willingful help and Granite Construction for donating their time and equipment for excavations at the Alabama Gates paleoseismic site. We acknowledge the Bureau of Land Management, Bishop Office for the use of their 1977 aerial photographs. We respectfully thank William Bryant, George Brogan and students, Gary Carver, Paul and Anita Hancock, Angela Jayco, Jeff Lee, Jim Macey, Rob Negrini, Nicholas Pinter, Tom Sawyer, Burt Slemmons, George Smith and colleagues, and many of our Pleistocene Friends for reviewing the trenches, walking out the scarps, and providing thoughtful and helpful comments.

We acknowledge Andrei M. Sarna-Wojcicki, U.S. Geological Survey, Menlo Park, California for his assistance in the identification and correlation of selected tephra. We thank Rob Negrini of California State University, Bakersfield for visiting and sampling the Alabama Gates paleoseismic site for paleomagnetics. Sincere thanks to the H-Crew: the many HSU students and volunteers for their cordial assistance during field work and trenching, in particular, Ronna Bowers, Bryan Dussel, Sarah Georgi, Tom Leroy, Jay Patton, Ian Pryor, Joanna Redwine,

Michelle Roberts, Jay Stallman, Dianne Sutherland, Cherri Taylor, Susan Taylor, and the members of the 1999 and 2001 HSU Quaternary field method and 2002 HSU geology field camp courses. Special thanks goes to Todd Williams from HSU who provided Global Positioning System (GPS) elevation control at the Quaker paleoseismic site and to Joanna Redwine for her pedologic expertise. We wish to acknowledge and give thanks to Jim Macey for use of the Keeler geologic field station during all the fieldwork for this project. S. Bacon acknowledges the University of California, White Mountain Research Station for awarding 1999-2001 travel minigrants.

REFERENCES

Adams, K.D., and Wesnousky, S.G., 1998, Shoreline processes and the age of the Lake Lahontan highstand in the Jessup embayment, Nevada: Geological Society of America Bulletin, v. 110, n. 10, p. 1318-1332.

Bacon, S.N., 2003, Latest Quaternary fluivo-deltaic and lacustrine stratigraphy in Owens Valley and paleoseismology on the Owens Valley fault near Lone Pine, eastern California: [M.S. thesis]: Humboldt State University, 227 p.

Bacon, S.N., Pezzopane, S.K., and Burke, R.M., 2002a. Stratigraphic evidence for only one Holocene paleoearthqauke since ca. 12 ka on the Owens Valley fault, near Lone Pine, eastern California: Geological Society of America, Abstracts with Programs., Vol. 33, No. 4., p. A-11.

Bacon, S.N., Pezzopane, S.K., and Burke, R.M., 2002b. Paleoseismology on the Owens Valley fault and Holocene stratigraphy of pluvial Owens Lake near Lone Pine, eastern California: Geological Society of America, Abstracts with Programs., Vol. 34, No. 6., p. 27.

Bacon, S.N., Pezzopane, S.K., and Burke, R.M., 2001. FY 2001 NEHRP Project Summary: Preliminary Paleoseismic Results on the Owens Valley Fault Zone and Latest Quaternary Stratigraphy in Owens Valley near Lone Pine, eastern California.

Bacon, S.N., and Burke, R.M., 2000, Preliminary paleoseismic investigations on the Owens Valley fault zone and latest Quaternary stratigraphy in Owens Valley near Lone Pine, eastern California: EOS Transactions, Am. Geophy. Union, v. 81, p. F856-F857.

Baucom, P.C., and Rigsby, C.A., 1999, Climate and lake-level history of the northern Altiplano, Bolivia, as recorded in Holocene sediments of the Rio Desaguadero: Journal of Sedimentary Research, v. 69, n. 3, p. 597-611.

Beanland, S., and Clark, M.M., 1994, The Owens Valley fault zone, eastern California, and surface rupture associated with the 1872 earthquake: U.S. Geological Survey Bulletin 1982.

Benson, L.V., 1994, Carbonate deposition, Pyramid Lake subbasin, Nevada: 1. Sequence of formation and elevational distribution of carbonate deposits (tufas): Palaeogeography, Palaeoclimatology, Palaeoecology, v. 109, p 55-87.

Benson, L.V., Burdett, J.W., Kashgarian, M., Lund, S.P., Phillips, F.M., and Rye, R.O., 1996, Climatic and hydrologic oscillations in the Owens Lake basin and adjacent Sierra Nevada, California: Science, v. 274, p. 746-748.

Benson, L., Burdett, J., Lund, S., Kashgarian, M., and Mensing, S., 1997, Nearly synchronous climate change in the Northern Hemisphere during the last glacial termination: Nature, v. 388, p. 263-265.

Bierman, P.R., Gillespie, A.R., and Caffee, M.W., 1995, Cosmogenic ages for earthquake recurrence intervals and debris flow fan deposition, Owens Valley, California: Science, v. 20, p. 447-450.

Bischoff, J.L., Stine, S., Rosenbauer, R.J., Fitzpatrick, J.A., and Stafford, T.W., Jr., 1993, Ikaite precipitation by mixing of shoreline springs and lake water, Mono Lake, California, USA: Geochimica et Cosmochimica Acta 57, p. 3855-3865.

Bryant, W.A., 1988, Owens Valley Fault Zone, Inyo County: California Department of Conservation, Division of Mines and Geology Fault Evaluation Report FER-192, reprinted in Division of Mines and Geology Open-File Report 90-14 (microfiche).

Burke, R.M., and Birkeland, P.W., 1979, Reevaluation of multiparameter relative dating techniques and their application t to the glacial sequences along the eastern escarpment of the Sierra Nevada, California: Quaternary Research, v. 11, p. 21-51.

Burke, R.M., Bacon, S.N., and Pezzopane, S.K., 2000, Paleoseismic investigations on the Owens Valley fault zone and Latest Quaternary stratigraphy in Owens Valley near Lone Pine, California: Seismogenic Behavior and Fault Mechanics: National Earthquake Hazards Reduction Program Proposal for Fiscal Year 2001, submitted May 9, 2000, variously paginated.

Burke, R.M., Bacon, S.N., and Pezzopane, S.K., 2001, Paleoseismic investigations on the Owens Valley fault zone and Latest Quaternary stratigraphy in Owens Valley near Lone Pine, California: National Earthquake Hazards Reduction Program Continuation Proposal for Fiscal Year 2002, submitted May 1, 2001, variously paginated.

Carver, G.A., 1970, Quaternary tectonism and surface faulting in Owens Lake basin, California: Reno, University of Nevada, MacKay School of Mines Technical Report AT2, 103 p.

CalTrans [State of California, Department of Transportation], 1993, Project plans for construction on state highway in Inyo County in and near Lone Pine from Begole Street to 0.1 mile south of Los Angeles Aqueduct bridge, 216 sheets.

Caskey, J.S., 1995, Geometric relations of dip slip to a faulted ground surface: new nomograms for estimating components of fault displacement, Journal of Structural Geology, 17 (8), pp. 1197-1202.
Caskey, J., 2002, Large-scale lateral-spread paleoscarps and Mazama-age lacustrine deposits at Dixie Hot Springs, *in* Caskey, J., ed., Historical faulting, chronostratigraphy, and paleoseismicity of the central Nevada Seismic Belt (guidebook for the 2002 Pacific Cell-Friends of the Pleistocene fieldtrip), p. 94-99 (Appendix 2-4).
dePolo, C.M., and Ramelli, A.R., 1987, Preliminary report on surface fractures along the White Mountain fault zone associated with the July 1986 Chalfant Valley earthquake sequence: Seismological Society of America Bulletin, v. 77, p. 290-296.
dePolo, C.M., 1989, Seismotectonics of the White Mountain fault system, eastern California and western Nevada [M.S. thesis]: Reno, University of Nevada, 354 p.
dePolo, C.M., Clark, D.G., Slemmons, D.B., and Ramelli, A.R., 1991, Historical surface faulting in the Basin and Range province, western North America: implications for fault segmentation: Journal of Structural Geology, v. 13, n. 2, p. 123-136.
dePolo, C.M., Peppin, W.A., and Johnson, P.A., 1993, Contemporary tectonics, seismicity, and potential earthquake sources in the White Mountain seismic gap, west-central Nevada and east-central California, USA: Tectonophysics, v. 225, p. 271-299.
Emery, D., and K.J. Myers, 1996, Sequence stratigraphy: Oxford, Blackwell Science, 297 p.
Einsele, G., 2000, Sedimentary basins: evolution, facies, and sediment budget. 2nd ed., New York, Springer-Verlag, 804 p.
Ellsworth, W.L., 1990, Earthquake history, 1769-1989, *in* Wallace, R.E., ed., The San Andreas fault system, California: U.S. Geological Survey Professional Paper 1515, p. 153-187.
Forester, R.M., 2000, An Ostracode Record of Holocene Climate Change from Owens Lake, California, in Impacts of Climate Change on Landscapes of the Eastern Sierra Nevada and Western Great Basin, U.C. White Mountain Research Station Workshop, Bishop, California.
Gale, H.S., 1915, Salines in the Owens, Searles, and Panamint basins, southeastern California: U.S. Geological Survey Bulletin 580, 281--323.
Gilbert, G.K., 1884, A theory of the earthquakes of the Great Basin, with a practical application: American Journal of Science, ser. 3, v. 27, p. 49-53.
Hill, M.R., 1972, A centennial....the great Owens Valley earthquake of 1872: California Geology, v. 25, p. 51-54.
Hollet, K.J., Danskin, W.R., McCafferey, W.F., and Walti, C.L., 1991, Geology and Water Resources of OwensValley, California: U.S. Geological Survey Water-Supply Paper 2370.
Jennings, C. W., 1994, Fault activity map of California and adjacent areas: scale 1:750,000, 2 plates with text, Calif. Div. of Mines and Geol., Sacramento.
Keefer, D.K., 1999, Earthquake induced landslides and their effects on alluvial fans: Journal of Sedimentary Research, Vol. 69, No. 1, p. 84-104.
Kirby, E., Burbank, D., Jager, J., and Reheis, M., 2002, Pleistocene slip rate on the White Mountain fault zone: Geological Society of America Abstracts with Programs, v. 34, no. 6, p. 249.
Langridge, R.M., 1998, Paleoseismic deformation in behind-arc lacustrine settings: Acambay, Mexico and Ana River, Oregon, [Ph.D. dissertation]: University of Oregon 188 p.
Lee, J., C. Rubin, M. Miller, J. Spencer, L. Owen, T. Dixon, 2000, Kinematics of the Eastern California shear zone north of the Garlock fault: Geol Soc. Am, Abstracts with Programs, v. 32, p. A105.
Lee, J., Spencer, J., and Owen, L., 2001, Holocene slip rates along the Owens Valley fault, California: Implications for the recent evolution of the Eastern California shear zone: Geology, v. 29, p. 819-822.
Lettis, W.R., and Kelson, K.I., 2000, Applying geochronology in paleoseismology, *in* Noller, J.S., Sowers, J.M., Lettis, W.R., eds., Quaternary geochronolgy: methods and applications, AGU reference shelf 4: American Geophysical Union, Washington D.C, p. 479-496.
Li, H., Bischoff, J.L., Ku, T., Lund, S.P., and Stott, L.D., 2000, Climate Variability in East-Central California during the Past 1000 Years Reflected by High-Resolution Geochemical and Isotopic Records from Owens Lake Sediments: Quaternary Research, v. 54, p. 187-197.
Lienkaemper, J.J., Pezzopane, S.K., Clark, M. M., and Rymer, M.J., 1987, Fault fractures formed in association with the 1986 Chalfant valley, California, earthquake sequence: Preliminary report: Seismological Society of America Bulletin, v. 77, no. 1, p. 297-305.
Lubetkin, L.K.C., and Clark, M.M., 1988, Late Quaternary activity along the Lone Pine fault, eastern California: Geological Society of America Bulletin, v. 100, p. 755-766.
Lund, S.P., Newton, M., Hammond, D., and Stott, L., 1998, Paleohydrology of the Owens River/Lake System as a Proxy Indicator of Late Quaternary Glacial Variations within the Sierra Nevada: Geol. Soc. Am, Abstracts with Programs, v. 30 n. 7, p. A61.
Martel, S.J., Harrison, T.M., and Gillespie, A.R., 1987, Late Quaternary vertical displacement rate across the Fish Springs fault, Owens Valley fault zone, California: Quaternary Research, v. 27, p. 113-129.
McCalpin, J.P., 1996a, Field techniques in paleoseismology, *in* McCalpin, J.P., ed., Paleoseismology, Volume 62 in the International Geophysics Series: Academic Press, New York, p. 33-83.

McCalpin, J.P., 1996b, Application of paleoseismic data to seismic hazard assessment and neotectonic research, *in* McCalpin, J.P., ed., Paleoseismology, Volume 62 in the International Geophysics Series: Academic Press, New York, p. 479.
Miller, W., III, 1989, Pleistocene freshwater mollusks on the floor of Owens Lake playa, eastern California: Tulane Studies in Geology and Peleoecology, Vol. 22, No. 2, p. 47-54.
Newton, M.S., 1991, Holocene stratigraphy and magnetostratigraphy of Owens and Mono Lakes, eastern California [Ph.D. thesis]: Los Angeles, Univeristy of Southern California, 330 p.
Oakeshott, G.B., Greensfelder, R.W., and Kahle, J.E., 1972, 1872-1972....One hundred years later: California Geology, v. 25, p. 55-61.
Orme, A.R., and Orme, A.J., 1993, Late Pleistocene oscillations of Lake Owens, eastern California: Geol. Soc. Am, Abstracts with Programs, v. 25, n. 5, p. 129-130.
Orme, A.R., and Orme, A.J., 2000, Deformation of Late Pleistocene shorelines at Owens Lake, eastern California: Tectonic and Hydrologic Implication: Geol. Soc. Am, Abstracts with Programs, v. 32, n. 7.
Pezzopane, S.K. and Weldon, R.J., 1993, Tectonic role of active faulting in central Oregon: Tectonic, v. 12, p. 1140-1169.
Pinter, N., Keller, E.A., and West, R.B., 1994, Relative dating of terraces of the Owens River, northern Owens Valley, California, and correlation with moraines of the Sierra Nevada, Quaternary Research, v. 42, p. 266-276.
Pinter, N., 1995, Faulting on the Volcanic Tableland, California: Journal of Geology, v. 103, p. 73-83.
Redwine, J.L., 2003, The Quaternary pluvial history and paleoclimate implications of Newark valley, east-central Nevada; derived from mapping and interpretation of surficial units and geomorphic features, [Masters thesis]: Humboldt State University, 250 p.
Sauber, J., Thatcher, W., Solomon, S.C., and Lisowski, M., 1994, Geodetic slip rate for the Eastern California shear zone and the recurrence time of Mojave Desert earthquakes: Nature, v. 367, p. 264-266.
Schroeder, J.M., Lee, J., Owen, L.A., and Finkel, R.C., 2002, Quaternary dextral fault slip history along the White Mountains fault zone, California: Geological Society of America Abstracts with Programs, v. 24, p. A87.
Schumacher, G., 1962, Deepest Valley-Guide to the Owens Valley and its mountain lakes, roadsides, and trails: Sierra Club, San Francisco, 206 p.
Schwartz, D.P., and Coppersmith, K.J., 1984, Fault behavior and characteristic earthquakes--examples from the Wasatch and San Andreas fault zones: Journal of Geophysical Research, v. 89, n. B7, p. 5681-5698.
Simpson, G.D., 1990, Late Quaternary tectonic development of the northwestern part of Summer Lake basin, south-central Oregon, [M.S. thesis]: Humboldt State University, 121 p
Slemmons, D.B., 1968, Geophoto archive, MacKay School of Mines, Reno, Nevada.
Slemmons, D.B. and Cluff, L.S., 1968, Historic faulting in Owens Valley, California: Geol. Soc. Am. Special Paper 121, Abstracts for 1968, p. 559-560.
Smith, G.I., 1997, Stratigraphy, lithologies, and sedimentary structures of Owens Lake core OL-92, *in* Smith, G.I., and Bischoff, J.L. eds., An 800,000 Year Paleoclimatic Record from Core OL-92, Owens Lake, Southeast California, Geology Society of America, Special Paper 317, p. 9-23.
Smith, G.I., and Street-Perrott, F.A., 1983, Pluvial lakes of the Western United States, Ch. 10 in Wright, H.E., Jr., ed., Late Quaternary environments of the United States: Minneapolis, University of Minnesota Press, v. 1, p. 190-212.
Smith, G.I., Bischoff, J.L., and Bradbury, J.P., 1997, Synthesis of the paleoclimatic record from Owens Lake core OL-92, in Smith, G.I., and Bischoff, J.L. eds., An 800,000 Year Paleoclimatic Record from Core OL-92, Owens Lake, Southeast California, Geol. Soc. of Am. Special Paper 317, p. 143-160.
Smoot, J.P., 1998, A Comparison of the Lacustrine Sedimentary Record for the Holocene and the Last Interglacial at Owens Lake, California: Geol. Soc. Am, Abstracts with Programs, v. 30 n. 7, p. A308.
Stone, P., Dunne, G.C., Moore, J.G., Smith, G.I., 2000, Geologic Map of the Lone Pine 15' Quadrangle, Inyo County, California. U.S. Geological Survey, Geological Investigation Series I-2617.
Sylvester, A.G., 1988, Strike-slip faults: Geological Society of America Bulletin, v. 100, p. 1666-1703.
Vittori, E., Michetti, A.M., Slemmons, D.B., and Carver, G.A., 1993, Style of recent surface deformation at the south end of the Owens Valley fault zone, eastern California: Geol. Soc. Am, Abstracts with Programs, v. 25, n. 5.
Weldon, R.J., McCalpin, J.P., and Rockwell, T.K., 1996, Paleoseismology of strike-slip tectonic environments, *in* McCalpin, J.P., ed., Paleoseismology, Volume 62 in the International Geophysics Series: Academic Press, New York, pp. 33-83.
Wesnousky, S.G., and Jones, C.H., 1994, Oblique slip, slip partitioning, spatial and temporal changes in the regional stress field, and the relative strength of active faults in the Basin and Range, western United States: Geology, v. 22, p. 1031-1034.
Whitney, J.D., 1872, The Owens Valley earthquake: Overland Monthly, v. 9, p. 130-140, 266-278. Reprinted by Goodyear, W.A., 1888, *in* Eighth Annual Report of the State Mineralogist: California State Mining Bureau, pp. 288-309.
Wills, C.J., 1996, Liquefaction in the California desert, an unexpected geologic hazard: California Geology, v. 49, no. 2, p. 31-35.
Zehfuss, P.H., Bierman, P.R., Gillespie, A.R., Burke, R.M., and Caffe, M.W., 2001, Slip rates on the Fish Springs fault, Owens Valley, California, deduced from cosmogenic 10 Be and 26 Al and soil development on fans: Geological Society of America Bulletin, v. 113, p. 241-255.